A Platinum Open Access Journal
for Organic Chemistry

Review

Free to Authors and Readers

DOAJ Seal

Arkivoc **2022**, part vi, 0-0
to be inserted by editorial office

"Copper catalyzed azide alkyne cycloaddition" based synthesis and applications of oligo-1, 2, 3-triazoles connected by suitable building blocks and "*N-(CH)$_n$-C*" linked triazole oligomers

Rashmita Pan, and Tanmaya Pathak*

Department of Chemisry, Indian Institute of Technology Kharagpur, Kharagpur 721302, India
Email: tpathak@chem.iitkgp.ac.in

Received mm-dd-yyyy **Accepted** mm-dd-yyyy **Published on line** mm-dd-yyyy

Dates to be inserted by editorial office

Abstract

A typical 1,2,3-triazoles are important aromatic heterocyclic compounds with three adjacent nitrogen atoms. These "unnatural" heterocycles found applications in pharmaceutical science, material science and chemical biology. Oligo-1,2,3-triazole linked molecules showed interesting applications in the field of DNA binding, self-assembly, surface modification, supramolecular chemistry etc. In this article, oligo-1,2,3-triazoles are broadly classified into two categories: (i) 1,2,3-triazoles are connected through varieties of organic molecules and (ii) triazole units are connected with one another either by N-(CH)n-C linkages or by amide bonds generated from amino acids. Syntheses and properties of some of these oligomers are reviewed in this article.

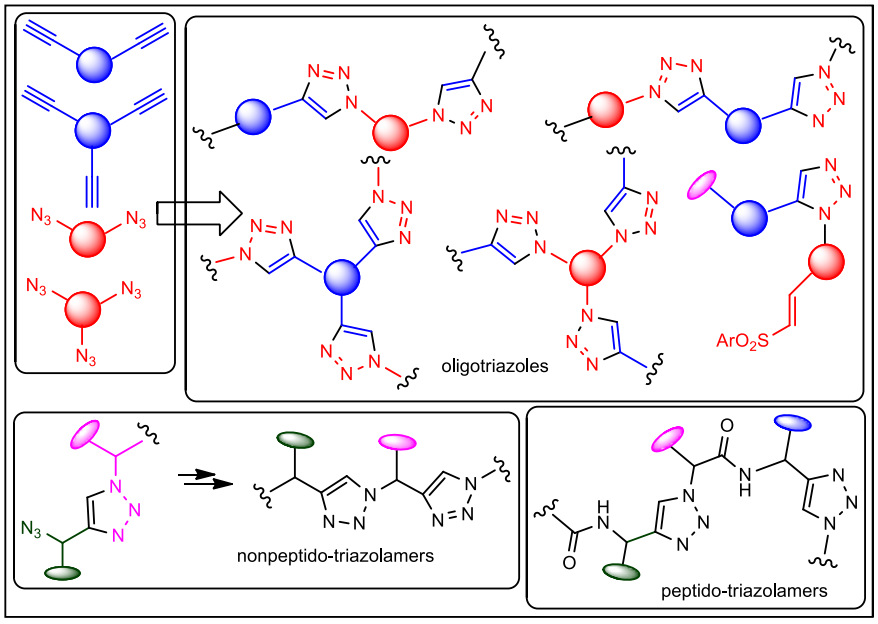

Keywords: Oligotriazoles, triazolamers, disubstituted 1, 2, 3-triazoles, click chemistry, peptidomimetic.

Table of Contents

1. Introduction

Nitrogen containing heterocyclic compounds are important component of life as they are part of essential building blocks like amino acids, nucleotides etc. 1,2,3-Triazoles are one of the most privileged five membered heterocycles with three adjacent nitrogen atoms. Although absent in nature, these heterocycles belong to a class of outstanding substances which are biologically active and are useful functionalized material.[1] Therefore, chemists are interested in devoloping facile and straightforward methodology for the synthesis of 1,2,3-triazoles. Synthesis of 1,2,3-triazole by thermal cycloaddition reaction of phenyl azide and diethyl acetylene-dicarboxylate was reported almost 130 years ago.[2] Later this class of reactions were thoroughly investigated and the scope of 1,3-dipolar cycloaddition reactions were widely expanded.[3] Despite high versatility, the reactions were slow and monosubstituted acetylenes lacked the regioselectivity to produce a mixture of 1,4-disubstituted 1,2,3-triazoles (1,4-DTs) and 1,5-disubstituted 1,2,3-triazoles (1,5-DTs) in almost equal ratios in most cases. In 2001, the usefulness of these reactions were revolutionized by applying Cu(I) catalyst in azide alkyne cycloaddition reactions which came to be known as Cu(I) catalyst azide alkyne cycloaddition or CuAAC.[4,5] The rate of the reaction was increased by a factor of 10^7 and exclusively 1,4-DTs were formed mostly at room temperature. Later, the Ru(II) catalyzed azide-alkyne cycloaddition (RuAAC) was introduced which afforded selectively 1,5-DTs although the reactions were much less efficient than CuAAC reactions (Scheme 1.1).[6]

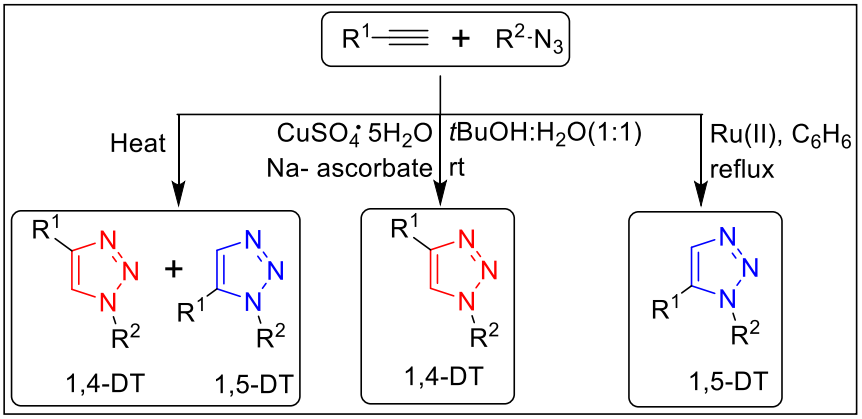

Scheme 1.1

1,2,3-Triazoles have several useful features like high chemical stability, aromatic character, strong dipole moments and hydrogen bonding ability. Some of these spectacular properties give a structural resemblance of 1,2,3-triazole unit with amide bond. Therefore, 1,5-DTs closely resemble a *cis*-configured amide bond, whereas 1,4-DTs mimic a *trans*-configured amide bond (Figure 1.1).[7] Because of the similarities with amide bonds 1,4-DT and 1,5-DT moieties are widely used as bioisosteres in biologically active molecules. 1,4-and 1,5-DTs, especially the 1,4-regioisomeric moiety are also used as "linkers" for the synthesis of hybrid organic molecules. Therefore, a large number of organic compounds containing 1,4 and 1,5-DTs possess a broad range of biological activities like antiviral, antimicrobial, anti-inflammatory, anticancer, antidiabetic etc.[8] This information has prompted researchers to incorporate more than one 1,4-DT moiety in several compounds. It should be noted that 1,4-DT moiety, because of its ease of synthesis, is used in overwhelming number.

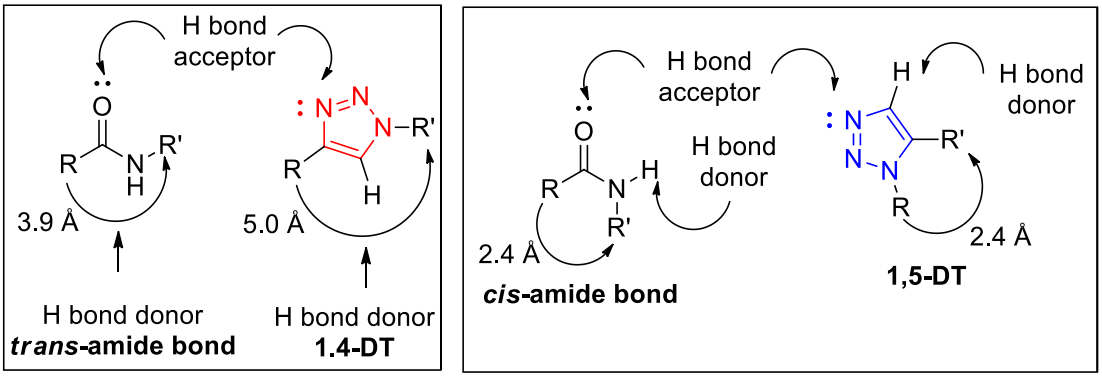

Figure 1.1

These oligotriazolylated compounds can be classified into two different catagories. In one case, triazole units are connected by a variety of functionalized organic molecules and in other case, one triazole unit is connected with another one by "*N-(CH)$_n$-C*" linkage to form triazole oligomer or triazolamer; a smaller fraction of the second class involves the use of natural amino acids [*N-CH(R)-C*]. This is not an exhaustive review article and monotriazoles are deliberately excluded almost all cases. Moreover, because of the research interests of the authors, special emphasis is given on the synthetic strategies of a variety of oligo-1,2,3-triazole based organic functional molecules. As mentioned above depending on the structural nature of the oligotriazoles, the molecules are summarised under two sections. Significant applications of the synthesized oligo-1,2,3-triazoles have also been highlighted directly after reporting the synthesis.

2. Oligotriazoles connected by situable building block

The diversity of oligotriazoles has been expanded by using more than one 1,2,3-triazole moieties connected by a variety of building blocks. These organic molecules are with aromatic and heteroaromatic motifs, carbohydrates, nucleoside analogues and in some cases acyclic compounds.[9] Generally, desired oligotriazoles can be prepared from various platform compounds bearing two or more clickable units (presence of two or more azide/alkyne unit) and triazoles were formed using a sequential conjugation strategy.[10] It was possible to react one particular molecule bearing two or more alkyne moieties selectively, with an organic azide by using a temporary masking group such as trialkylsilyl group.[11] However, platform molecules, such as diynes, diazides, triynes, and triazides containing either azido and alkyne component may lead to the generation of

multitriazoles.[10] In presence of anion, oligomers were shown to fold into ordered conformations in solution via non covalent interactions and resulted in the formation of anion templated foldamer, an interesting chemical entity.[12] A wide spectrum of potential applications are expected for oligo-1,2,3-triazole-based functional materials, such as supermolecules, fluorescence probes, and biological proteins.[13]

Several oligotriazoles were designed from a variety of organic polyazides and alkyne by 1,3-dipolar cycloaddition reaction. The aim of this study was to perform the reactions at lowest possible temperature using microwave irradiation or conventional method. It was observed that reactions took place at lower temperature (~50^{O}C) in case of alkyne substituted with electron withdrawing group. Thus the polyazides **2.1**-**2.12** were prepared using conventional methodologies. On the other hand several alkynes were also prepared. Reactions of **2.4** with ethyl propiolate under solvent-free microwave irradiation afforded a mixture of compounds. After repeated purifications a mixture of triazoles **2.19** was obtained with 80% purity. The tris-alkyne **2.18** on reactions with benzylazide afforded a mixture of regioisomeric triazoles; recrystallization afforded the major isomer **2.20** (Scheme 2.1). [14]

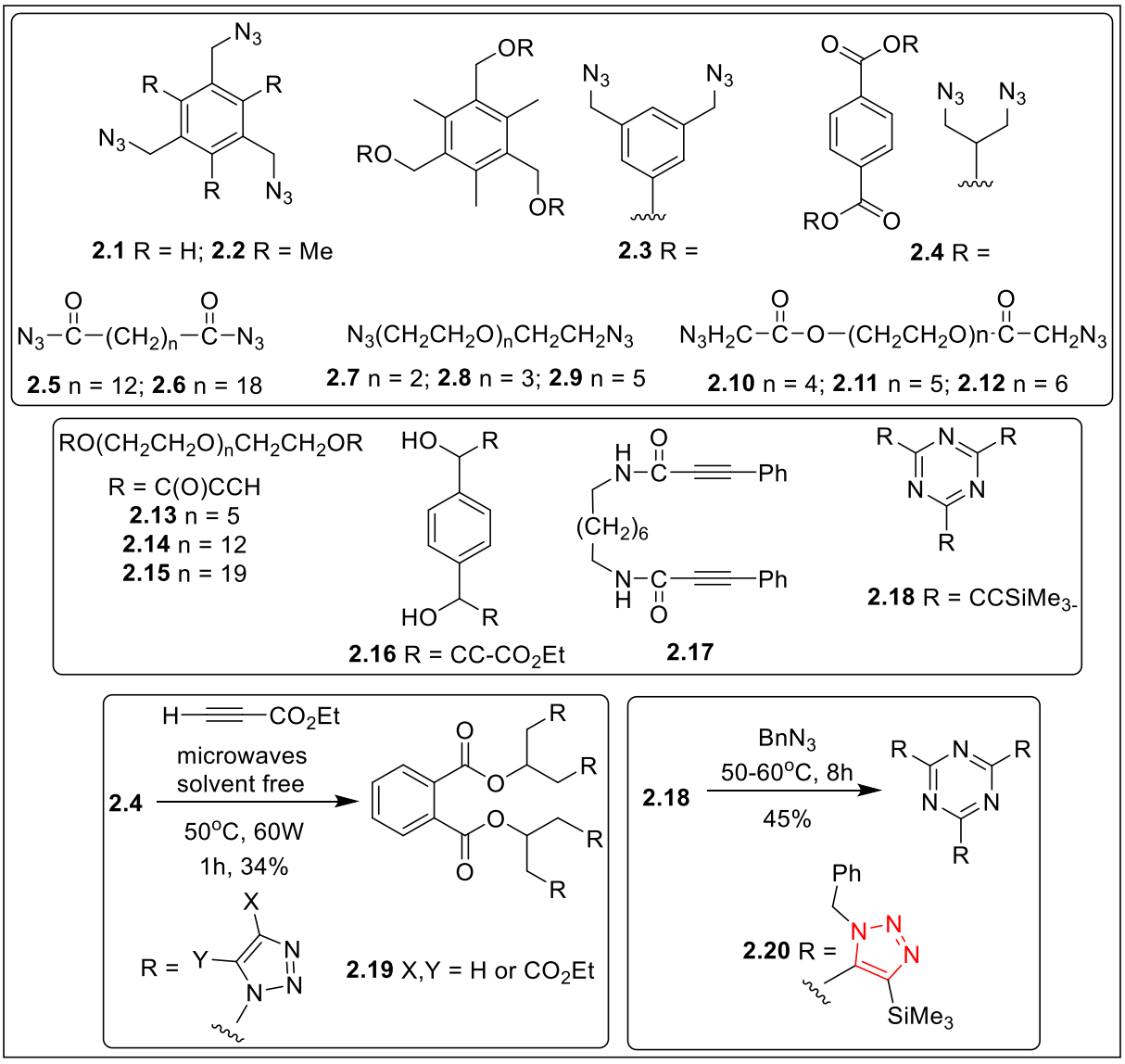

Scheme 2.1

The CuAAC strategy was utilized to couple an ethynyl α-*C*-mannoside and alkyl 6-azidoa-*C*-mannoside derivatives to generate a new class of 1,2,3-triazole linked (1,6)-α-D-oligomannoses or 1,4-DT linked triazolomannoses **2.24** (Scheme 2.2). Here, triazole moiety acted as stable and rigid linker between α-D-mannose units and resulted in the formation of linear oligomer with alternating triazole and mannose fragment upto triazolo pentamannose derivative. The orthogonally substituted ethynyl α-*C*-mannoside **2.21** and the ethyl methoxymethyl (MOM) protected alkyl 6-azido-α-C-mannoside **2.22** were chosen as the starting materials to afford triazolo-dimannose as a cycloadduct **2.23**; the free hydroxyl group of **2.21** on azidation afforded **2.24** which was coupled with **2.21** to get a trimer. The whole sequence of reactions was repeated to afford the protected pentamer **2.25**. Two steps deprotection generated the desired triazolo pentamannose **2.26** in overall good yield.[15] The synthetic strategy was extended further to synthesize 1,4-DT tethered 1,6-oligomannosides mimicking the cell wall constituents of *Micobacterium tuberculosis* which contains high oligomannose cores. The capping of 6-deoxymannose fragment in one side of the chain was necessary to make the oligomers stable to enzymatic degradation and unreactive to mannosyltransferase-promoted glycosylation, the key process for the *Mycobacterium tuberc*ulosis cell-wall biosynthesis.[16] Thus, the partially protected sugar alkyne **2.21** was deoxygenated to **2.27** and the latter was utilized for the synthesis of several C6 capped triazole-linked oigomannosides. Polyprenolphosphomannose (PPM)-dependent R-(1,6)-mannosyltransferases (from *Mycobacterium smegmatis)*, involved in the synthesis of the R-1,6-linked mannoside core present in the mycobacterial cell wall lipoarabinomannans, was targeted with these molecules; the highest activity (IC_{50} = 0.14-0.22 mM) was shown by the hexamannoside and octamannoside. Probably the 1,4-DT ring spacers contributed substantially to the overall length of these non-natural oligomannosides. Moreover, the triazole linkers did not disturb the molecular recognition properties toward these mycobacterial R-(1,6)-mannosyltransferases (Scheme 2.2).[17]

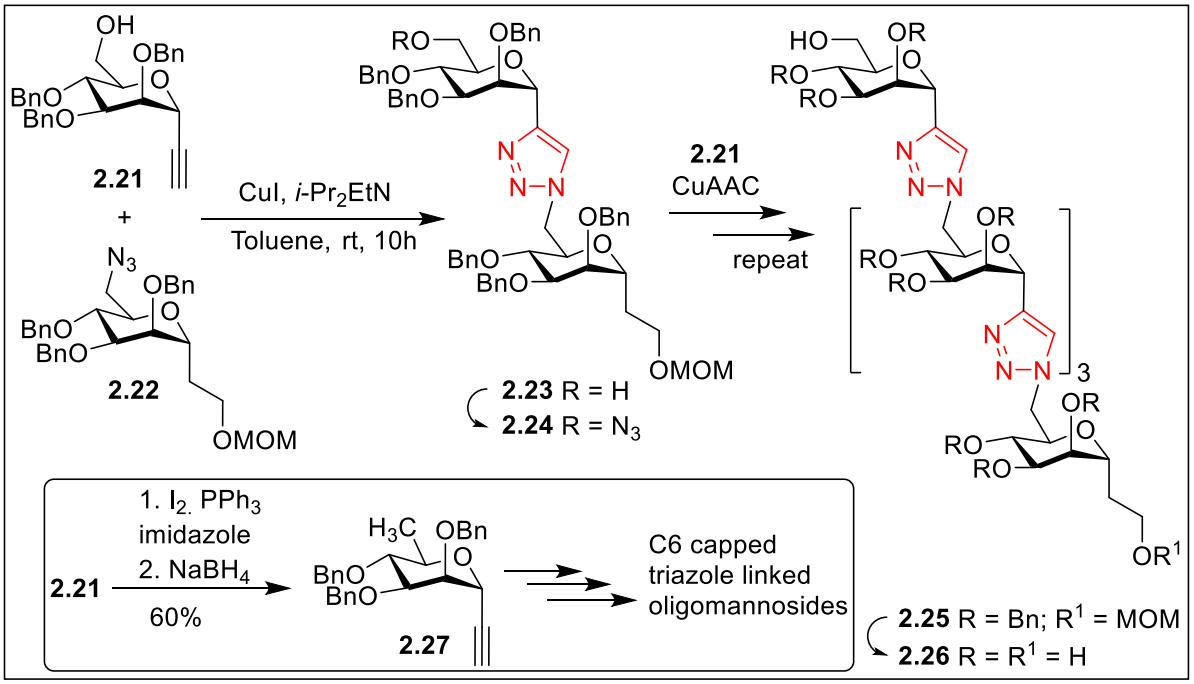

Scheme 2.2

It was expected that an oligomer like **2.32** (Scheme 2.3) would fold in a manner similar to other linear, flexible oligomers to generate a cavity. The electropositive C-H side of 1,4-DT would be involved in

intermolecular interaction(s) with a negatively charged guest anion. Synthetic strategy involved the conventional CuAAC method at an elevated temperature to couple the bisazido ester **2.28** with a monoalkyne **2.29a** or a bisalkyne **2.29b** in the presence of a catalytic amount of tris(benzyltriazolylmethyl)amine (TBTA). To increase the length of the oligomer, bistrazole **2.30b** was coupled further with azido ester **2.31** under similar conditions. The ^{1}H-NMR experiment established the existence of a 1:1 interaction between diaryl triazole **2.30** and chloride ions in acetone. The strength of the interaction (based on the binding constant values) increased with the increasing number of 1,4-DT groups in the oligomer and most importantly these effects triggered the folding of arylated 1,4-DT linked oligomers in solution and in the solid state (as shown in **2.33**). On the other hand, chloride ion containing molecules have better binding constant value in comparison to bromide and iodide.[18] Further studies established that fluoride ion catalyzed proton/deuteron exchange between the host triazoles and d_6-acetone in a process that was mediated by the formation of HF_2 (Scheme 2.3).[19]

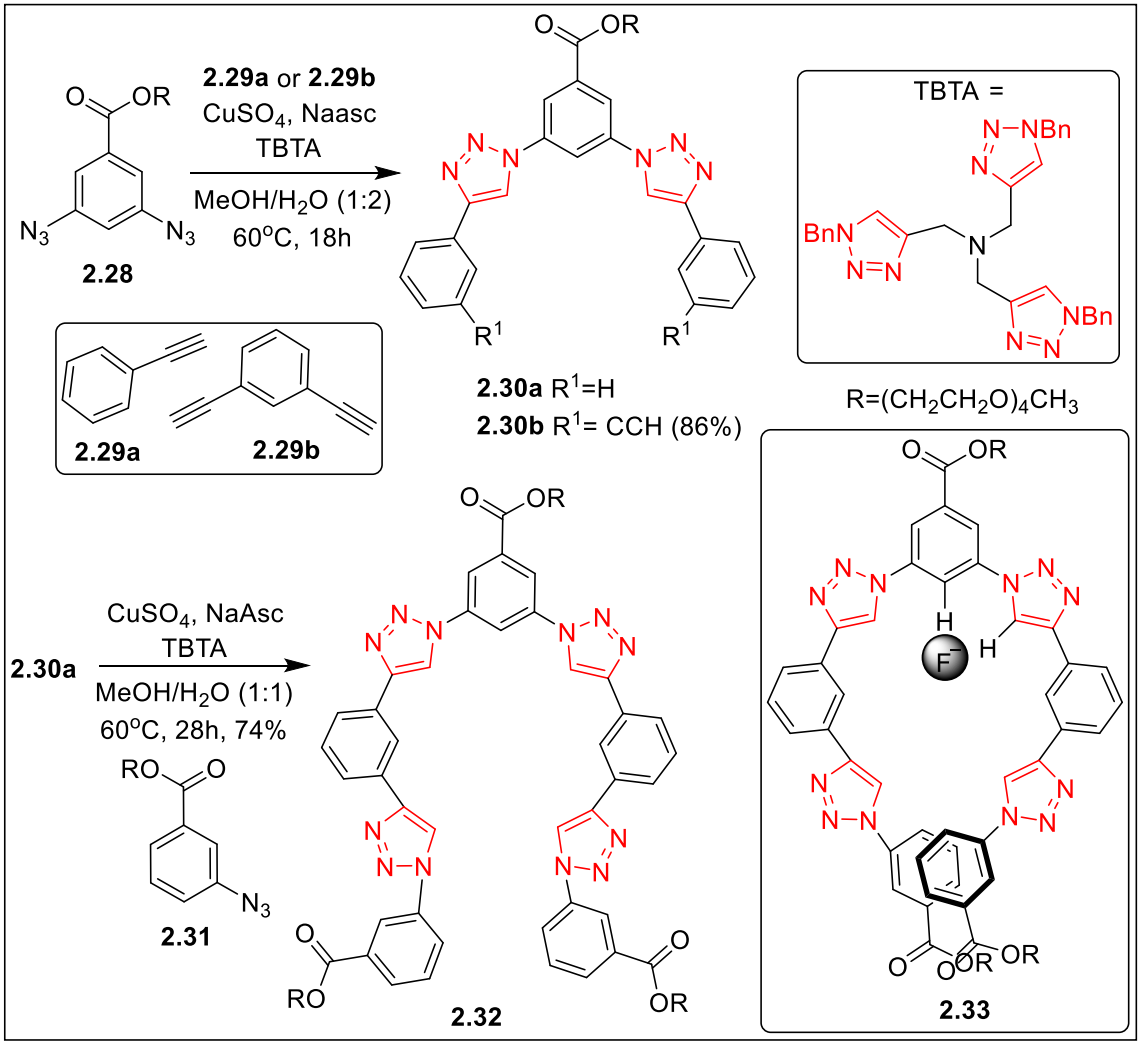

Scheme 2.3

1,2,3-Triazole unit emerged as a useful tool in polymer science. In order to synthesize hyperbranched polytriazole (*hb*-PTAs), A_2+B_3 route was established as an effective technique. Thus, the diazide **2.34** and triyne **2.35** were chosen as monomers, which were free of self-oligomerization concerns. Thermal reaction afforded a mixture of 1,4-/1,5-PTA linked polymers; CuAAC reaction afforded the soluble *hb*-1,4-PTA, whereas, RuAAC

based click polymerizations furnished the desired *hb*-1,5-PTA in good yields. The *hb*-1,4-PTA, and *hb*-1,5-PTA are soluble and formed films. By irradiating 1.4-/1,5-PTA, *hb*-1,4-PTA and *hb*-1,5-PTA films, fluorescent images were generated with white, blue and yellow emissions respectively. The important outcome of this study was that the emission colour of a polymer film was tuned by simply changing the reaction conditions to generate different regioisomeric polymers rather than synthesizing new polymers with different starting materials (Scheme 2.4).[20]

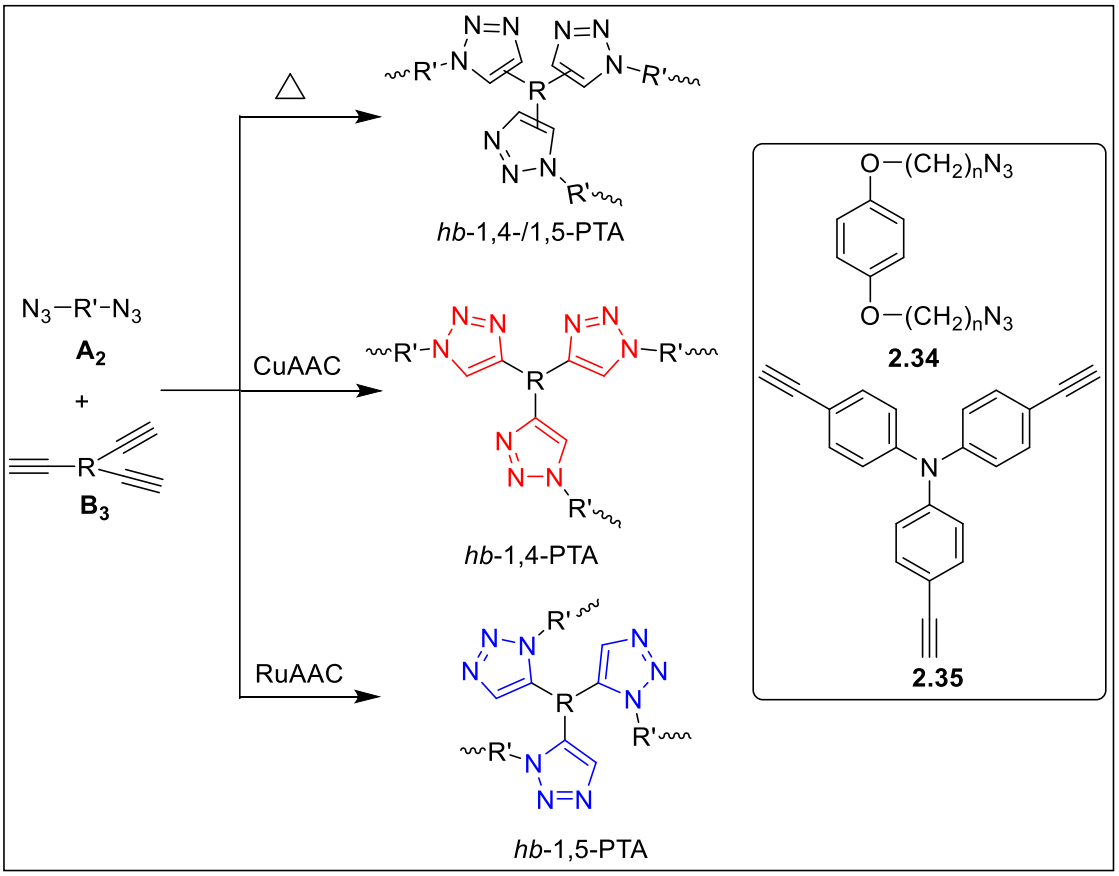

Scheme 2.4

In order to study folding and aggregation of cationic oligo(aryl-triazole)s in aqueous solution a new family of 1,4-DT linked aryl based cationic oligomers with different chain lengths, compounds **2.41a-c**, were synthesized using click chemistry (Scheme 2.5). Judiciously functionalized monomer **2.36** with TMS "protected" alkyne and an azido group was reacted with **2.37** with a reactive alkyne; the 3-amino group was useful for the post-coupling generation of azido function to afford the 1,4-DT **2.38**. Different reaction conditions were applied to **2.40** (2.38) to generate two reactive dimers, the alkyne **2.39a** and the azido **2.39b** which were coupled again under CuAAC conditions to afford the bistriazolylated trimer **2.40**. The strategy was reapeated to generate a tetramer and a pentamer. Finally, the Boc group was removed from all three products using trifluoroacetic acid to generate the oligomers **2.41a-c** with the cationic amide linkages. These cationic oligo(*m*-phenylene-1,2,3-triazole)s were designed in such a way that they folded into a helical conformation in water/methanol mixture. The foldamers imparted a concentration dependent self-assembly nature in both water/methanol mixtures and pure water. The formation of helical structure and aggregation behaviour were determined by chain length. Circular dichroism spectroscopy and dynamic light scattering experiments

revealed that oligotriazoles formed aggregates with sizes in the range from 100 to 500 nm. Foldamers had the ability to recognize chloride and fluoride anions in aqueous solution through the internal cavity in the mixture of water/methanol (75:25 v/v). This binding was effective to prevent the aggregation of the foldamers (Scheme 2.5).[21]

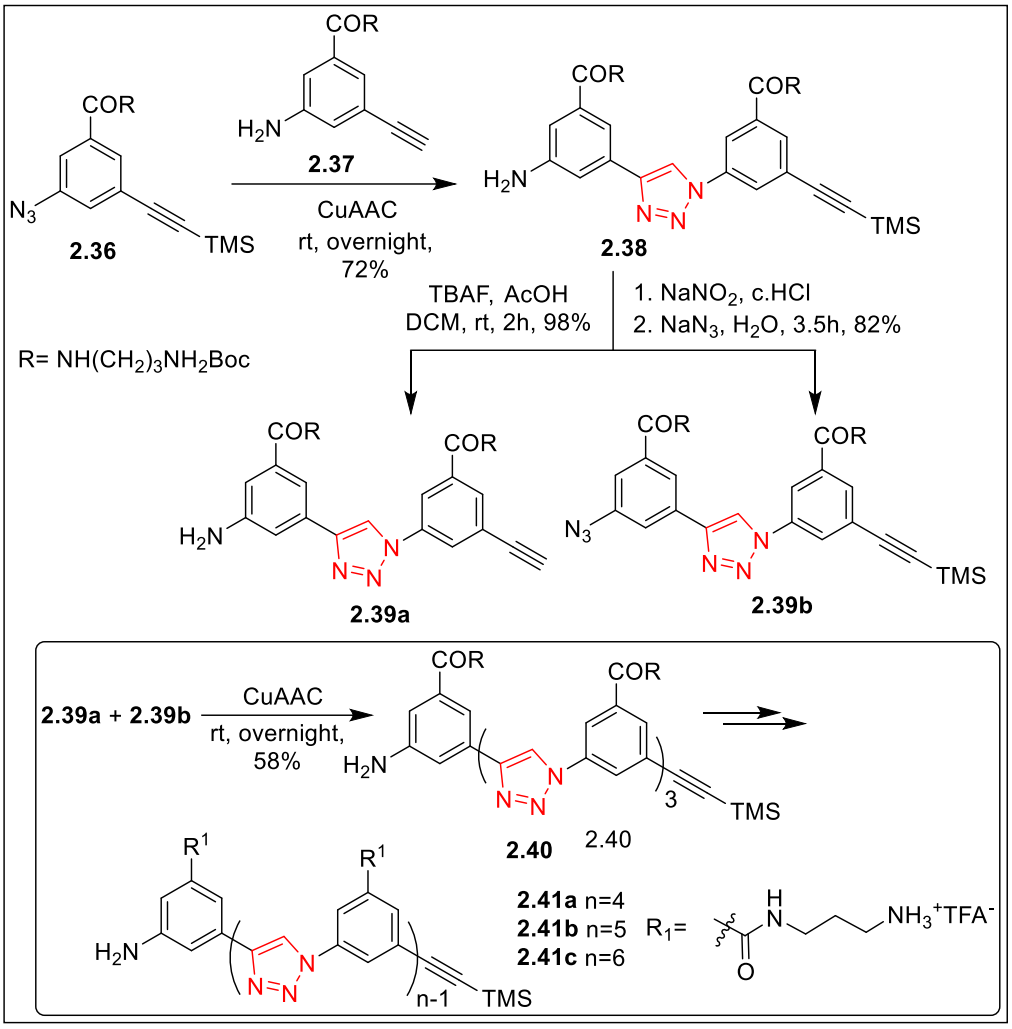

Scheme 2.5

1,4-DT linked nucleoside trimer was synthesized using CuAAC strategy. The required nucleoside alkynes **2.43** and **2.45** were prepared from the corresponding aldehydes **2.42a** and **2.44** respectively using Bestmann reagent. The desired azido nucleosides **2.46a** and **2.46b** were easily synthesized using standard protocols. 3'-Alkyne nucleoside **2.43** and 5'-azidothymidine **2.46a** were coupled in 36h to get a dinucleoside **2.47**. On the other hand, 5'-alkyne nucleoside **2.43** and 3'-azidothymidine **2.46b** under similar conditions afforded the isomeric dimer **2.48**. The free 5'-hydroxyl group of **2.48** was oxidized and the aldehyde group was converted to the alkyne functionalized dimer **2.49**. The 3'-azido-3'-deoxythymidine **2.42b** under CuAAC conditions afforded the trinucleoside **2.50** (Scheme 2.6).[22] One and two units of T-triazole-T **2.48** were introduced in a natural oligonucleotide T12 and the melting temperatures with a complementary deoxyadenosine sequence were determined. A decrease in stability of 10°C per modification led to the conclusion that these 1,4-DT-thymidine hybrids were not suitable for antisense strategy. The length of the triazoles spacers was probably shorter than

the natural phosphodiester linkage which contributed to the decrease of melting temperatures. (Scheme 2.6).[23]

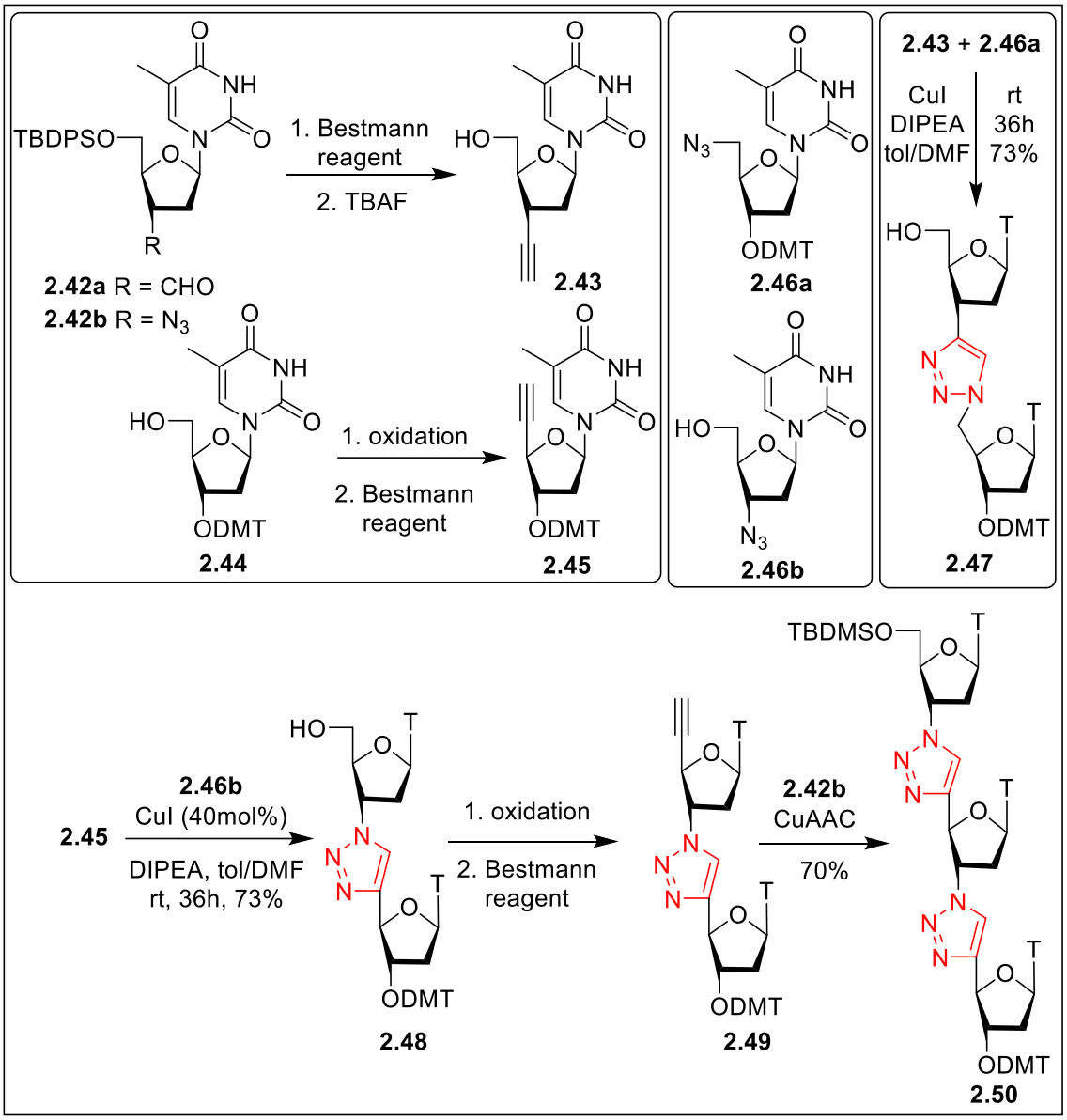

Scheme 2.6

The model system of dicarboxylic acid functionalized 1,4-DT-terminated alkyl oligomers is represented as a new chemical entity for obtaining high proton conductivity in proton solvating heterocycles. The model compounds **2.52a-c** were synthesized by 1,3-dipolar cycloaddition reaction of diazido derivative **2.51** with acetylene dicarboxylic acid. From, thermogravimetric analysis it was observed that the samples were thermally stable up to 150 ˚C. Differential scanning calorimetry revealed the crystalline nature of the organic electrolytes. The spacer length showed significant influence on conductivity and the maximum conductivity of about 10^{-5} S/cm was recorded at 130˚C for $(CH_2)_6$-bis-TriA **2.52b** (n=6) system in pure and dry state (Scheme 2.7).[24]

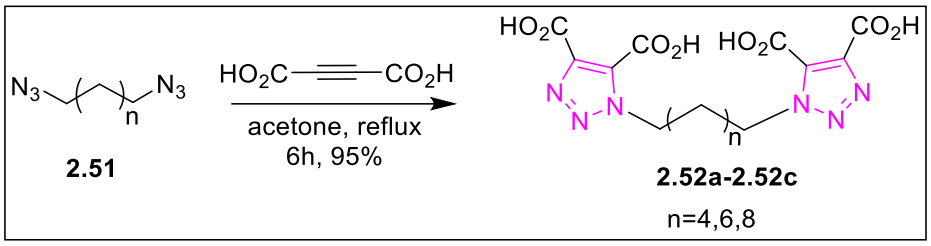

Scheme 2.7

A 1,4-linked hybrid triazole/amide macrocycle was designed by cyclooligomerization of a chiral pseudo dipeptide derived from furanoid sugar molecules. The conformation of this macrocycle resembles the D-L-α amino acid based cyclic peptide with identical backbone chirality. The key intermediate for the synthesis of peptide macrocycle **2.58** is the 1,2,3-triazole di-β-peptide isostere **2.55**, which was readily synthesized from cis-furanoid homopropargyl sugar amine **2.54**, and cis-furanoid azido ester **2.53** via CuAAC reaction (**2.55** → **2.56a,b** → **2.57** → **2.58a,b**). Structures **2.58a** and **2.58b** represent two rotamers of the pseudo cyclic β-peptide. Macrocycle imparts a unique behaviour of self-assembly through an antiparallel backbone to backbone intermolecular H-bonding involving amide NH and triazole N2/N3 as well as parallel stacking via amide NH and carbonyl oxygen H-bonding, leading to the formation of a tubular nanostructure (Scheme 2.8).[25] The library of bis-1,2,3-triazole containing isothiazolidine-1,1-dioxide was reported using a one-pot click/aza-Michael protocol. Here, the building block N-propargylated dihydroisothiazole 1,1-dioxide scaffold **2.59** was prepared rapidly on multigram scale. This compound was subjected to bis-click/aza-Michael in presence to generate a 180-triazole-containing isothiazole 1,1-dioxide library as represented by **2.60**. All 180 compounds were prepared, with 167 possessing >90% final purity (Scheme 2.9).[26]

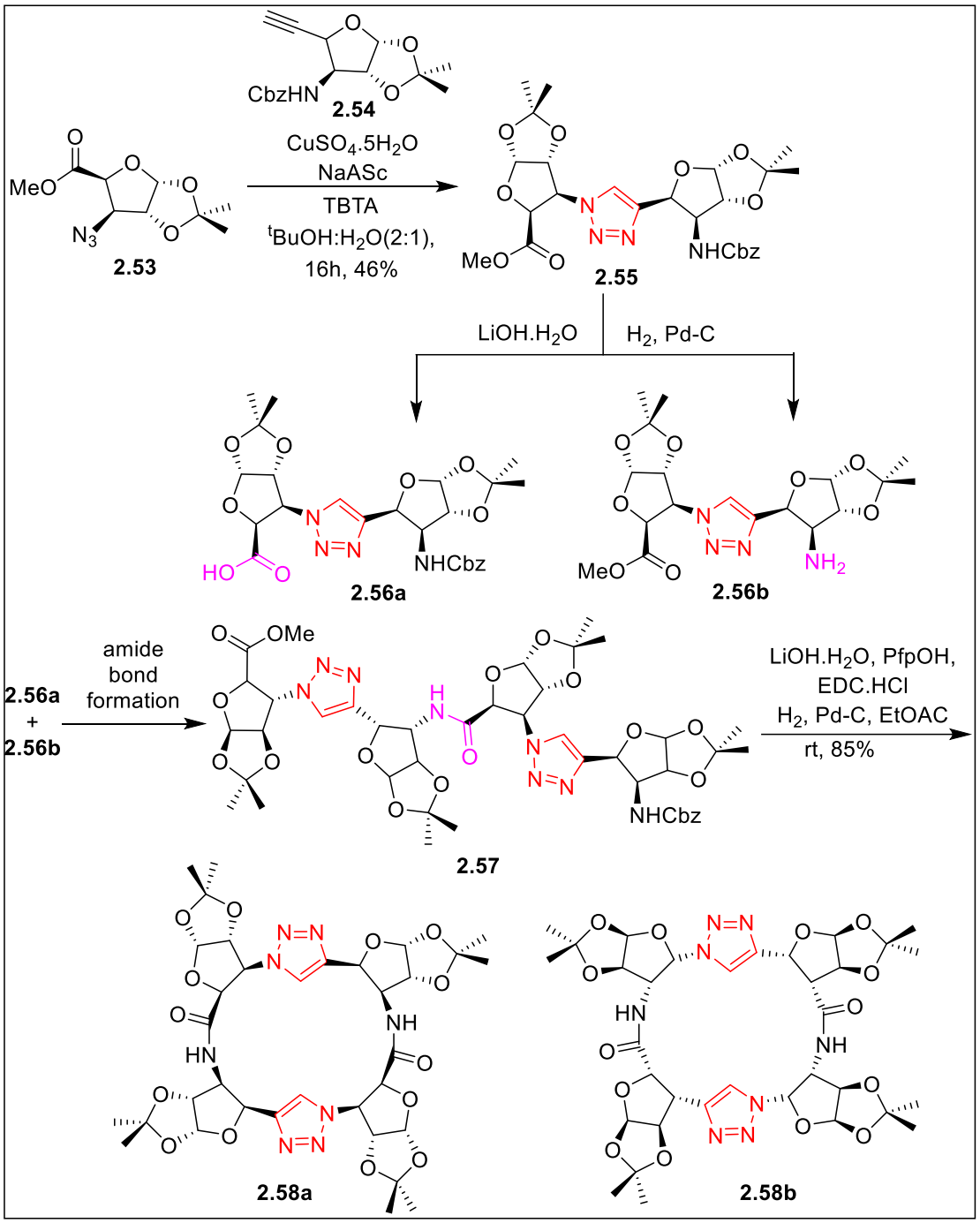

Scheme 2.8

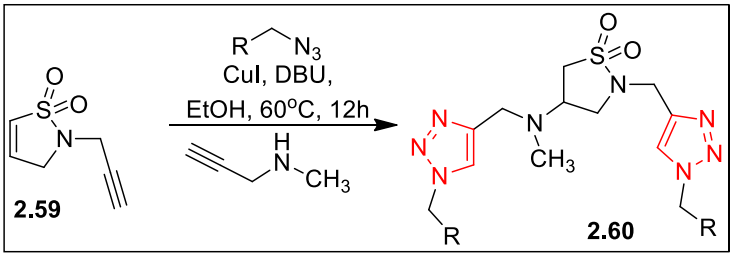

Scheme 2.9

1,4-DT was used linking the 6-thiopurine building block with CH_2CO_2R functionality. Thus bispropargylated thiopurine **2.61** was reacted with azidoacetic acid under CuAAC conditions to generate the bistriazolylated derivative **2.62**. Compound **2.62** exhibited potential antimalarial activity and it was found to be equipotent with standard reference chloroquine at same dosage. The monotriazolyl derivatives **2.63** and **2.64** also showed similar biological activities. These compounds also exhibited antileishmanial activities (Scheme 2.10).[27]

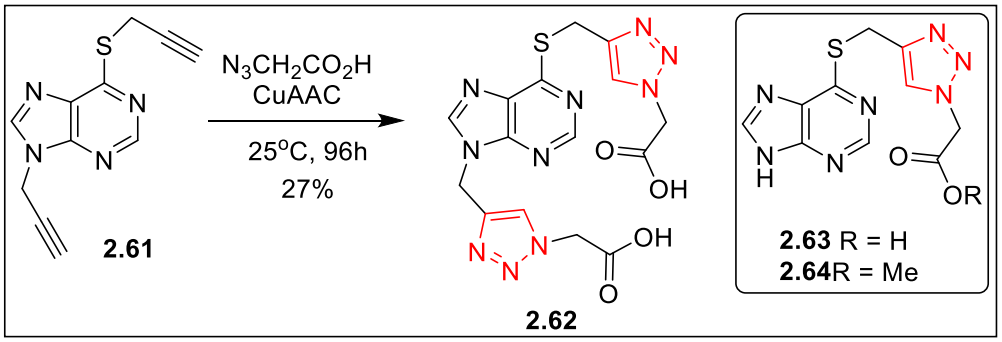

Scheme 2.10

In order to generate conformationally restricted molecular architectures various 1,4-DT-based foldamers with adjacent heteroatom substituents were designed and studied. For example, bisalkynyl pyridyl compound **2.65** (Scheme 2.11) was coupled with *meta*- azidofluorobenzene **2.66** to generate the bistriazolylated architecture **2.67**. In this type of model compound, the 2,6-bis(1-aryl-1,2,3-triazol-4-yl)pyridine core showed a horse-shoe like structure. Several other motifs such as **2.68**, **2.69** were also thoroughly studied. In general, the results showed that the presence of N-, O-, and F-substituents induced rotational constraints around the single bonds attached to the 1- and 4-positions of the 1,2,3-triazoles. Therefore, this study provides a kind of foldamer construction kit, which should enable the design of various clickamers with specific shape and incorporated functionality (Scheme 2.11).

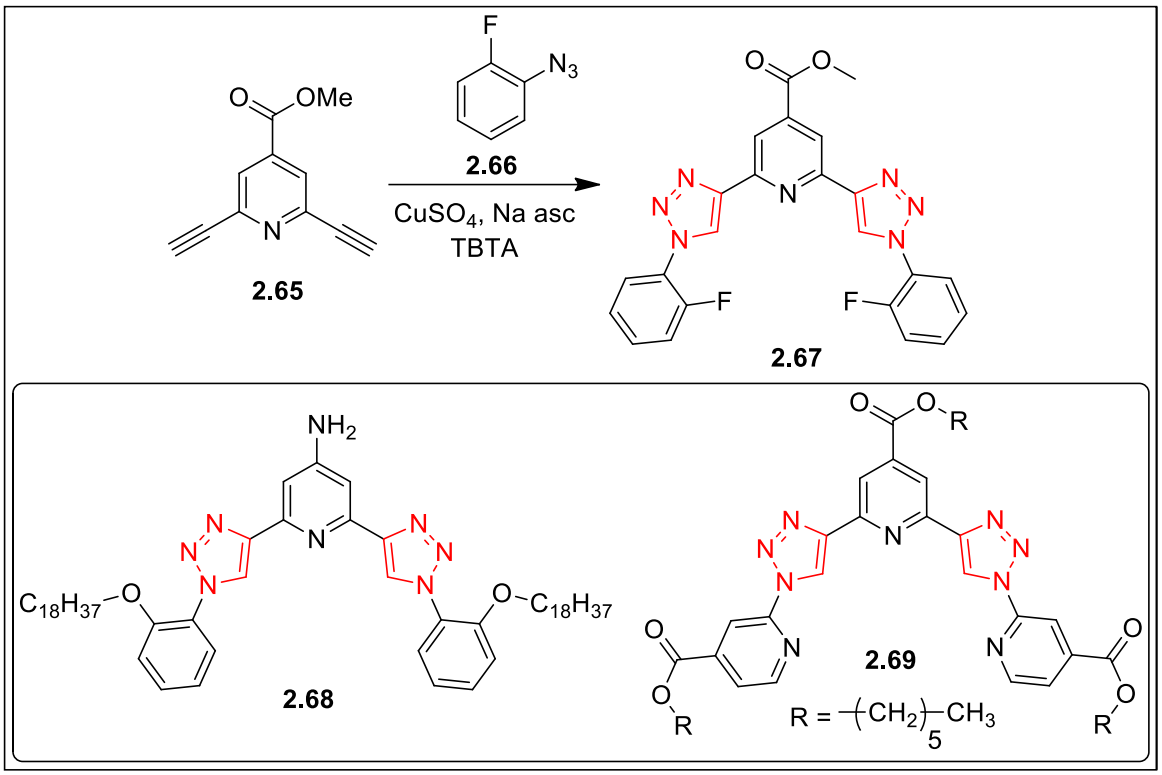

Scheme 2.11

A 1,2,3-triazole linked mannooligomer **2.72** (Scheme 2.12) was synthesized by coupling the suitably propargylated bismannoside **2.70** with α-D-mannopyranosyl azide **2.71** under microwave irradiation. Debenzylation and hydroxylation of the anomeric carbon of **2.72** afforded the pseudo-Man_8 **2.73** in excellent yield. Although the original Man_8, which binds to mannose-specific lectin concanavalin A (Con-A) is made of eight mannose units, the mannooligomer **2.73** with only five mannose units was compared with Man_8 activity. Thus the binding affinity of **2.73** towards concanavalin A was strikingly similar to that of natural Man_8. The new compound also compared favourably with other Con A-binding ''click'' clusters reported so far (Scheme 2.12).[29]

A series of β-lactam-bis(triazole-quinoline) bifunctional hybrids **2.76** (Scheme 2.13) were synthesized by coupling bisalkyne **2.74** with azidochoroquine **2.75** using click chemistry and their antimalarial activity was evaluated. it was envisaged that the combination of two intrinsically antimalarial moieties, 7-chloroquinoline and a β-lactam linked via a triazole would result in the development of potent antimalarials. Compound **2.76** (R = p-C_6H_4-F) was the most potent (IC_{50}= 1.1 µM) in this series and bis triazolylated compound fared better than their mono triazolylated analogues. The experimentally observed activities were justified by docking the compounds with of *Plasmodium falciparum* dihydrofolate reductase, a potential target for anti-malarial compounds (Scheme 2.13).[30]

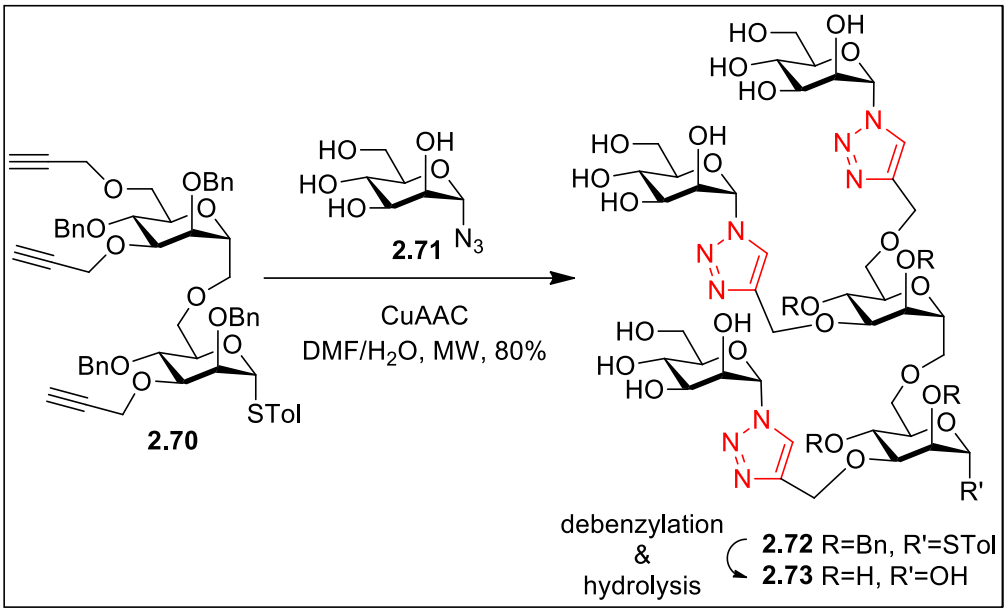

Scheme 2.12

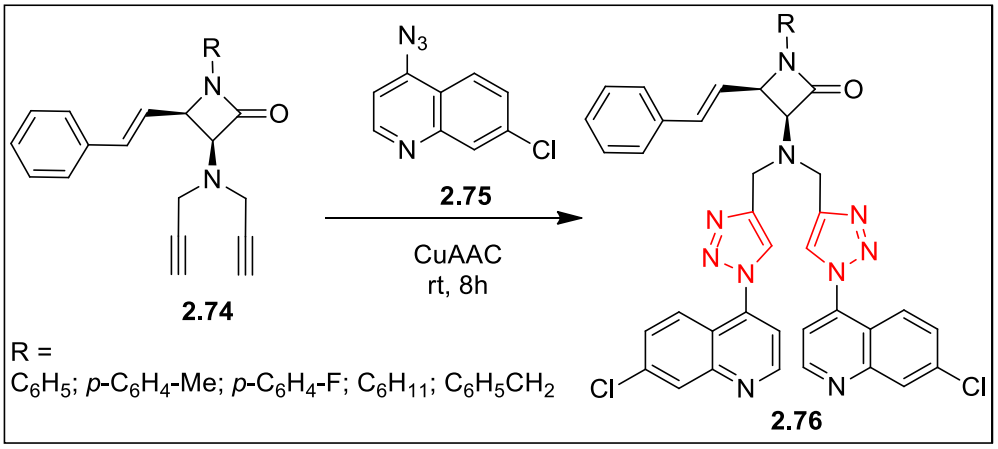

Scheme 2.13

1,4-Dibromobenzene **2.77**, 2-ethynylthiophene **2.78** (Scheme 2.14) and sodium azide were reacted under CuAAC conditions to afford the disubstituted product **2.79** with the in situ generation of 1,4-diazidobenzene. This combination was expected to generate a donor–acceptor–donor model in which, thiophene moieties acted as donor and 1,4-DT as acceptor units. In general, a weak electronic conjugation of 1,2,3-triazole ring was observed from spectroscopic and redox properties (Scheme 2.14).[31]

Intramolecular triazolyl C-H···O hydrogen bonding has been utilized to create new aromatic triazole foldamers. Several smaller units were studied (Scheme 2.15A) and the geometry of the crystals of two model compounds suggested that oligomers with eight repeated triazole units would give rise to one turn; this turn was expected to produce a cavity (approximately 1.8 nm in diameter). Thus, this example (and many others reported in the paper) demonstrated that intramolecular C-H···O hydrogen bonding can be utilized to induce aromatic 1,2,3-triazole oligomers to form folded and helical secondary structures. For a selective example of the synthesis, the bistriazol derivative **2.80** was converted to the corresponding bisalkyne compound **2.81** in three steps. The

pyrene functionalized alkyne **2.82** was reacted selectively with one of the azido groups of the bisazide **2.83** to obtain a monotriazole **2.84**. The CuAAC reaction between one equivalent of the alkyne unit **2.81** with two equivalents of the azido derivative **2.82** afforded the foldamer **2.85** (Scheme 2.15A).[32]

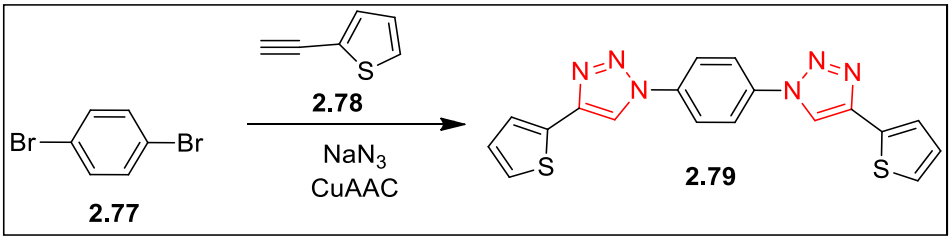

Scheme 2.14

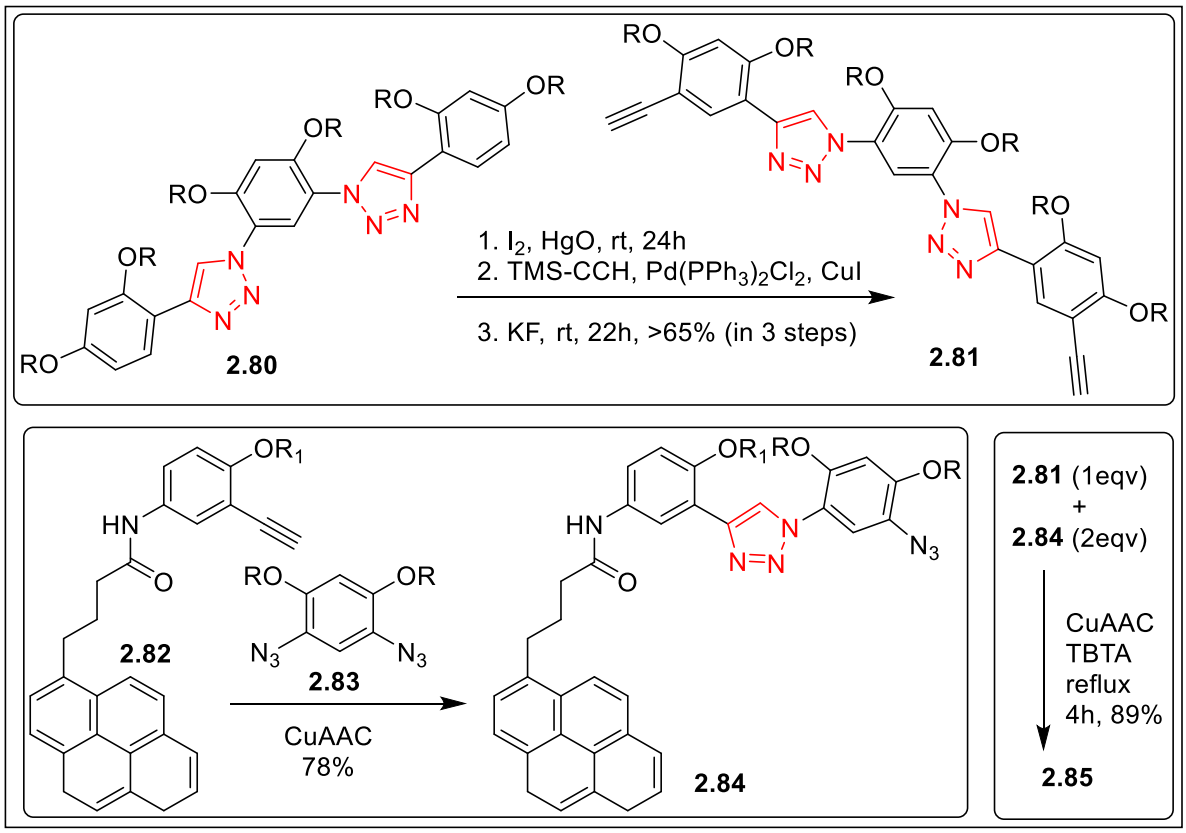

Scheme 2.15A

All the triazole units of the new foldamers are positioned inward to form a cavity which could accommodate a tridentate organohalogen guests. The addition of 1 equivalent of the foldamer **2.85** to a solution of **2.86** (10 mM) in dichloromethane caused the CF_2 signal of **2.86** in the ^{19}F NMR spectrum to shift upfield (Scheme 2.15B). The addition of **2.86** to the dichloromethane solution of **2.85** caused its excimer emission to increase. The resulting 1:1 complexes are remarkably stable as a result of the cooperativity of the formed halogen bonds and the complexation further stabilized the folded state of **2.85**. Both observations indicated that the foldamer **2.85** complexed the organohalogens as shown in the host-guest complex **2.85-2.86** (Scheme 2.15B).

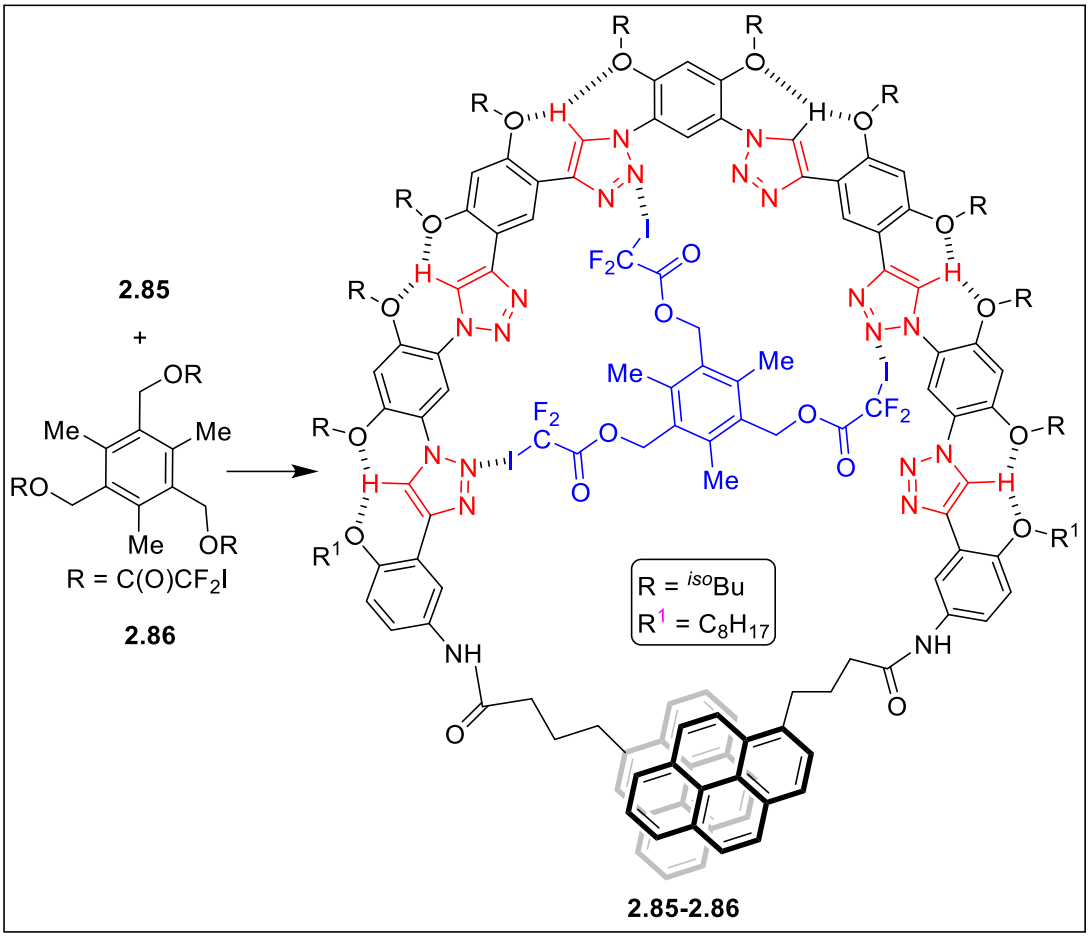

Scheme 2.15B

The same group of researches, designed a series of 1,2,3-triazole oligomers containing two, four, six and eight triazole units where triazole rings were connected by 4,6-difluoro-*meta* phenylene linker(s). In this case, the intramolecular C–H···F hydrogen bonding was utilized to induce conjugated 1,2,3-triazole oligomers to form folded or helical secondary structures (Scheme 2.16). Thus, the azide **2.87**, the bisalkyne **2.88** and the terminal azido compound **2.89** were combined in various orders under CuAAC conditions to afford the smaller or the larger oligomers (as in **2.90**). Two triphenylmethyl groups were appended at the ends of the backbones to suppress the stacking of the backbones which also increased solubility. NMR and X-ray experiments established that the 1,4-DT units exhibited folded or helical conformations due to the formation of continuous three-centred C–H···F intramolecular hydrogen bonding. In this case also, the theoretical calculations revealed that the longest 8-mer foldamer could form a one-turn helical cavity with a diameter of ca. 1.7 nm. The intramolecular C–H···F hydrogen bonding was more stable than the well-established intermolecular C–H···X– (X = Cl and I) hydrogen bonding (Scheme 2.16).[33]

A homologous series of oligo(amide–triazole)s (such as **2.92;** Scheme 2.17) were synthesized using CuAAC method from an orthogonally functionalized azido-alkyne **2.91**. The self-assembly and organogelating properties of the synthesized compounds were also studied. It was observed that their self-assembly and gelation strength depended on the number of hydrogen-bonding moieties in the oligomers. Beyond a threshold number of the CONH hydrogen-bonding units, above which all the oligomers were organogelating. Hence, at a concentration of 2.5% w/v in aromatic solvents, oligomers with more than 4 CONH units were all

organogelators, and the Tgel value increased monotonically with increasing number of primary amide units. Finally, it was concluded that oligomers with different numbers of hydrogen-bonding units exhibited self-sorting to maximize the enthaplic and entropic gains during the self-assembly process (Scheme 2.17).[34]

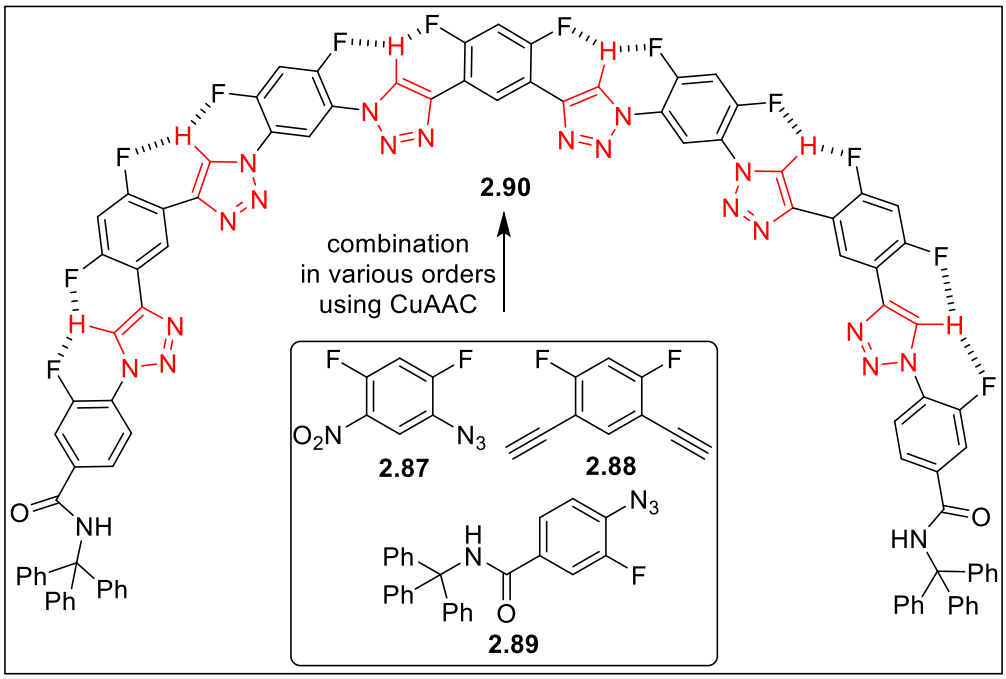

Scheme 2.16

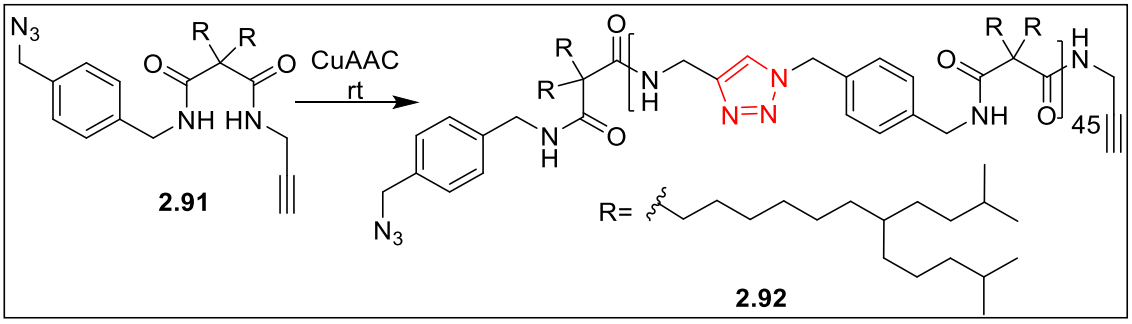

Scheme 2.17

4-(Bromomethyl)benzaldehyde **2.93** (Scheme 2.18) was reacted with pyrrole followed by azide substitution of the resulting bromoporphyrins (not shown) and subsequent zinc metallation afforded **2.94**. Different alkynes (e.g. $MeC(O)OCH_2CCH$) were reacted with the tetraazide **2.94** to afford the triazolylated porphyrine **2.95**. Thus, the efficient "click" synthesis and self-assembly of AB_2- and AB_4-type multitopic porphyrin–polymer conjugates were prepared which consisted of linear polystyrene, poly(butyl acrylate), or poly(-*tert*-butyl acrylate) arms attached to a zinc(II) porphyrin core via triazole linkages. The 1,4-DTs helped to direct the self-assembly of the PPCs into short oligomers via intermolecular porphyrinatozinc–triazole coordination. The modular synthesis and tunable self-assembly of the triazole-linked PPCs represent a supramolecular platform for building functional nanostructured materials (Scheme 2.18).[35]

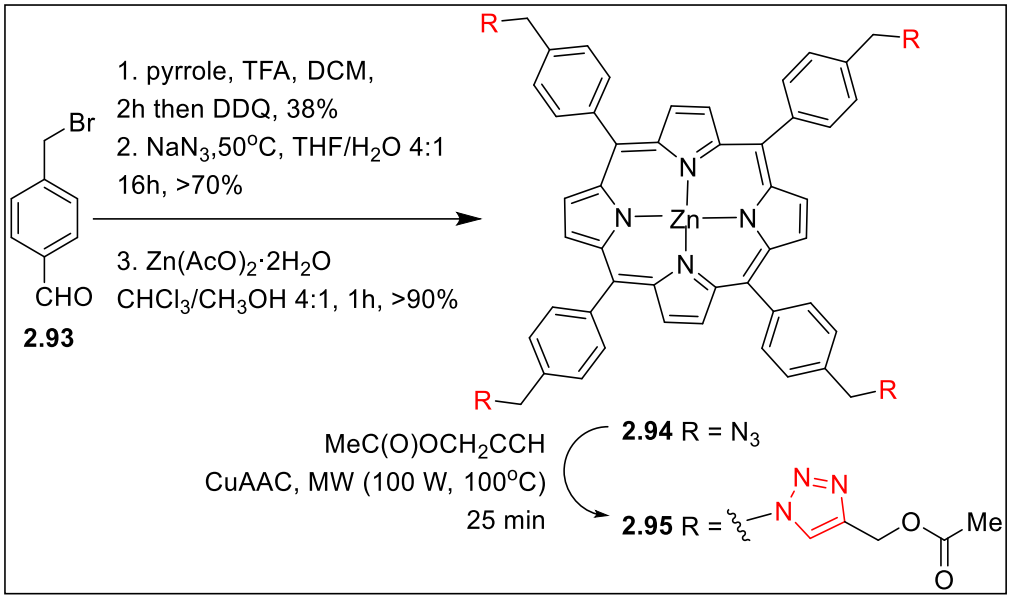

Scheme 2.18

Fluorine- and chlorine- substituted aryl-triazole oligomers were designed and synthesized using click chemistry. For example, the bisazide **2.96**, the bisalkyne **2.97** and the terminal azido compound **2.98** were combined in various orders under CuAAC conditions to afford the oligomers **2.99** (Scheme 2.19). Crystal structure ananlysis and NMR experiments established that the oligomers folded into stable helical conformation, which were induced by C5−H···X−C (X = F, Cl) intramolecular hydrogen bonding between triazole protons and halogen atoms. DFT calculations indicated the large energy differences between their folded and unfolded states, which determined their strong conformational preferences. The hydrogen-bonding networks were disrupted in solvents like DMSO where competitive H-bonding generated the unfolded oligomers (Scheme 2.19).[36]

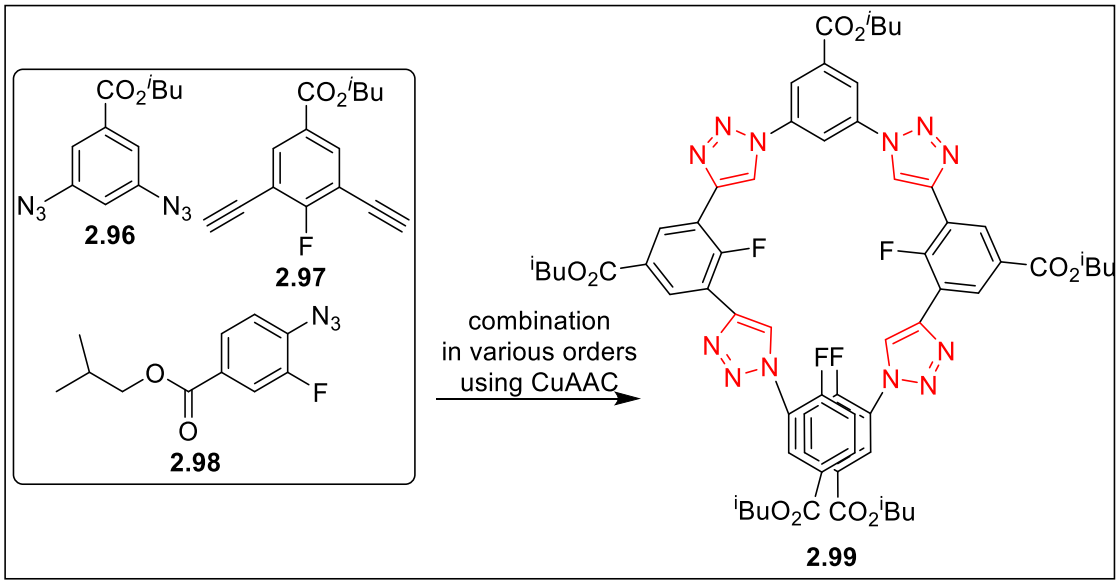

Scheme 2.19

Aryl triazole oligomer with two long C_{18} alkyl tails have been synthesized by coupling bisalkyne **2.100** and the azide(s) **2.101** to afford bistriazoles **2.102**-**2.104** (Scheme 2.20). Bi-phasic 2D monolayers were generated in the self-assembly of these oligomers at the solution-graphite interface bearing two long C18 alkyl tails and a large 16 debye molecular dipole. An important result of this study was the application of synthetic design strategies to search for a bi-phasic behavior in 2D self-assembly. Scanning tunnelling microscopy experiment determined the packing and structure of two principle phases, α and β. The bi-phasic behavior was explined as a balance between electrostatic interactions and van der Waals contacts. These findings were expected to be helpful in designing environmentally responsive 2D supramolecular arrays (Scheme 2.20).[37]

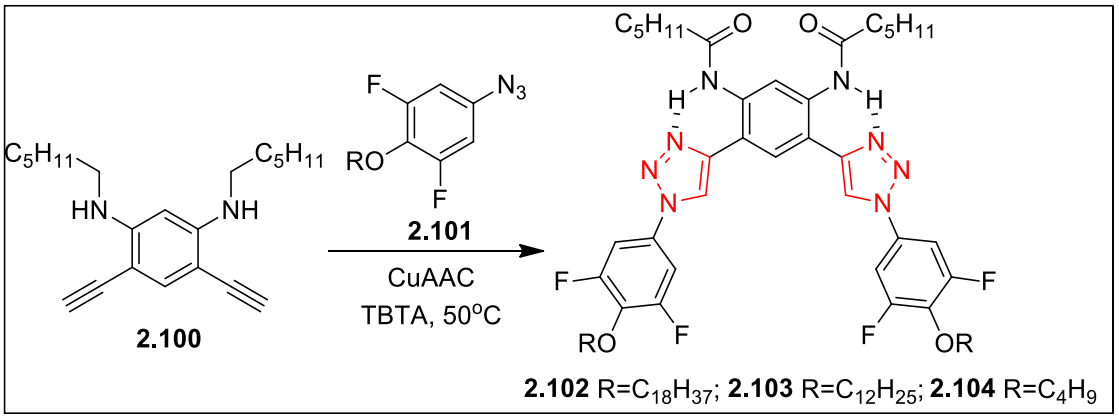

Scheme 2.20

In order to access 1,2,3-triazolium-based poly(ionic liquid)s the polymer **2.105** and 6-(2-azidoethoxy) coumarin **2.106** was reacted in the presence of $CuIP(OEt)_3$ and diisopropylethyl amine in DMF to afford functionalized poly(ionic liquid) **2.107**. Several other varieties of functional groups were introduced by reacting **2.105** with other organic moieties under CuAAC conditions (Scheme 2.21).[38]

An azido-alkyne-functionalized galactose building block **2.108** carrying the azidoethyleneglycol moiety under various CuAAC conditions afforded linear oligomers and sevral cyclic oligomers (such as **2.109a**). Spontaneous cyclization, on the other hand, generated a mixture of compounds where both 1,4-DT (such as **2.109b**) and 1,5-DT (such as **2.109c**) residues were incorporated in the ring and several 1,4-DT and 1,5-DT linked linear oligomers (Scheme 2.22). The flexible ethyleneglycol based linker resulted in the random formation of mixed population of linear and cyclic triazole-linked oligomers. Although the method had very little synthetic utility, the cyclic compounds were separable from each other and from the corresponding linear materials. Triazole linked cyclic oligomeric compound were tested for their ability to act as substrate for *Trypanosoma cruzi trans*-sialidase (TcTS) and demonstrated their potential activity against the parasite (Scheme 2.22).[39]

In continuation with related search for novel structures of foldamers mentioned above, aryl-triazole oligomers (such as, **2.113**) based on pyridinium moiety were designed from diazide **2.111** and bisalkyne-pyridine **2.110** precursors; the monoazide **2.112** was chosen for the terminal ends. Alkylation of pyridine unit helped in increasing the anion binding properties of oligo(phenyl-triazole-pyridine)s. It was observed that the resulting foldamers bound halides strongly in 6:94 (v/v) D_2O/pyridine-d_5 (Scheme 2.23).[40]

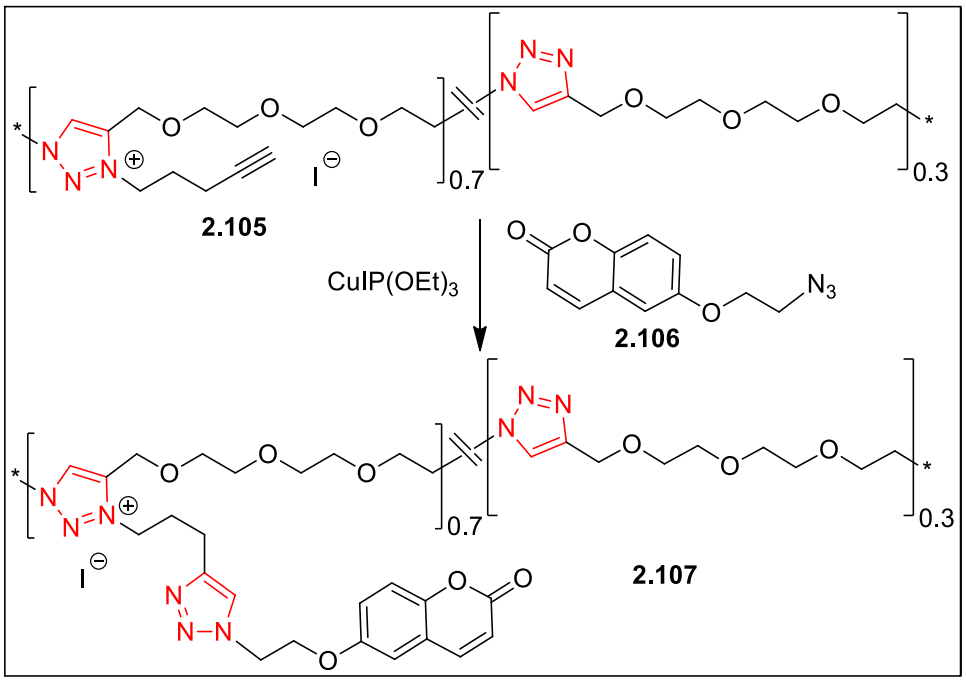

Scheme 2.21

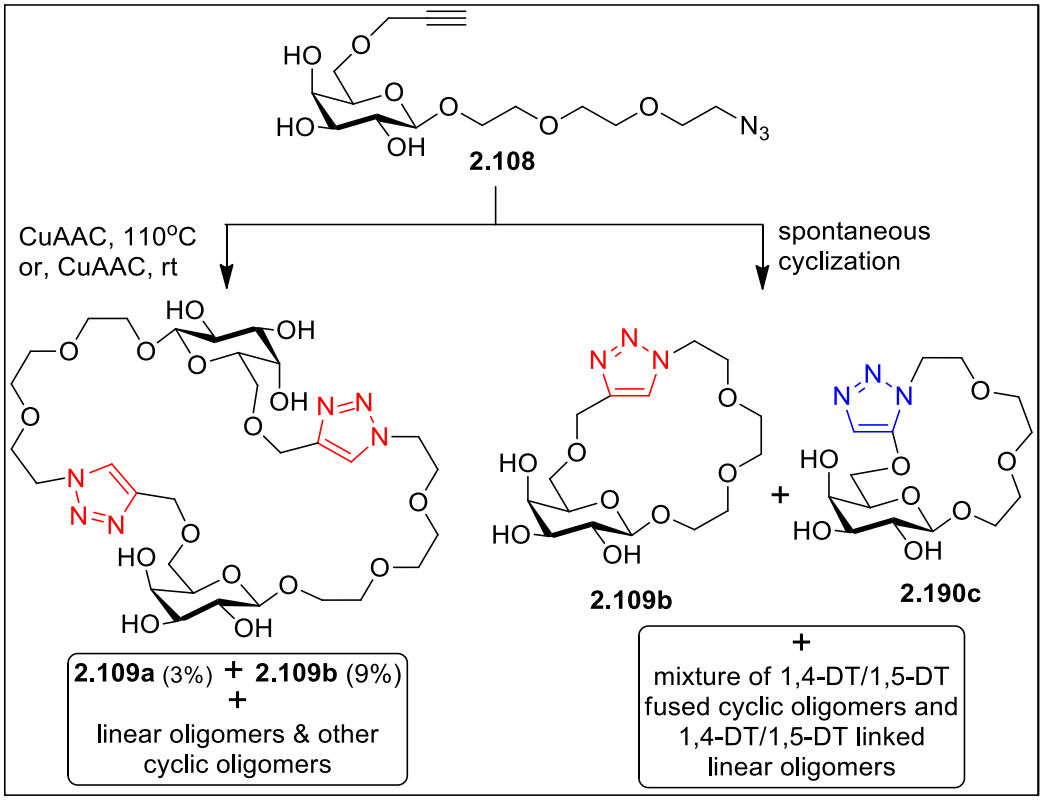

Scheme 2.22

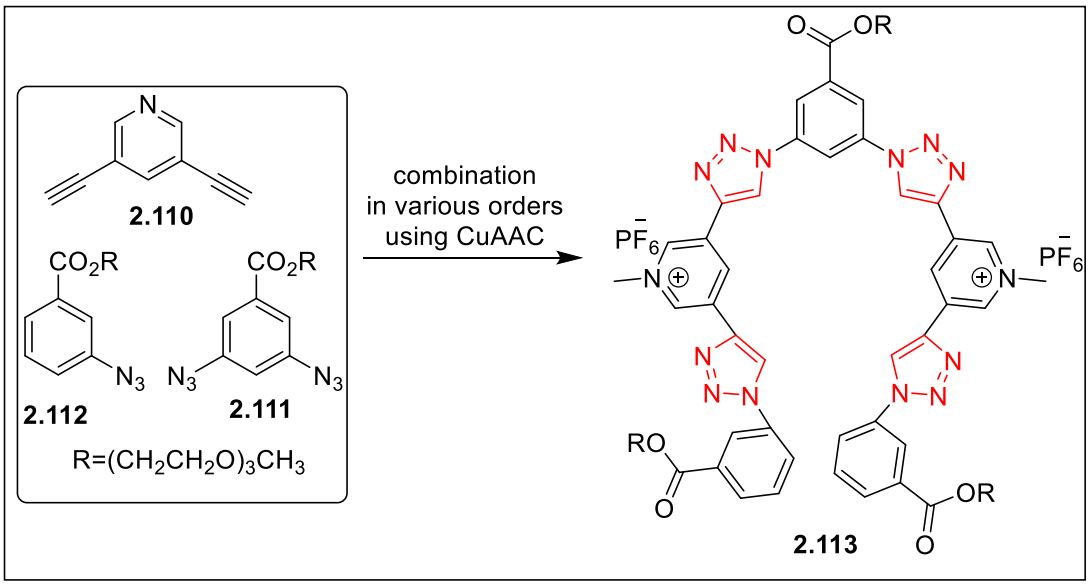

Scheme 2.23

New aryl-triazole receptors with ethynyl spacer were designed using an azide **2.114** and an alkyne-tiazine derivative **2.115** as the starting materials. The first step was a click reaction and after several steps of synthetic manipulation the foldamaer **2.116** was prepared. From, UV–Vis spectroscopic titration, the foldamers were found to bind various halides and oxyanions with high affinities but low selectivities. The lack of anion selectivity might provide an opportunity for designing new type of anion transporters (Scheme 2.24).[41]

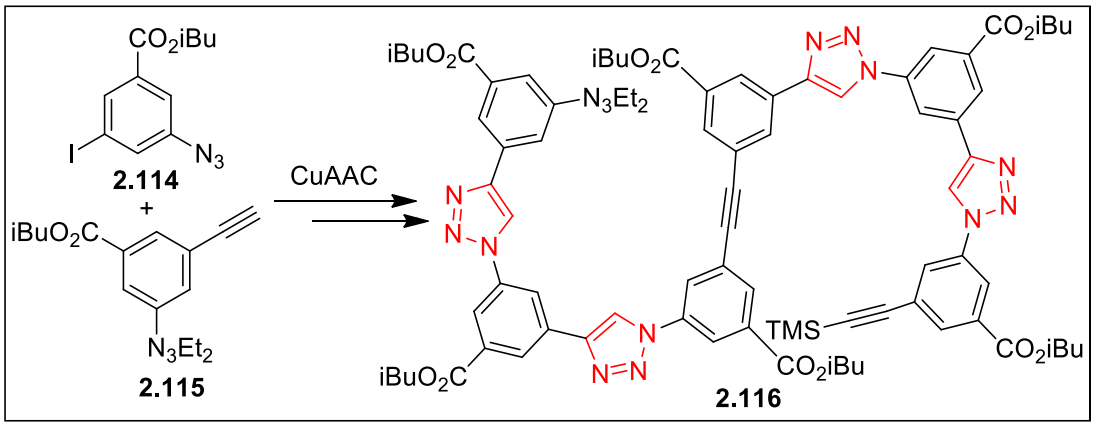

Scheme 2.24

Ruthenium (II) complexes of oligo(bipyridine–phenyl triazole)s were designed as receptors for anions. Click coupling of alkyne **2.117** and azide **2.118** and components afforded bistriazole **2.119** under CuAAC conditions (Scheme 2.25). Compound **2.119** was converted to a tetrazolide **2.121** using the monoazide **2.120**. Oligomers **2.119** and **2.121** were subjected to complexation reaction with $[Ru(bpy)_2Cl_2]\cdot 2H_2O$ resulting into the formation of ruthenium (II) complexes **2.122** and **2.123** respectively. The receptors **2.119** and **2.121** were partially preorganized through metal–ligand interactions and folded into a helical conformation to bind different halides or nitrate anions in their inner cavities. The short receptor **2.119** folded into a helical conformation to bind chloride, bromide, iodide, and nitrate anions. In the competitive H-bonding solvent DMSO, the short

receptor still complexed the anions in a 1:1 binding stoichiometry, whereas the longer receptor **2.121** formed double helices with an anion trapped inside (Scheme 2.25).[42]

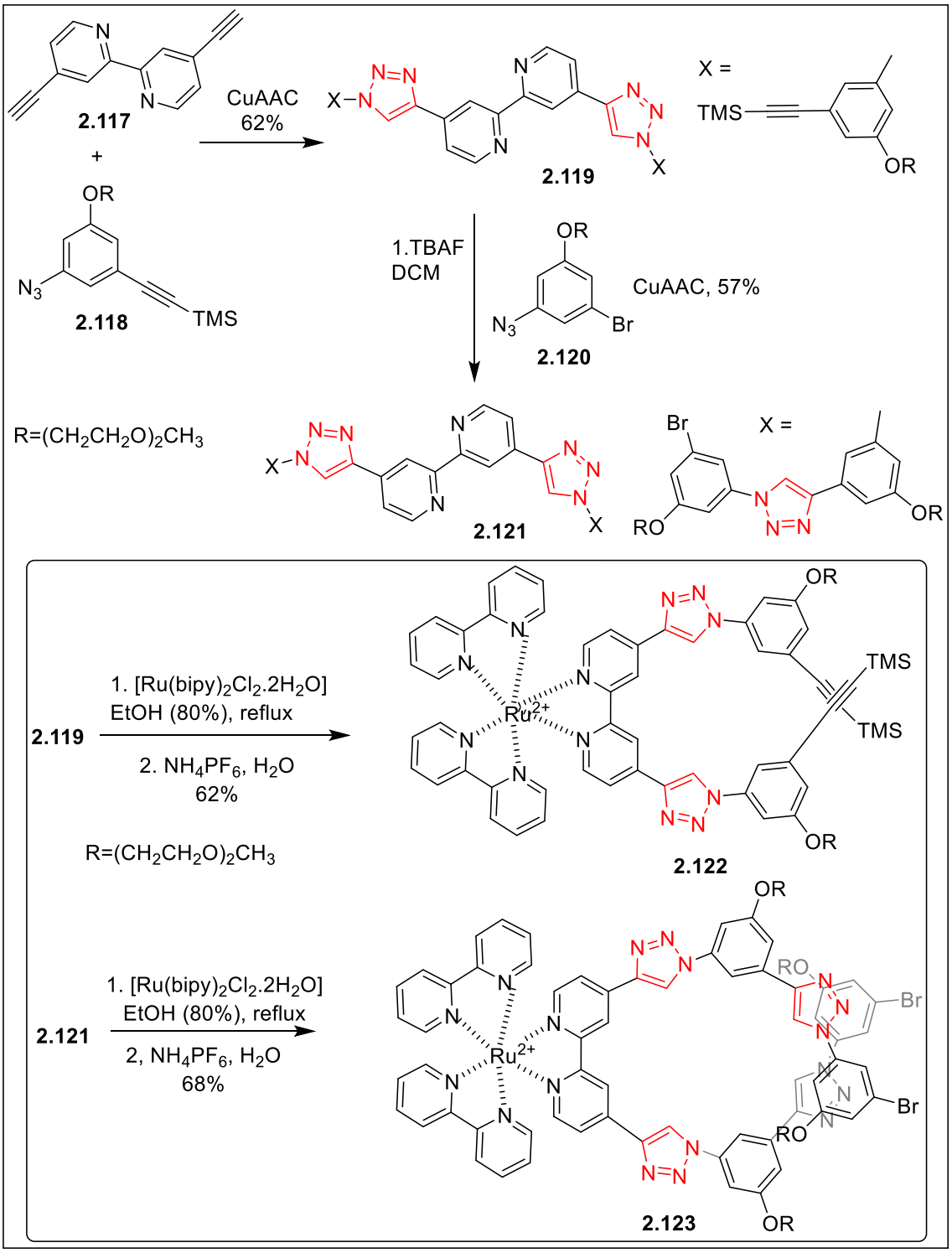

Scheme 2.25

In order to synthesize chimeric oligonucleotides by incorporating purine nucleobases and multiple triazole linkers in natural, phosphate-linked structures of RNA, a solution-phase strategy was developed. A representative bistriazole linked phosphoramdite **2.130** was synthesized starting with the click coupling of an

uridine alkyne **2.125** and an alkyne azido uridine **2.124** (Scheme 2.26). The dimer **2.126**, thus obtained was made ready for coupling with the azidouridine **2.128** and the trimer **2.129** was converted to a phorphoamdite trimer UUC **2.130**. The UUC unit was incorporated into a natural RNA fragment to obtain several oligomers having several combinations of nucleobases in **2.131** (Base = U, C, G, A). The chimeric oligonucleotide, 5'-GpApUpGpU$_{TR}$U$_{TR}$CpUpApApGpCpU was subjected to translation reactions and the products were separated. The results showed that the chimeric RNA was recognized as mRNA and the UUC codon was translated into phenylalanine in the peptide product. During the translation reaction, single nucleotide misreading was noted (Scheme 2.26).[43]

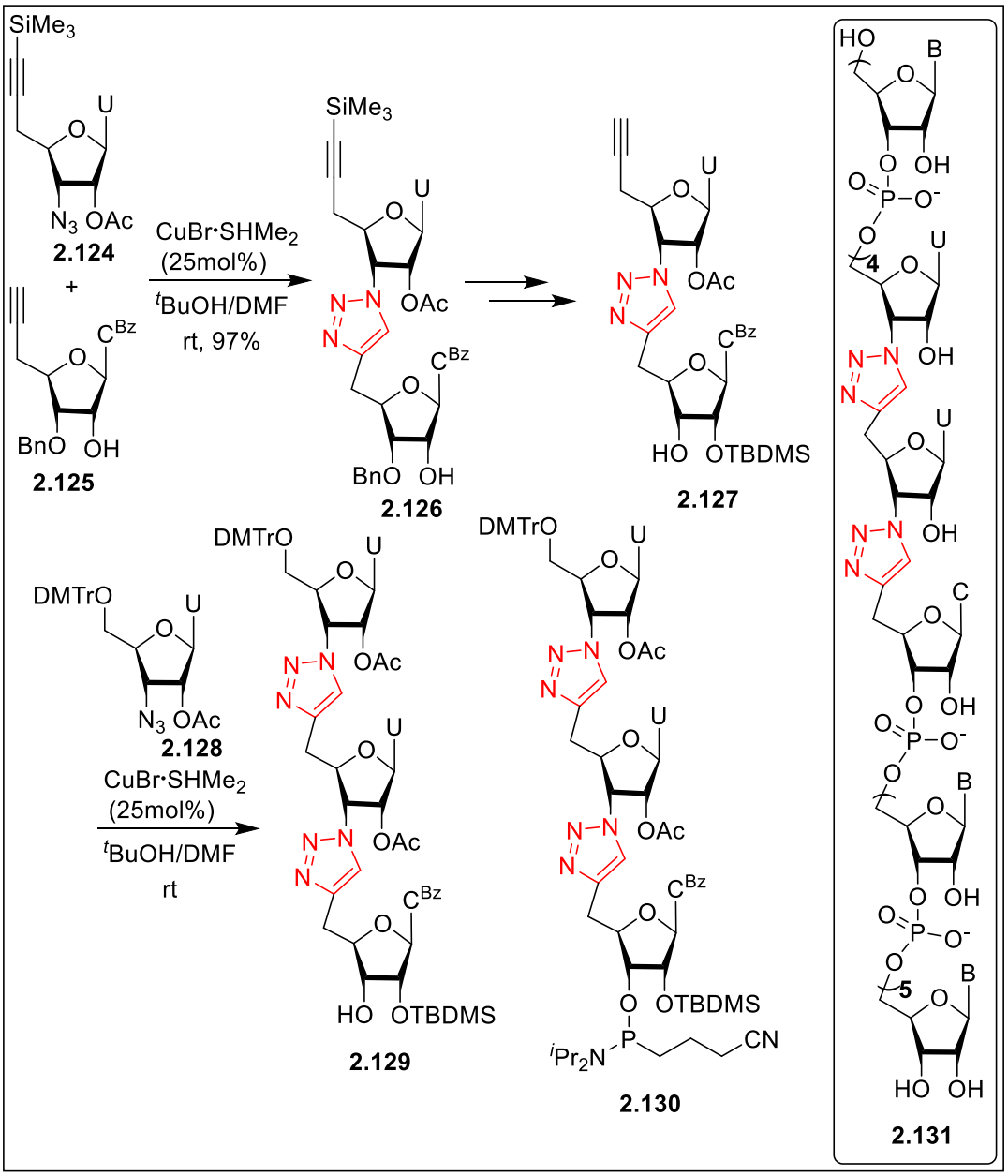

Scheme 2.26

In an attempt to demonstrate the utility of CuAAC reaction for the generation of mixed poly heterocycles, bistetrazole **2.132** was used as the starting material. Propargylaion of the sodium salt of bistetrazoleethane

afforded a mixture of three isomers from which **2.133** was isolated in 10% yield. The structure was unambiguously established using X-ray diffraction analysis. This compound readily underwent CuAAC based triazolylation with *p*-tolyl azide, *p*-nitrophenyl azide, and benzyl azide to give heterocyclic assembles **2.134**-**2.136** bearing 1,2,3-triazole and tetrazole heterocycles (Scheme 2.27).[44]

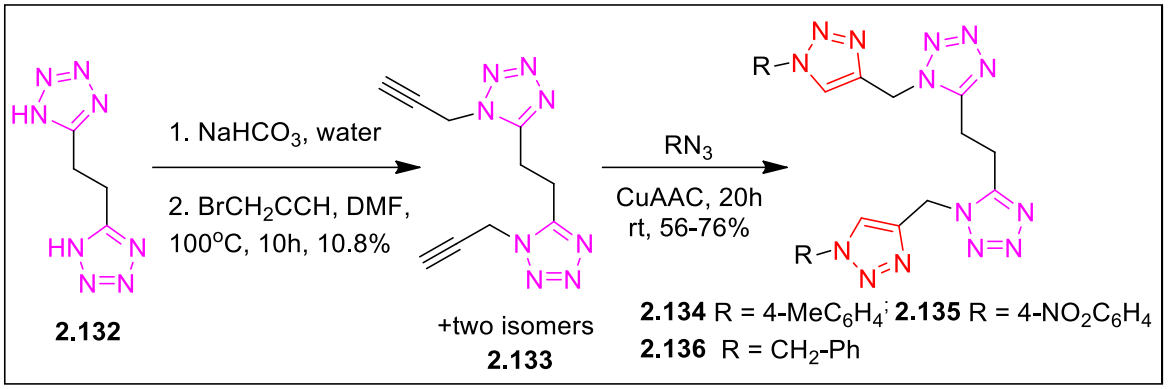

Scheme 2.27

In order to synthesize hetero-oligotriazoles with 1,4-DT/1,5-DT combination a partial metal-free strategy was applied. Vinyl sulfone group has been used extensively as a 2π partner for the regioselective synthesis of 1,5-DTs.[45] The strategy was used for the synthesis of vinyl sulfone modified carbohydrates as well. Thus, 1,5-DT linked disaccharides were synthesized from a orthogonally functionalized building block **2.137** having both vinyl sulfone and azido groups using aqueous ionic-liquid (water: *N,N*-dimethylethanol ammoniumformate) media (Scheme 2.28). This building block **2.137** containing secondary azido groups did not undergo self-coupling but reacted with the externally delivered primary azidosugar **2.138** to afford a pseudo disaccharide **2.139**. The disaccharide was coupled with an alkyne sugar block **2.140** for the preparation of the first ever 1,4-/1,5-DT-linked trisaccharide **2.141** using aqueous ionic-liquid and water–butanol based "click" chemistry. Similar strategy with different building blocks afforded another trisaccharide **2.142** (Scheme 2.28).[45]

It was observed that CuAAC reaction of geminal diazide **2.143** with methyl propiolated under standard conditions afforded only the deacetylated bistriazole **2.144**. Other alkynes also produced similar bis 1,4-DTs. The CO_2Et group was easily replaced by the treatment of IBX-SO_3K, NaN_3 and a catalytic amount of NaI to afford **2.145**. A series of geminal tris- triazoles (such as **2.146**) were easily synthesized from 2.143. The reaction of tripropargylamine with excess of azidobistriazole **2.143** afforded N-linked geminal oligotriazoles **2.146a** (Scheme 2.29).[46]

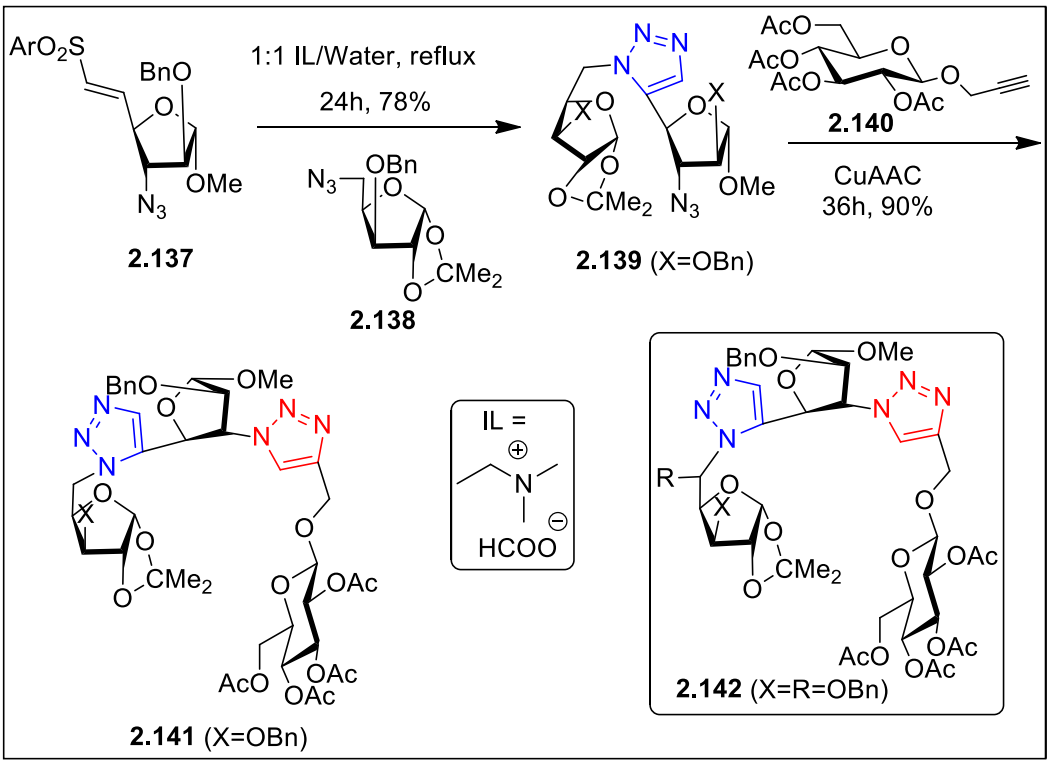

Scheme 2.28

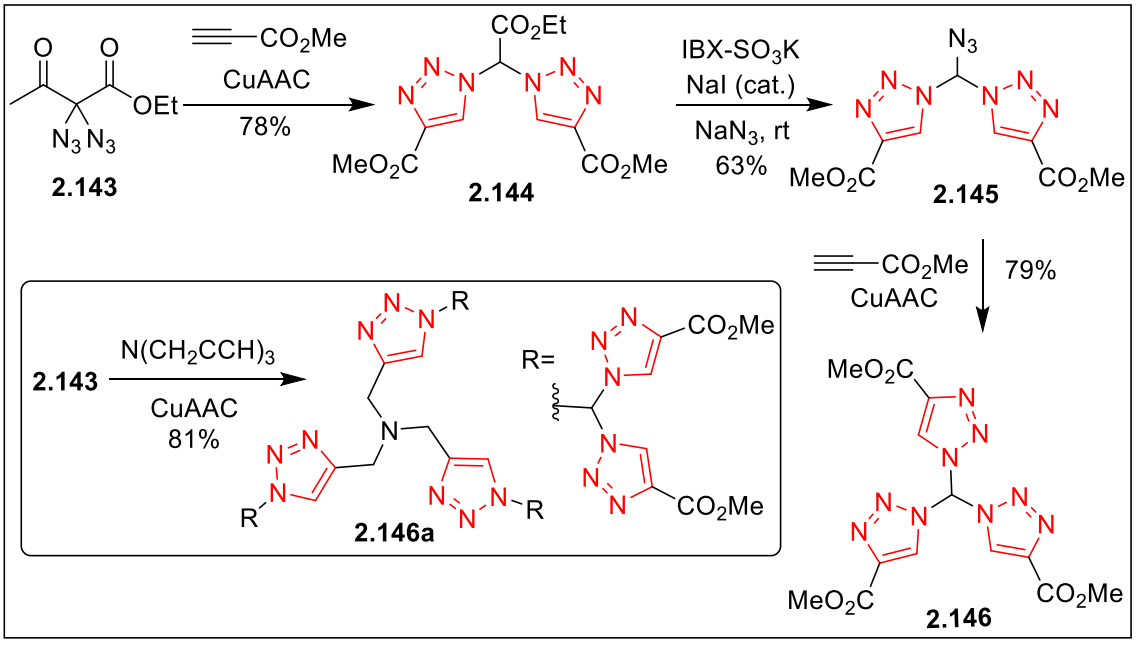

Scheme 2.29

Two isomeric (1,4- and 1,5-DT) 1,2,3-bis triazole scaffolds **2.147** and **2.148** were designed where the triazole moieties were connected by isophthaloyl group and naphthyl thiourea based spacer (Scheme 2.30). The 1,4-DT was prepared using the usual CuAAC strategy. The starting 1,5-DT **2.149** required for the synthesis of **2.148** was also prepared using vinyl sulfone as the 2π partner under metal free conditions as mentioned

above.[45] Thus, the vinyl sulfone **2.149** was reacted with the azido derivative generated in situ from $MsOCH_2CH_2NHBoc$ to afford the 1,5-DT **2.150**. Stepwise transformation of **2.150** via **2.151** afforded the amino triazole **2.152**. Two equivalents of **2.152** on reactions with disulfonyl chloride afforded the bistriazole **2.154**. Deprotection of **2.154** followed by the reaction of the free amine with the naphthyl thiocyanate **2.155** afforded the required scaffold **2.148**. Molecular recognition potential of these molecules was studied against different inorganic phosphate and phosphate based biomolecules such as ATP, ADP, AMP etc in semi aqueous system. From fluorometric study, it was observed that both the sensors recognised ATP with considerable increase in emission and 1,4-DT linked device **2.147** acted as a better chemosensor in comparison to 1,5-regioisomer **2.148** (Scheme 2.30).[47]

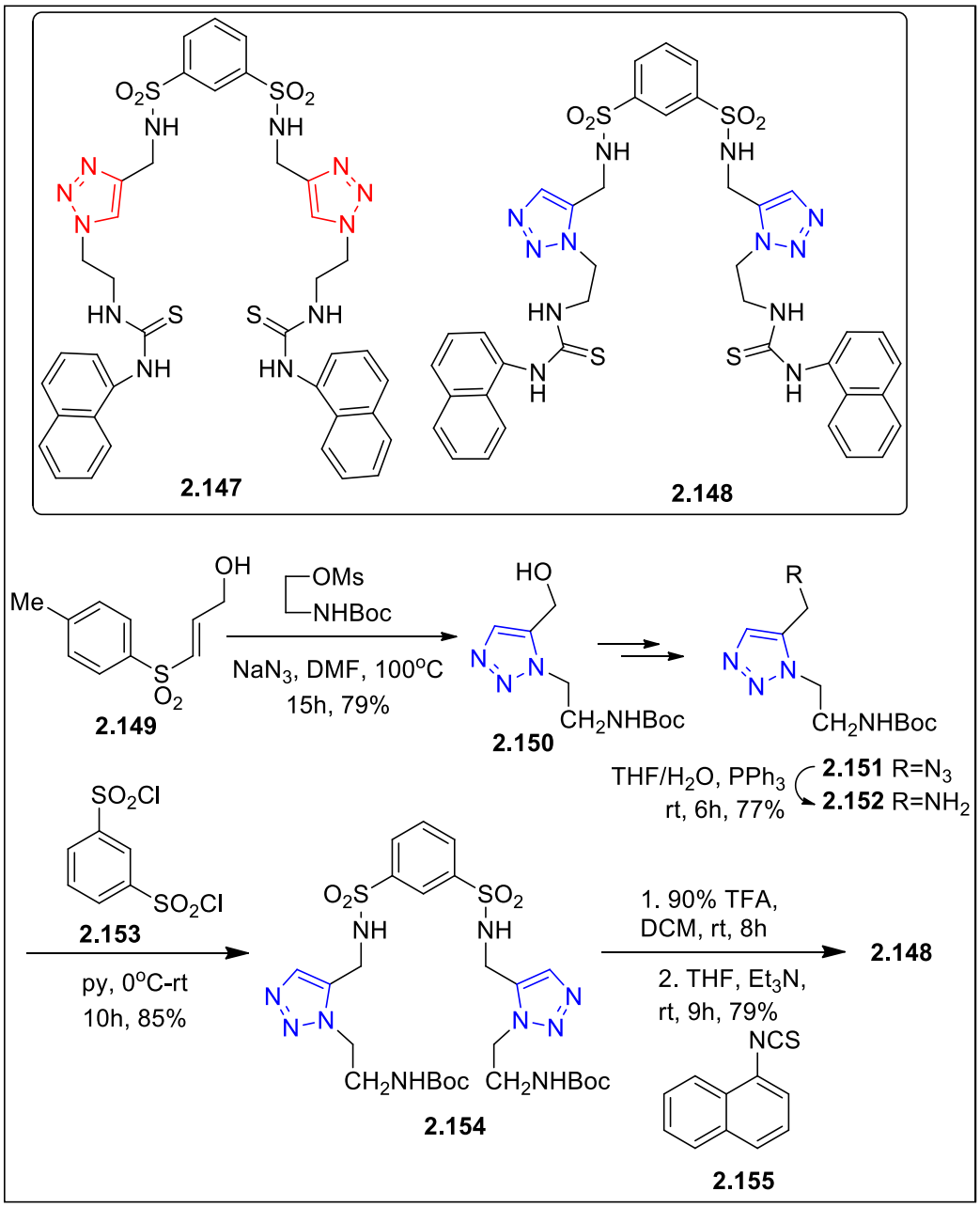

Scheme 2.30

A series of triazole tethered hybrid molecules based on coumarin, uracil and benzimidazolone were designed by employing click chemistry. Synthetic strategy involved the cycloaddition reaction between azido derivative of coumarin **2.157** and bispropargyl derivative of 6-methyl uracil **2.156** as well as benzimidazolone. All synthetic compounds like **2.158** and **2.159** were tested for the inhibition of *Micobacterium tuberculosis* strain *H37Rv*. The uracil linked bistriazoles 2.158 showed moderate inhibition whereas benzimidazolone linked triazoles **2.159** performed better. The docking study revealed an additional interaction of bezimidazolone oxygen, which made compounds **2.159** conformationally more flexible (Scheme 2.31).[48]

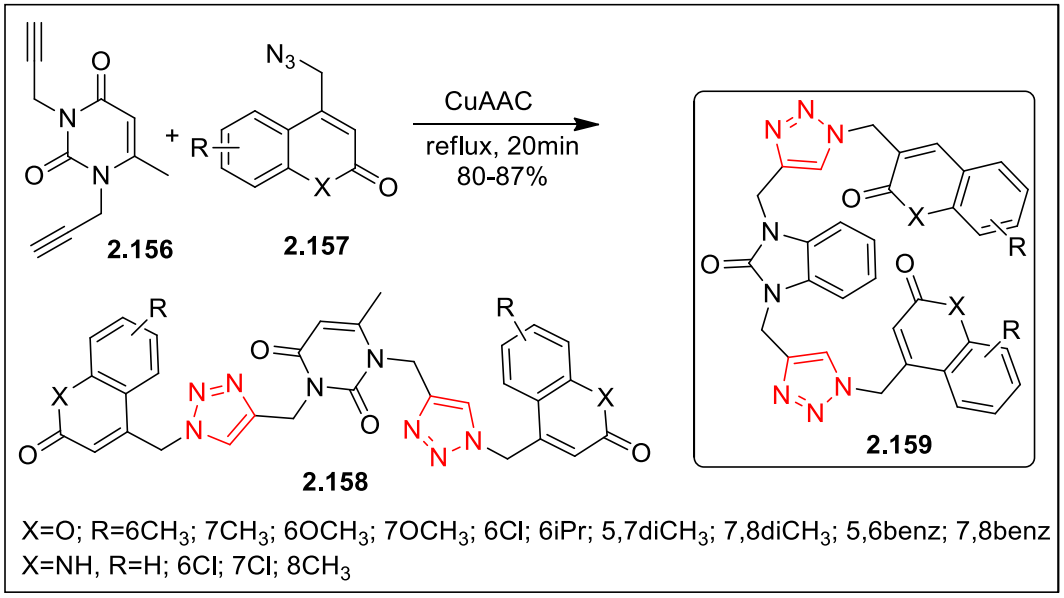

Scheme 2.31

An enantiopure 3-amino-substituted pyran derivative **2.160** was converted to 3-azido-substituted pyran **2.161** by copper-catalyzed diazo transfer reaction using nonafluorobutanesulfonyl azide (Scheme 2.32). Compound **2.161** was sulfated and the product was converted to a pyran-1,4-DT hybrid **2.163.** A wide range of di-propargylated molecules were reacted with the azido compound **2.161** to obtain several divalent triazole-pyran hybrid molecules. *O*-sulfation of some of these compounds afforded five products in sufficient purity. Compound **2.164** showed the lowest IC_{50} value for binding to L-Selectine whereas **2.165-2.166** showed the values in the range of 20 to 50 µm (Scheme 2.32).[49] Using a similar approach, a series of multivalent 1,2,3-triazole-linked molecules were reacted with the azido compound **2.161** to obtain several divalent triazole-pyran hybrid molecules. *O*-sulfation of some of these compounds afforded five products in sufficient purity. Compound **2.164** showed the lowest IC_{50} value for binding to L-Selectine whereas **2.165-2.166** showed the values in the range of 20 to 50 µm (Scheme 2.32).[49] Using a similar approach, a series of multivalent 1,2,3-triazole-linked carbohydrate mimetics was synthesized. For example compound **2.168** prepared by coupling **2.167** with **2.161** was converted to pure *O*-sulfated derivative **2.169**. Thus, compound **2.169** and **2.170** were evaluated as L- and P-selectin ligands; **2.169** showed IC_{50} values of 1.1–1.5 µM for L-selectin and 1.1–4.5 µM for P-selectin whereas **2.170** gave an IC_{50} value of 30 µM for P-Selectin. Although synthesized and tested, the purity of an *O*-sulfated C_{60}-fullerene based dodecavalent similar system could not be established (Scheme 2.33).[50]

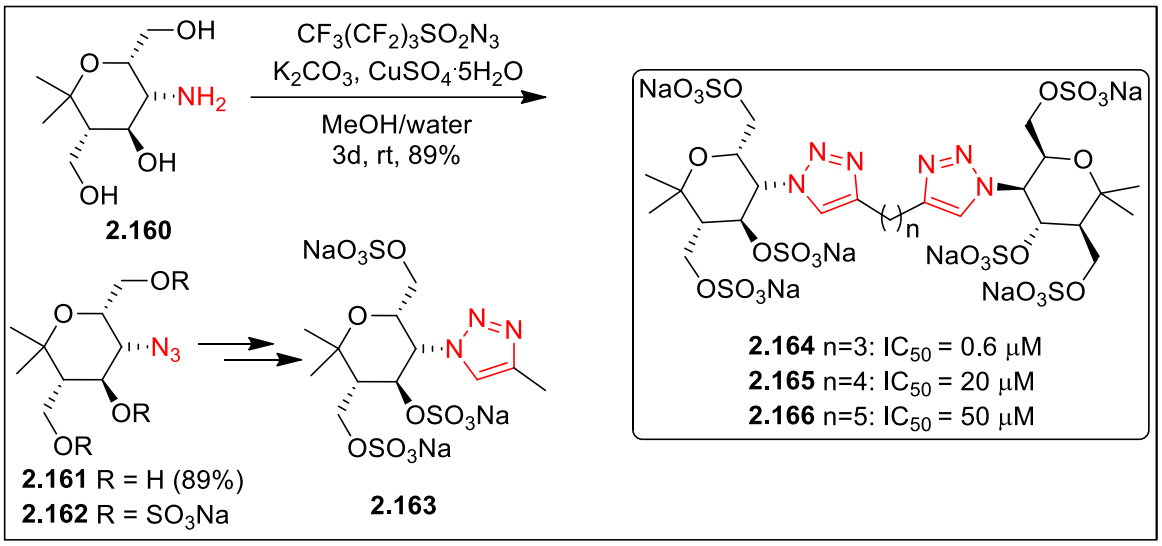

Scheme 2.32

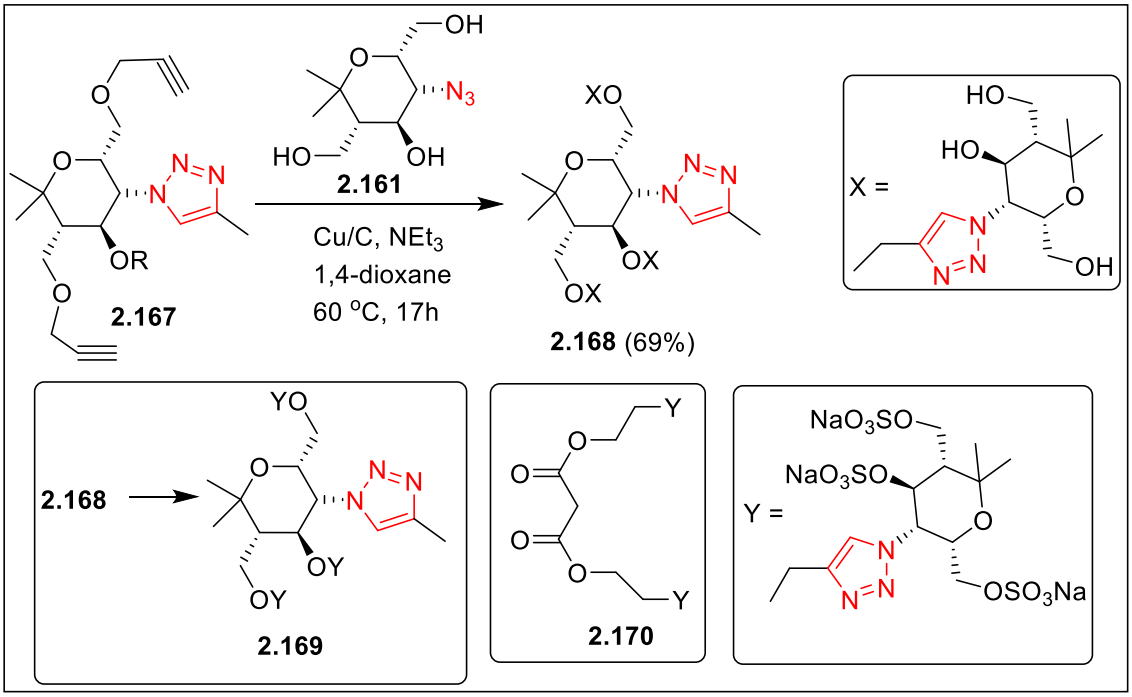

Scheme 2.33

Recently, two different bistriazolylated β-D-ribose structures were designed where the triazole moieties were used as carriers of different acidic functions. These acidic functions were expected to reach the positively charged active site of ribonuclease A (RNase A) and inhibit the functions of the enzyme. Thus, two synthetic routes were followed to achieve the sulfonic acid-modified bistriazoles **2.179** and **2.180** from a common precursor **2.175**, which was prepared by reacting sugar alkyne **2.171** with 2-azidoethyl mesylate under CuAAC cnditions (Scheme 2.34). The triazole derivative **2.172** upon treatment with methyl thioglycolate afforded the sulfide derivative **2.173** and the latter was converted to the azido derivative **2.175** via **2.174**. The azido-derivative **2.175** was then separately subjected to the multistep transformation to the monocarboxylated sulfonic acid derivative **2.179** (**2.175** → **2.176** → **2.177** → **2.178**→**2.179**). The azido-derivative **2.175** was also

converted to the disulfonic acid derivative **2**.**180** in a similar fashion. Compounds **2**.**179** and **2**.**180** were shown to act as RNase A inhibitors with inhibition constant (Ki) values 46 and 29 μM respectively. Docking studies indicated that all of these inhibitors mostly occupied the B1, P1 and P2 subsites. The strong electrostatic interactions between the sulfonic acid groups and the active P1 subsite residues resulted in a more potent inhibition RNase A. The triazole moieties also interacted with the catalytic site residues (Scheme 2.34).[51]

A family of carbohydrate conjugated G-quadruplex ligands based on a phenyl ditriazole (PDTZ) motif were synthesized leading to symmetrical and dissymmetrical carb-PDTZ derivatives containing a phenyl pyrrolidinyl side-chain. The symmetrical ones are prepared in the usual way using CuAAC reaction. .For the unsymmetrical ligands, one equivalent of 2-azidoethyl 2,3,4,6-tetra-O-acetyl-β-D-glucopyranoside **2.181** (Scheme 2.35) was reacted with the 1,3- diethynylbenzene **2.182** under controlled conditions to afford the mono 1,4-DT derivative **2.183** and the product on reactions with the azide **2.184** followed by deprotection generated the desired **2.185**. The dissymmetric monosaccharide- phenyl ditriazole hybrid molecule **2.185** stabilized G-quadruplex and showed much higher G-quadruplex vs duplex DNA selectivity than the non-saccharide control phenyl ditriazole **2.186**. NMR experiments established that ligand **2.185** interacted with the edgewise-loops and the adjacent tetrad in contrast to the non-specific binding mode of 2.186 with the three G-quadruplex studied. All carb-PDTZ hybrid molecules showed poorer antiproliferative activities than **2.186** (Scheme 2.35).[52]

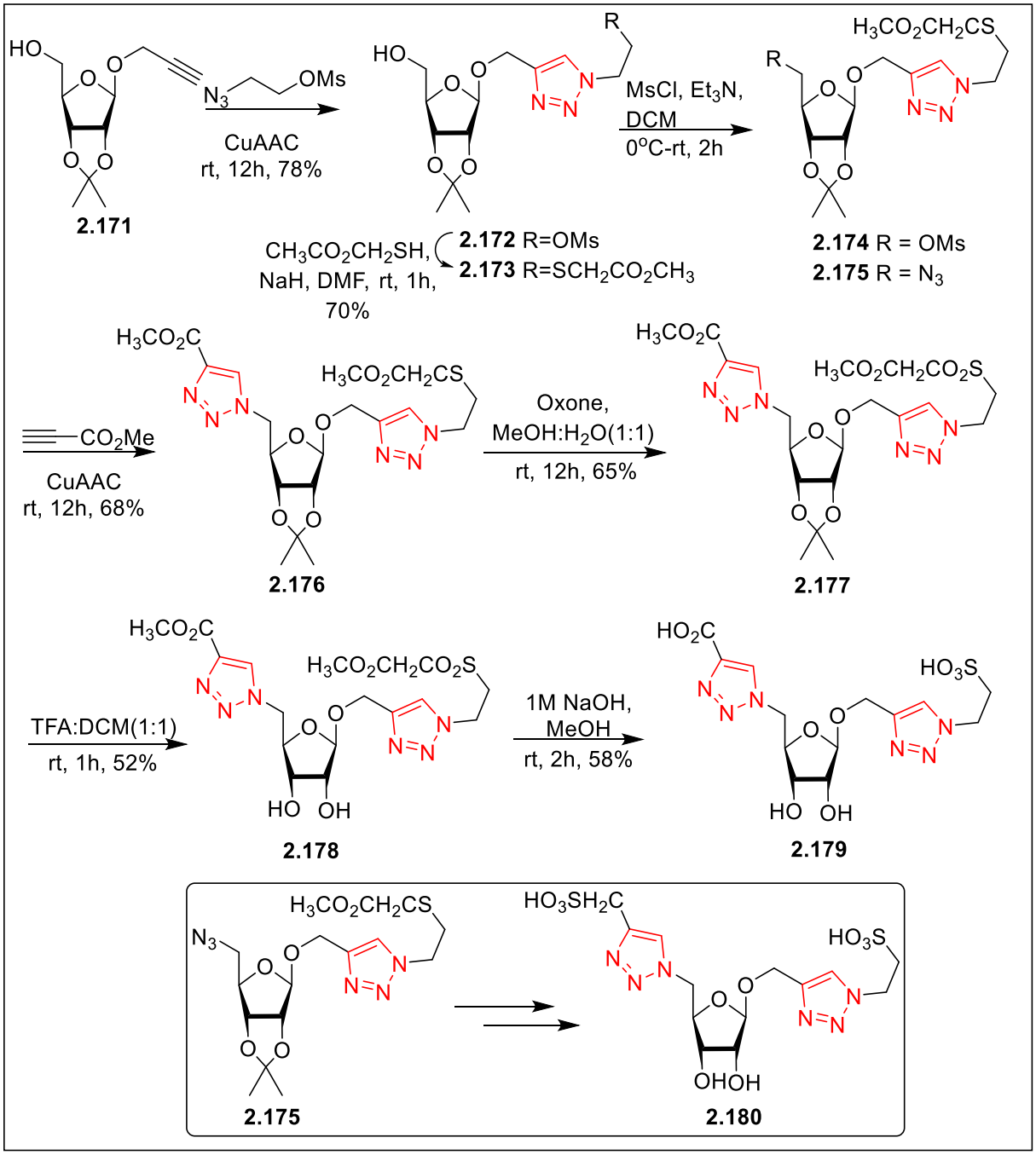

Scheme 2.34

A series of 1,4-DT linked dihydropyrimidone type hybrid molecules was synthesized by multicomponent click-Biginelli reactions. Thus, azide **2.187** (Scheme 2.36) and styrene formed the triazoles **2.191** whereas, urea and the aldehyde **2.188** formed the intermediate **2.192** [shown as the Cu(I) complex]. The Cu(I) complex **2.191a** and **2.192** under Cu(I) catalysis formed the monotriazole **2.189** via intermediate **2.192a**. The monotriazole **2.189** involving bromination, azidation and CuAAC afforded compounds like **2.190**. Some of these hybrids were potent cell proliferation inhibitors of non-small-cell lung cancer, cervix cancer, breast cancer, and colon cancer. The hybrid molecule **2.190** was identified as the best growth inhibitor (Scheme 2.36).[53]

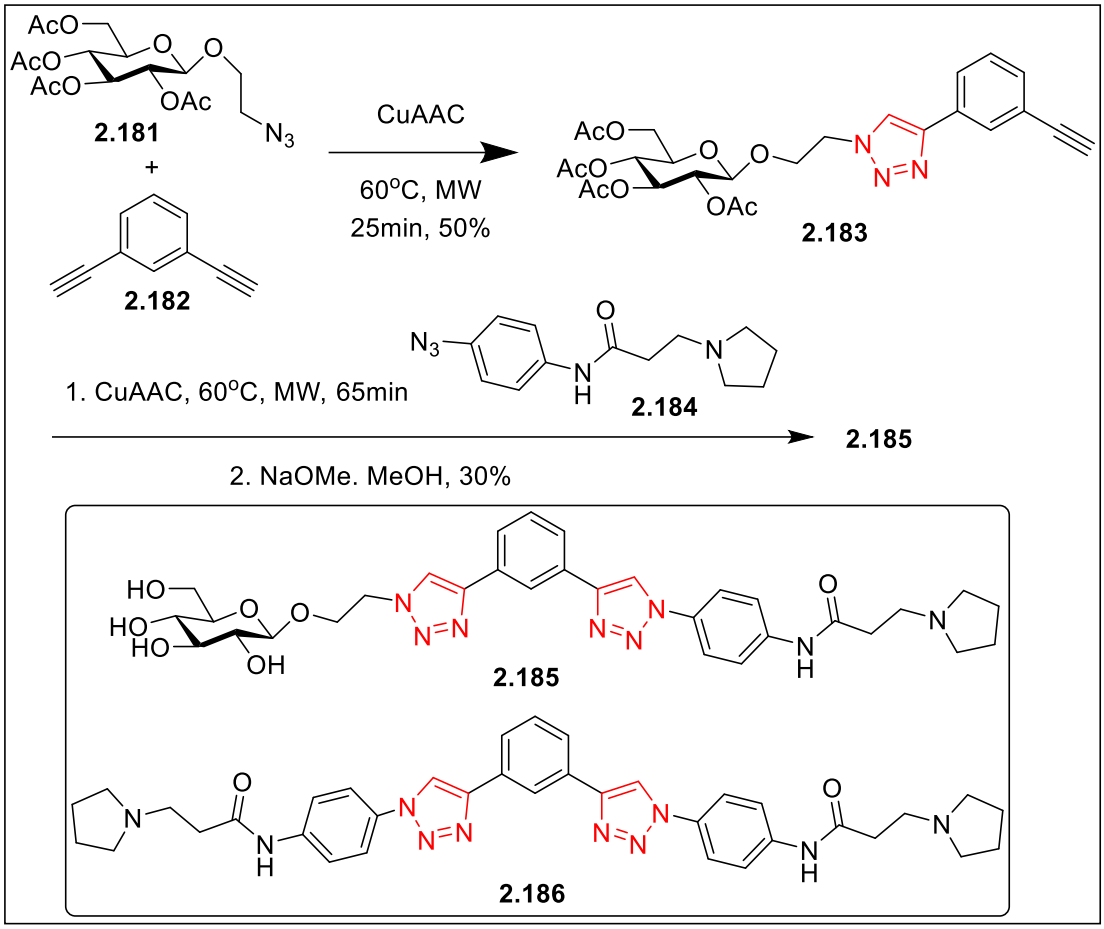

Scheme 2.35

A series of unsymmetrical bis-1,4-DT-Daidzein hybrid derivatives were designed by the propargylation of two phenolic hydroxy groups of the naturally occurring isoflavone Daidzein **2.193** to bisalkyne **2.194**. A series of organic azides were reacted with **2.194** to generate more than a dozen bistriazoles like **2.195**. Compounds **2.195a-c** showed selective potency against A549 cancer cell line. Compounds **2.195d-e** showed significant activity against HeLa and MDA-MB-231 cell lines. Compound **2.195f** was found to be a close competitor of the positive control against breast cancer cell line (MDA-MB-231) (Scheme 2.37).[54]

A series of heteroditopic receptors were synthesized to study the cooperative recognition of halide anions via sodium cation–benzo-crown ether binding. For example, the synthesis of the iodo containing receptor **2.198** (Scheme 2.38), two equivalents of 4-azido-benzo-15-crown-5 **2.197** and 3,5-diiodoethynylpyridine **2.196** were reacted under modified CuAAC conditions to get the desired compound in 84% yield after recrystallization. Compound **2.198** was converted to **2.200** in two steps. NMR based ion pair binding investigations revealed that sodium cation–benzo-crown ether binding dramatically enhanced the recognition of bromide and iodide halide anions. Crystals of the complex **2.199**.2 NaI showed that the triazole-bound iodide anion was bonding encapsulated within each of the 3,5-bis-triazole pyridine anion-binding clefts via an array of CH···I^- hydrogen interactions. Theoretical calculations indicated that the crown ether-sodium cation complexation induced a polarization of the σ-holes of **2.198** and **2.200**, which triggered the unique cooperativity exhibited by these triazole-crown ether hybrid systems (Scheme 2.38).[55]

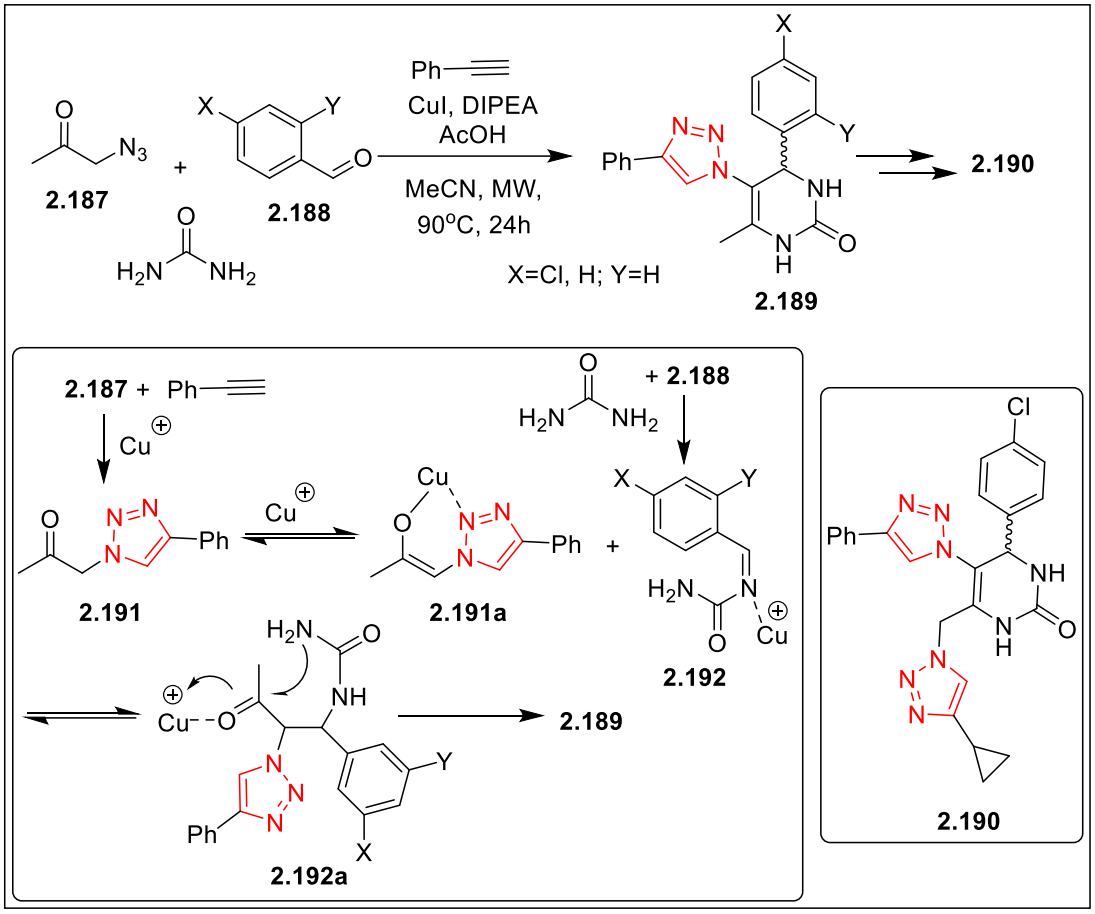

Scheme 2.36

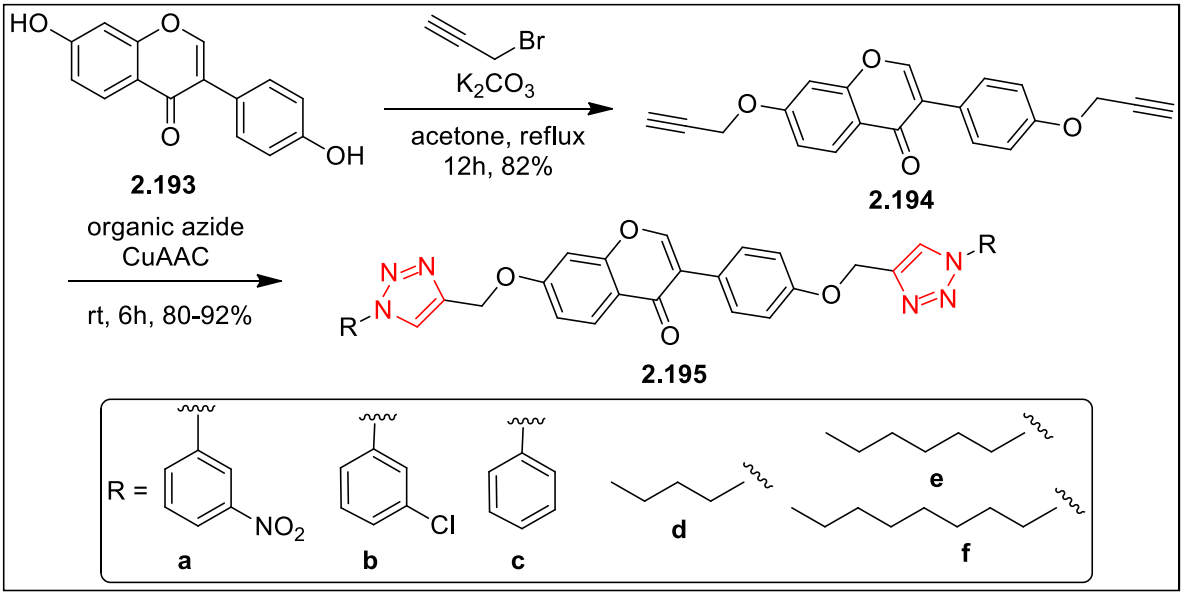

Scheme 2.37

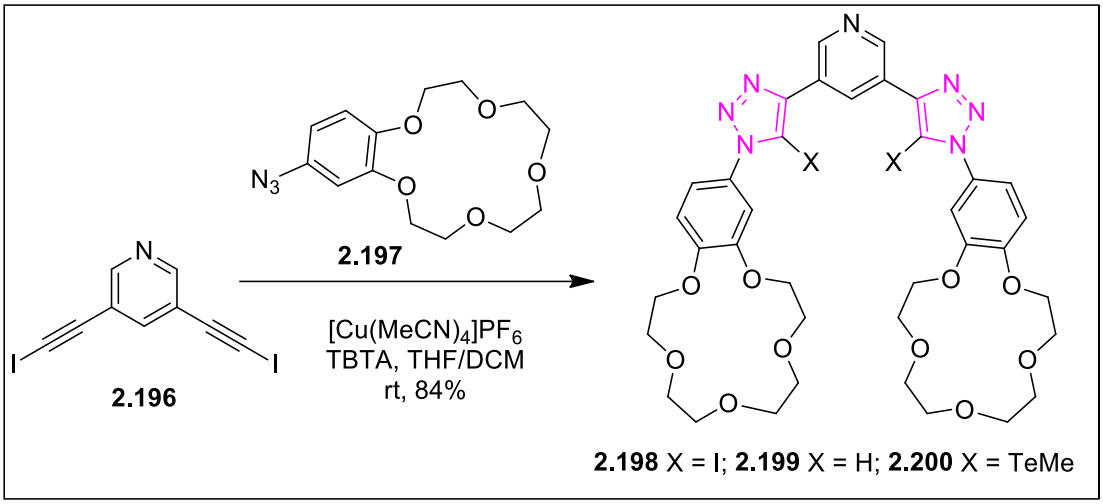

Scheme 2.38

Compounds **2.202** (X = a-c) and several other related compounds were prepared by coupling bipropargyl piperazine **2.201** with the corresponding amido-azides under CuAAC conditions. These three compounds have shown antitubercular activity against *Mycobacterium tuberculosis* (Mtb) H37Rv with minimum inhibitory concentration value 12.5mg/mL. Docking studies revealed that **2.202** (X = a) was tightly bound to the active site of *Mtb* enoyl reductase (InhA). Some of these compounds also showed antifungal and antioxidant activities (Scheme 2.39).[56]

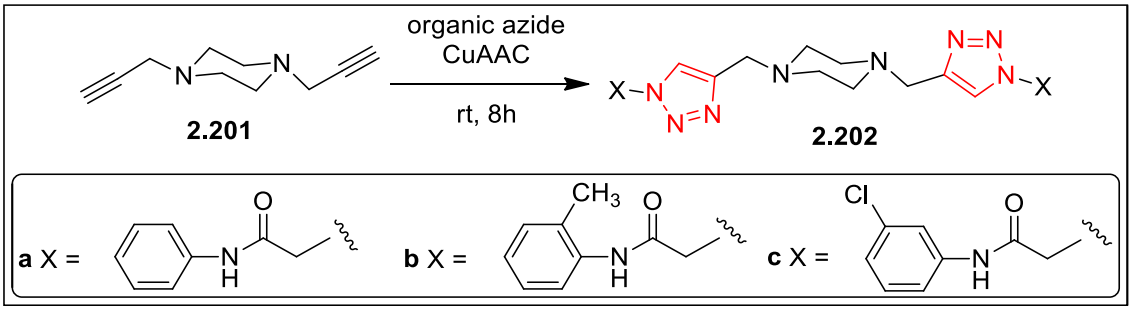

Scheme 2.39

1,4-DT **2.204** was prepared from the alkyne **2.203** (Scheme 2.40) using CuAAC strategy and the former was converted to the triazolium salt **2.205**. Room temperature Schiff base condensation of **2.205** with 1,4-diaminobutane afforded the symmetrical bis-imino- functionalized triazolium salt **2.206**. The single crystal X-ray diffraction results revealed that **2.206** crystallized in the *ρ*-1 space group of the triclinic system. The dihedral angles between the planes of the triazole rings in **2.206** and the planes of the respective phenyl rings indicated strong deviation from coplanarity. The solid-state structure of **2.206** was further stabilized by weak intramolecular C–H…π and intermolecular C–H … X (X = F, I) non-bonded interactions. Results of Hirshfeld surface contacts analysis and associated two-dimensional fingerprint plots also correlate with the observed intermolecular interactions in the crystals of **2.206**. The 1,2,3-triazole based compounds may serve as potential NHC type ligand precursors for application in organometallic chemistry and catalysis (Scheme 2.40).[57]

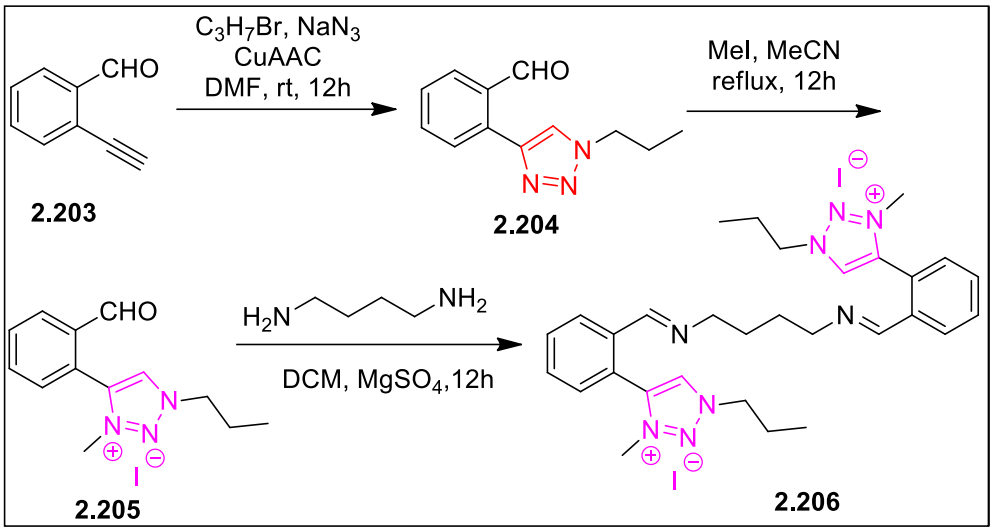

Scheme 2.40

1,2,3-Bistriazole derivative **2.209** of 2,5-dihydroxy-3-undecyl-1,4-benzoquinone (embelin) derivative was synthesized by using the bisalkyne **2.207** and the azido derivative generated in situ from the bromo compound **2.208** followed by the conventional click chemistry. The hybrid molecule **2.209** was found to have potential antidiabetic activity in the HFD-STZ type 2 diabetic rats. The derivative **2.209** (30 mg/kg) exhibited a distinct effect in PPARγ and GLUT4 expression in epididymal adipose tissue. The measured biochemical parameters, electrostatic potential analysis and molecular docking studies extensively supported the activity of the molecule. Hence, this 1,4-DT derivative enhanced the therapeutic activity of embelin for obesity-related T2DM (Scheme 2.41).[58]

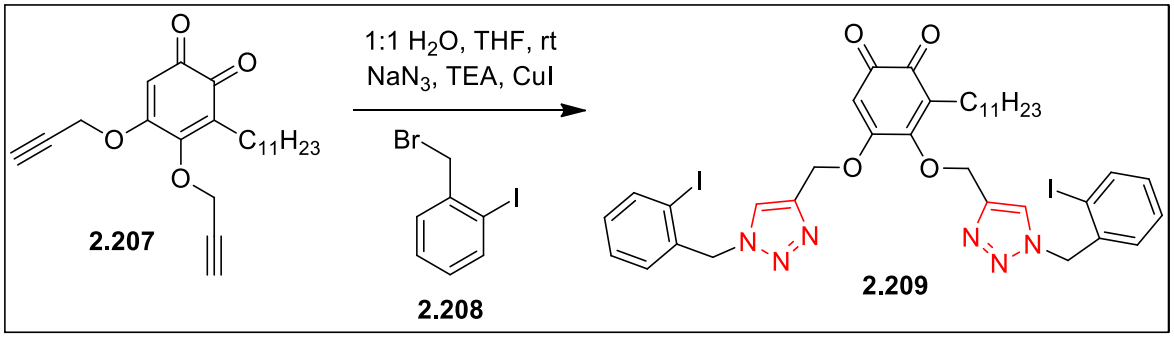

Scheme 2.41

Propargylation of the bisphenol **2.210** afforded the bisalkyne **2.211** which was separately reacted with hexylazide and cyclohexylazide to afford two bistrizoles **2.212** and **2.213** respectively. These intermediates were condensed with a variety of substituted benzaldehydes under basic conditions affording a dozen of bis 1,3-triazolyl chalcones **2.214**. Some of these compounds shoed potent antimicrobial activities (Scheme 2.42).[59]

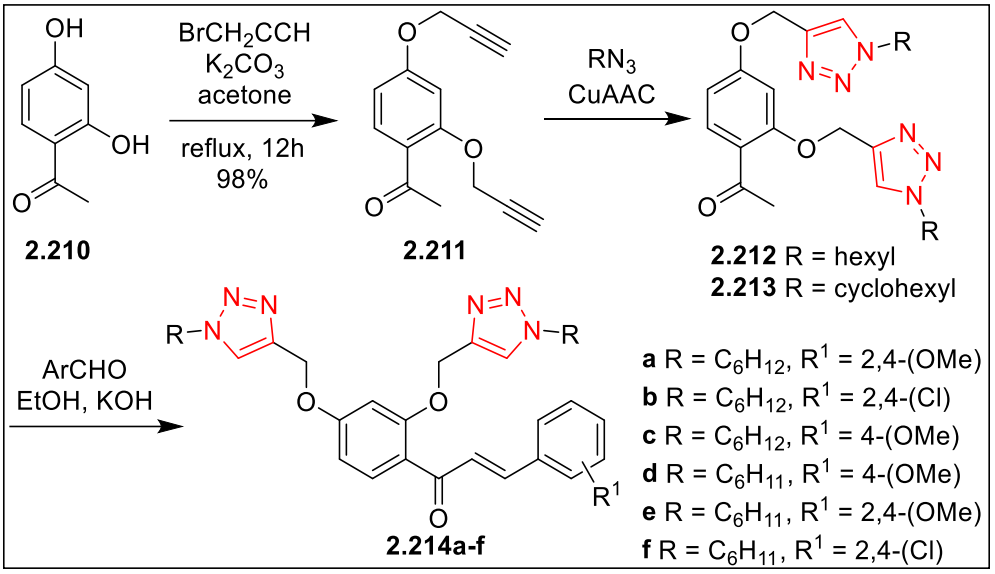

Scheme 2.42

The synthesis of a water soluble decamine derivative of pillar[5]arene **2.218** (Scheme 2.43) decorated with three different functional groups, such as amide, triazole and primary amine was taken up. Thus, the bisalkyne **2.215** was reacted with paraformaldehyde and $BF_3{\cdot}OEt_2$ in dichloromethane to yield the cyclized pillar[5]arene derivative **2.216**. CuAAC mediated reaction transformed **2.216** to 1,4-DT functionalized **2.217**. Further functionalization of **2.217** afforded the desired molecule **2.218** with 10 amino groups at the both ends. The molecule provided a flexible binding core during its interaction with various ions and molecules. Water-soluble **2.218** selectively detected Fe^{3+} with a minimum detection limit of 689 ppm and the in situ prepared Fe-**2.218** exhibited chemosensor activity towards F^- anion and cysteine amino acid. The minimum detection limits of Fe-**2.218** for F^- and Cys were 434 and 1740 ppm respectively (Scheme 2.43).[60]

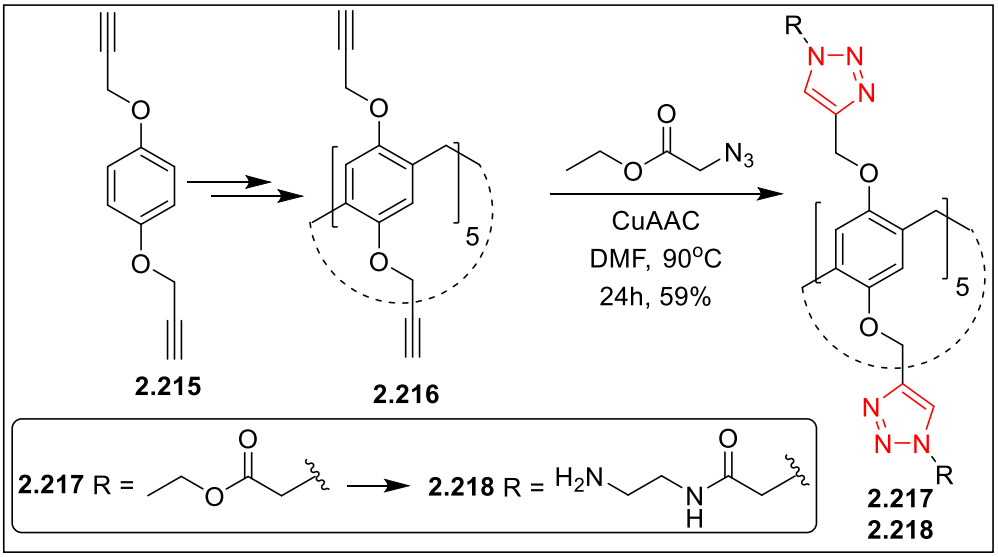

Scheme 2.43

A bimodal triazole-bridged pyrene-appended calix-[4]arene **2.221** was synthesized by coupling bispropargylated tetra-*tert*-butylcalix[4]arene **2.220** and bis(azidomethylpyrenyl)alkane **2.219**. Enhanced monomer and declining excimer emission fluorescence spectral changes demonstrated the binding of Cd(II) and Zn(II) with the chemosensor **2.221**. The observed monomer formation in the fluorescence spectra with Cd(II) and Zn(II) was probably linked not just to the diminished parallel orientations of the pyrene rings but with the magnitude of the resulting HOMO-LUMO gaps (Scheme 2.44).[61]

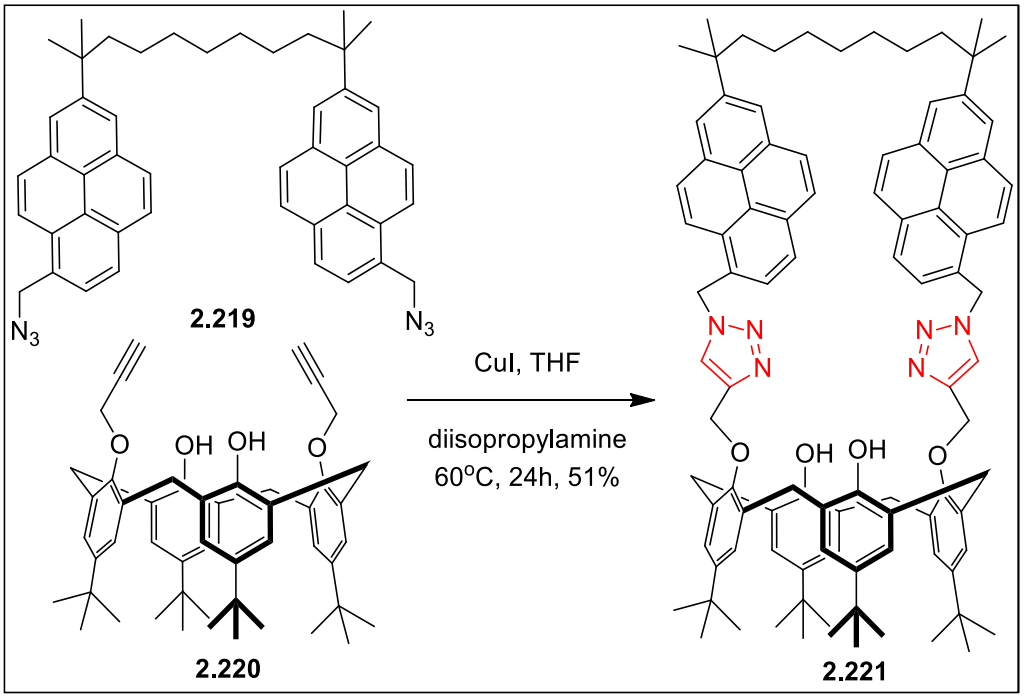

Scheme 2.44

Bis-1,2,3-triazole ligands (for example **2.224)** were designed for complex formation with Cu(II) and Zinc(II) ions. Thus, a suitable bispopargylated para-benzoicaniline derivative **2.222** was coupled with phenylazide using Cu(II) reagent to afford **2.223** (Scheme 2.45). The bistriazole **2.223** was then converted to the amino acid bioconjugate **2.224** via amide coupling reactions. The crystal structure of one such ligand **2.225** and two Cu(II) complexes, **2.225Cu** and **2.226Cu** were recorded (not shown). The Cu(II) complexes were characterized in solution by UV-Vis spectroscopy and for Zn(II) complexes NMR spectroscopy was used. DFT calculations indicated that in **2.225Cu** and **2.226Cu** the triazole groups were coordinated to Cu in the equatorial plane, while the Cu–N2 distance is elongated; thus, the complexes can be considered as pseudo trans-fac isomers. The UV-Vis titrations showed the formation of complexes of ML and ML_2 stoichiometry for Cu(II) complexes of ligands **2.225** and **2.224**. Zn(II) complexes of **ML** and **ML_2** stoichiometry are in fast exchange compared to the NMR timescale. Theoretical studied indicated that the most stable isomer of complexes $[Cu(\mathbf{2.227})_2]_2$+ and $[Cu(\mathbf{2.228})_2]_2$+ is *trans-fac*, which was in agreement with the experimental structures **2.225Cu** and **2.226Cu** (Scheme 2.45).[62]

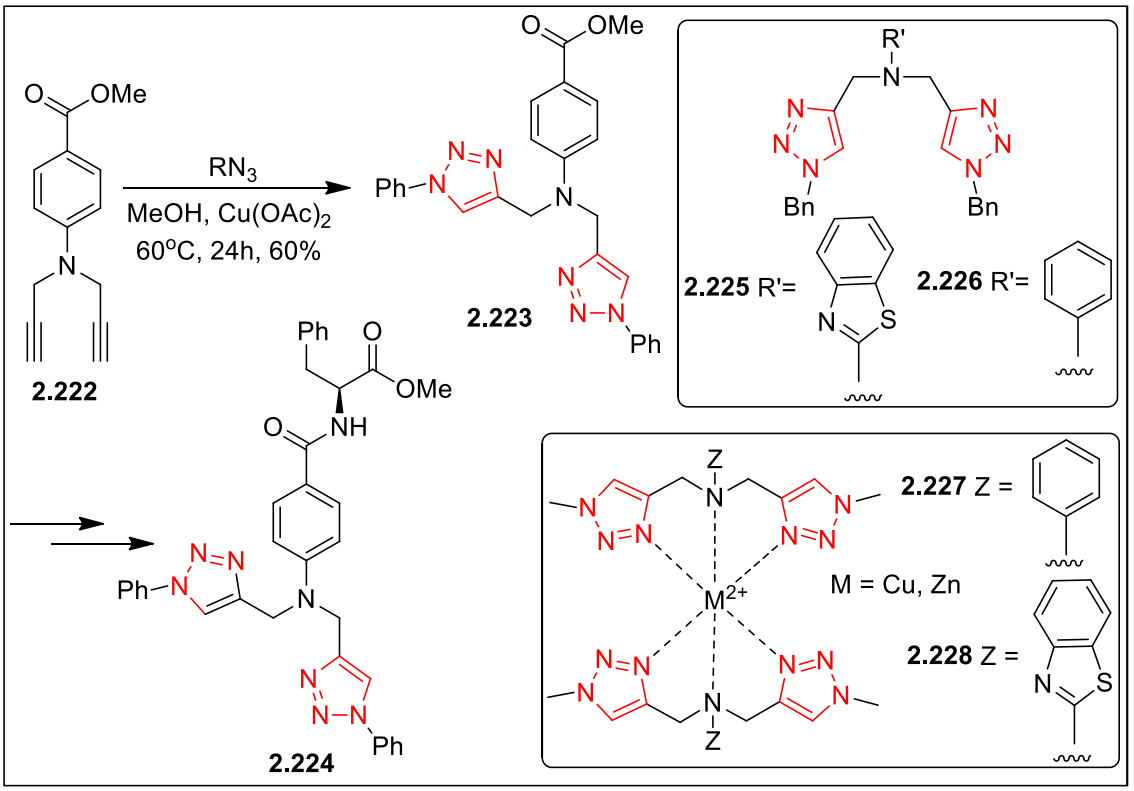

Scheme 2.45

Isomannide derived 1,2,3-bistriazole-bridged ketoxime was designed and used as a diol source for the synthesis of a new class of biobased polyurethanes. The 1,2,3-triazole linked dioxime was synthesized by condensing diazido isomannide **2.229** with two equivalents of 2,4-pentandione **2.230** to afford trisubstituted bistriazolide **2.231**. The keto groups of **2.231** were converted to ketoxime **2.232** and the latter was used in a polyaddition reaction with a diisocyanate **2.233** to afford several 1,2,3-triazole-bridged oximepolyurethanes (for example, **2.234**). The surface characteristics of the synthesized polymers were also examined (Scheme 2.46).[63]

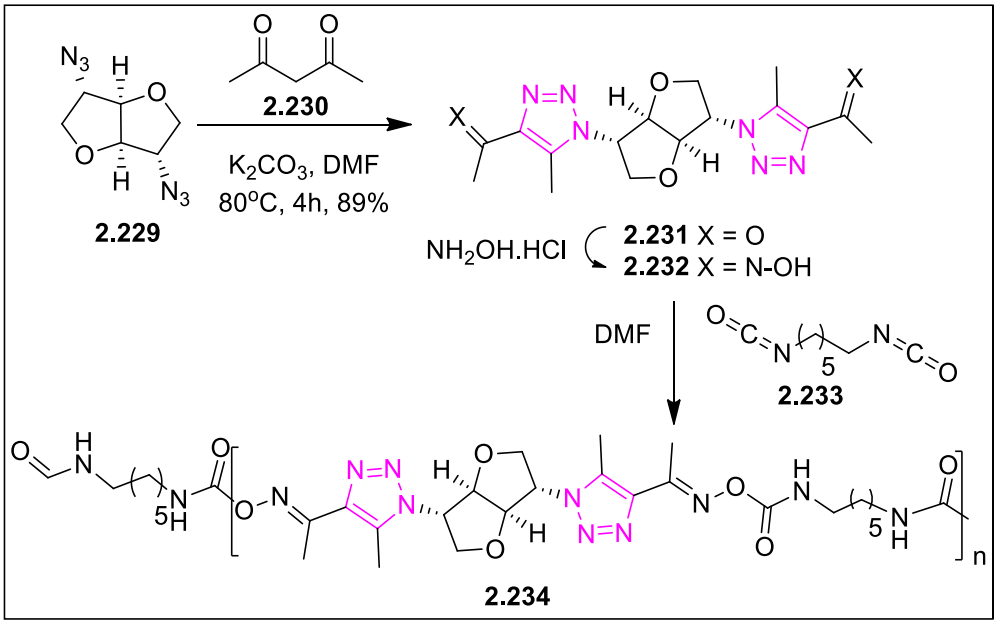

Scheme 2.46

The bis-triazole-bispyrenyl-based sugar derivative **2.237** was synthesized by coupling 1-azidopyrene **2.235** with the bisalkyne D-xylose derivative **2.236** using CuAAC strategy (Scheme 2.47). The bistriazolylated compound **2.237** exhibited selective and sensitive fluorescence quenching effect in the presence of Cu(II) ions over a wide range of cations and anions in acetonitrile. The ON-OFF type fluorescenc response of **2.237** was probably because of the conformational changes from strong excimer emission of pyrene to weak pyrene monomer emission due to an interaction between Cu(II) and inward-facing triazole groups. The interference experiment indicated the ability of the sensor to detect Cu(II) ions in the presence of other metal ions. The limit of detection of sensor **2.237** for Cu^{2+} was found to be 0.15 µM, which is within WHO's guidelines (Scheme 2.47).[64]

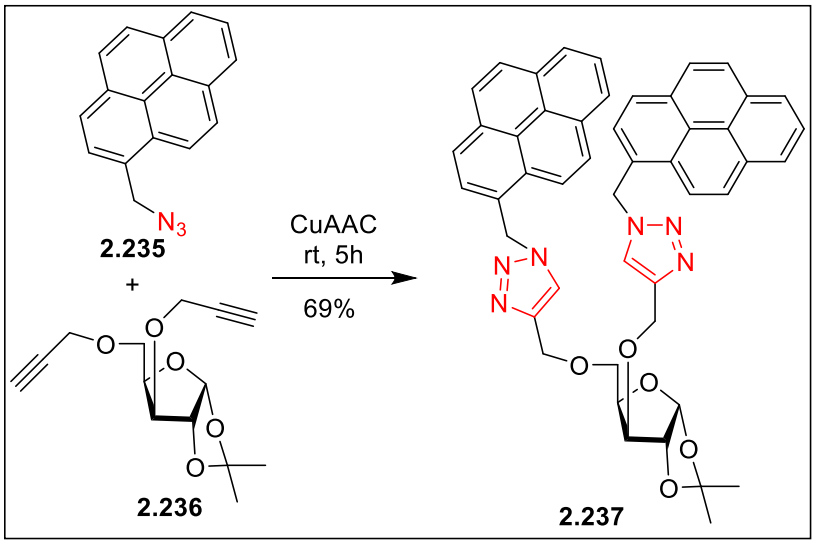

Scheme 2.47

A sequence defined oligotriazole architecture was reported with excellent stereoregularity on the basis of 1,4,5-trisubstituted chiral monomers. The chiral triazole monomers were synthesized from the reaction of one L-prolinol-derived azide **2.239** (Scheme 2.48) with different internal 1-thioalkynes **2.238** under mild IrAAC (Ir-catalyzed azide-alkyne cycloaddition)conditions. The triazole-prolinol hybrid **2.240** was deprotected to get **2.242** and on the other hand the same molecule was brominated to **2.241**. These two building blocks **2.241** and **2.242** were coupled through a simple displacement to afford a bistriazolyalted dimer **2.243**. This strategy was also used to couple two different SR containing monomers prepared by selecting alkynes **2.238a-d**. A judicial choice of this strategy led to the synthesis of a polymer **2.244** made of octatriazoles functionalized with all the alkynes under complete control. The stereoregularity was identified by circular dichroism (Scheme 2.48).[65]

A propargylated chalcone derivative **2.245** was subjected to click reactions with 1,4-diazobutane or 1,6-diazohexane to afford bistriazolides **2.246** and **2.247**. These compounds along with several other mono- and bistriazolides were tested for their inhibitory effects against the glutathione S-transferase, acetylcholinesterase, and butyrylcholinesterase. These two compounds showed efficient inhibition agains all

these molecules at micromolar levels. Docking experiments validated the experimental results by showing the most efficient binding with the active sites of these enzymes (Scheme 2.49).[66]

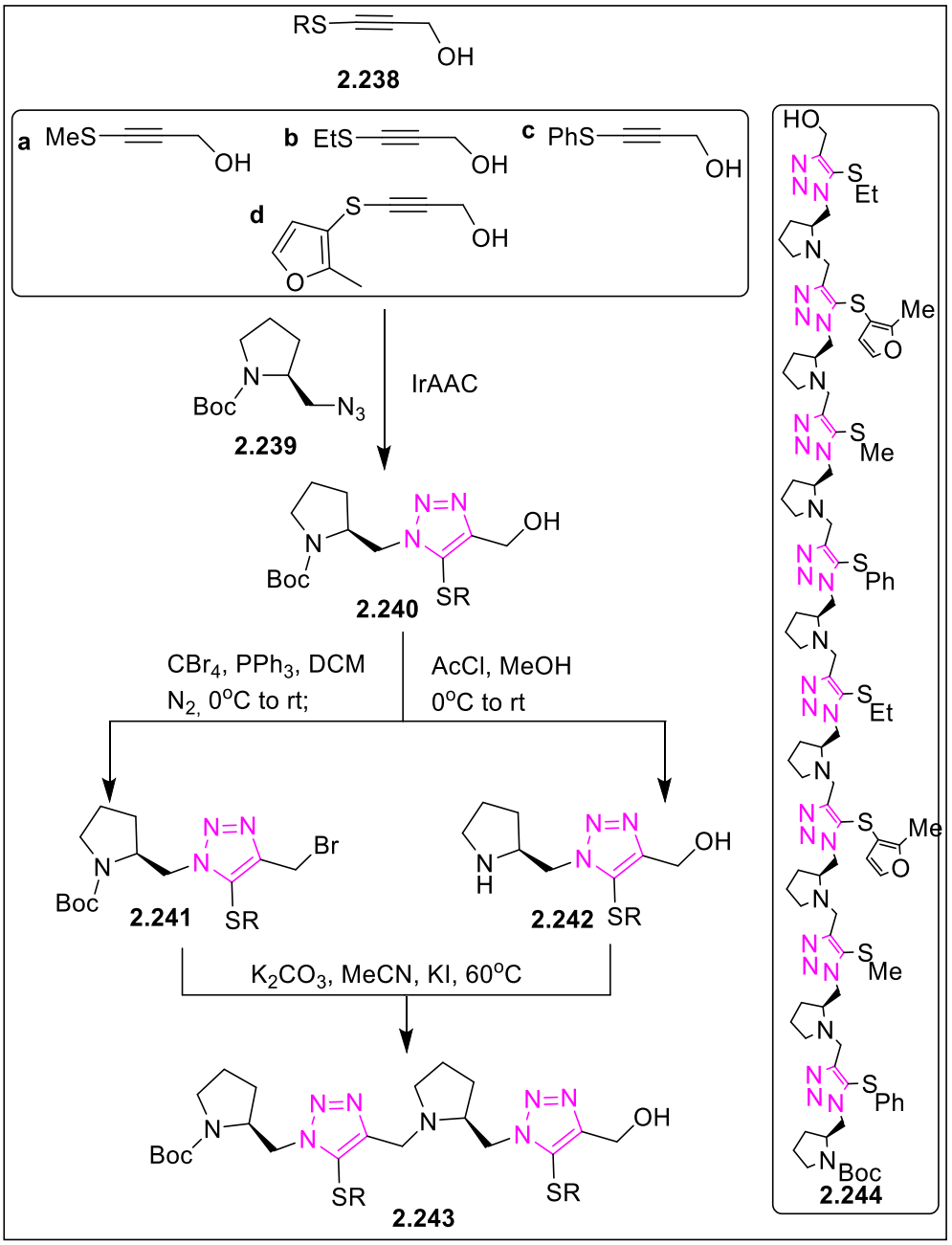

Scheme 2.48

A new family of water-soluble carbohydrate polymers based on chitosan was recently reported. C-2 primary amino groups of chitosan were converted to the corresponding azide by using imidazole sulfonyl azide. The azido derivative of chitosan **2.248** (Scheme 2.50) was reacted, for example with N-propargyl-*N,N,N*-trimethylammonium bromide **2.249** to afford the triethylammonium tethered 1,4-DT functionalized chitosan or chitotriazolan **2.250**. Several cationinc, anionic and neutral deivatives with 1,4-DT residues **a-i** were prepared using similar strategies. Some of these derivatives were soluble in water under neutral or basic

conditions. The cationic chitotriazolan, such as **2.250** showed significant antibacterial activity against *S. aureus* and *E. coli* at pH 7.2, whereas the anionic derivatives were found to be inactive (Scheme 2.50).[67]

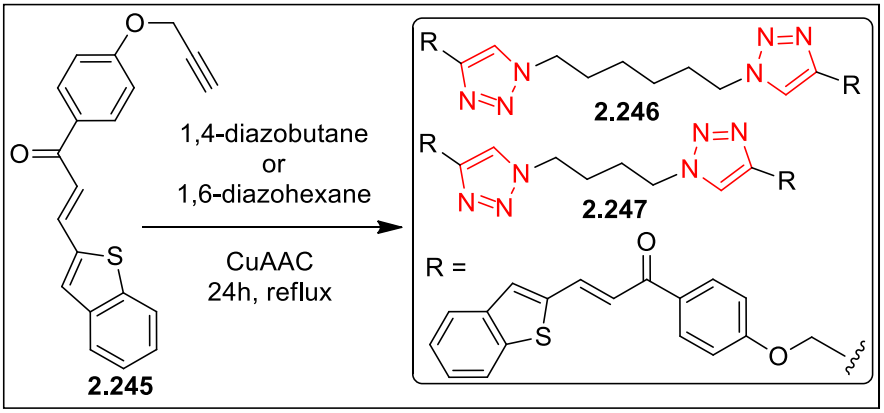

Scheme 2.49

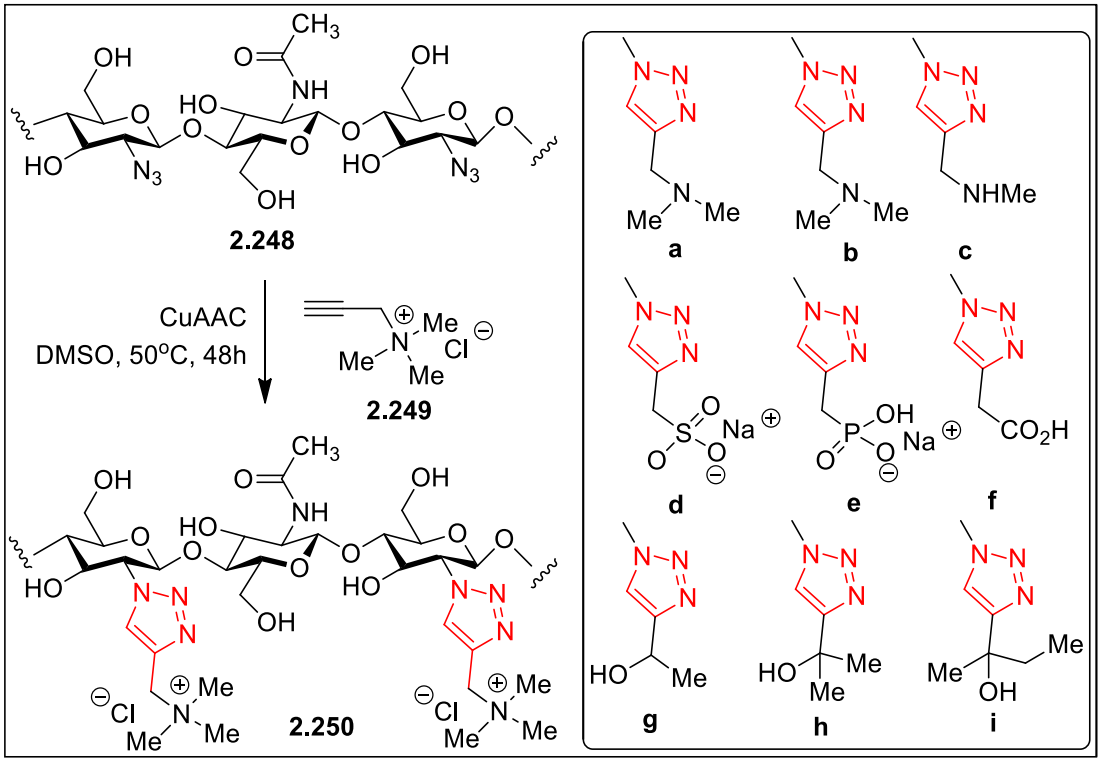

Scheme 2.50

Replication of sequence information with mutation is the molecular basis for the evolution of functional biopolymers. Template **2.251** (Scheme 2.51) was reacted with different proportions of monomers **2.252** and **2.256** via ester coupling using N-(3-dimethylaminopropyl)-N'-ethylcarbodiimide (EDC)/dimethylaminopyridine as coupling reagents. This step determined the mutation ratios of the process, as the pre ZIP intermediates (such as **2.253**) were enriched in phenol or benzoic acid monomers (0%, 38%, 54%, 75% or 100%) according to the initial ratio of monomers **2.252** and **2.256** used mixed in various ratios (0%, 38%, 54%, 75% or 100%). Then the products (e.g. **2.253** when only **2.252** was used) were "zipped" using CuAAC chemistry to form the 1,4-DT

linkages (such as **2.254**) in the newly attached **2.252** and/or **2.256**. The products were then hydrolyzed to remove the 4,4'-biphenol linker (represented by thick black bond) to generate a new strand from each experiment. Exclusive use of **2.252** and **2.256** generated the same **2.255** or complimentary sequence **2.257** respectively and the template **2.251** was released for a new cycle of reaction. The terminal *tert*-butyl group, delivered by the capping alkyne differentiated the copied products (e.g. **2.255** or **2.257**) from the original template **2.251**. This report demonstrated that the covalent "base-pairing" strategies were capable of introducing controlled mutation in synthetic oligomers (Scheme 2.51).[68]

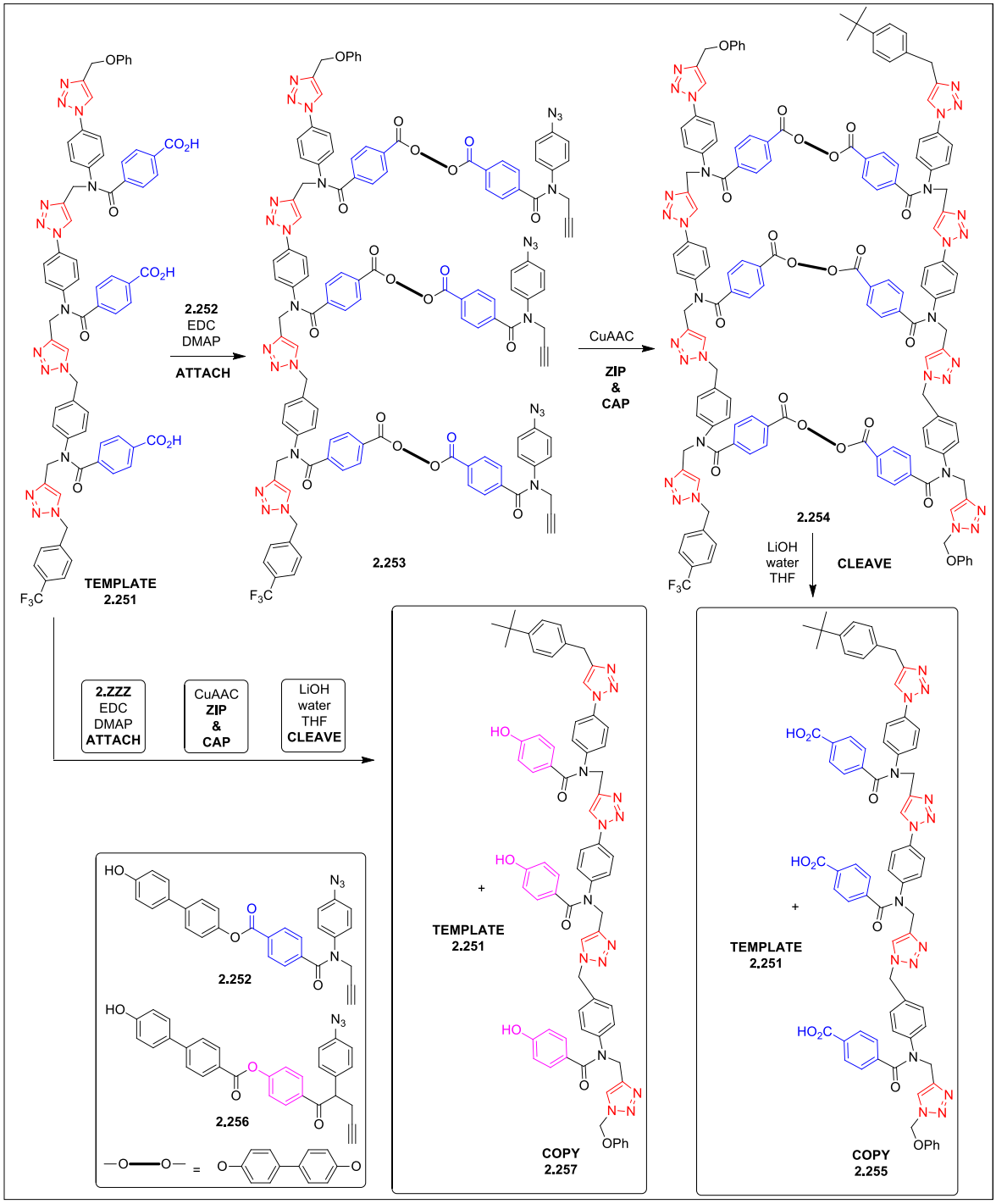

Scheme 2.51

A chelation assisted CuAAC domino reaction was reported. In this case, aryl azides (e.g. **2.258;** Scheme 2.52) containing polar $X^+–O^-$ group ($X^+–O^-$ = $P(O)(NR_2)_2$, $P(O)Ph_2$, SO_3H) at the *ortho* position performed a Cu(I) catalyzed cycloaddition with terminal alkynes followed by in situ electrophilic trapping with a second equivalent of azide to produce fully decorated 1,2,3- triazoles with a triazenyl moiety chemo- and regioselectively. For example, the reactions of 4 equivalents of **2.258** with 1,3-diethynylbenzene **2.30** afforded a bis(triazenyltriazole) **2.261** from a mixture of products **2.259** and **2.260**. On the other hand, reaction of **2.258** with 1 equivalent of pre-formed 1-copper (I) 4- fluorophenylacetyene afforded the dicopper(I) triazoletriazenide **2.262** in 56% yield. The active catalytic species **2.262** was characterized by X-ray diffraction and its catalytic activity was demonstrated in a standard azide−alkyne−azide coupling reaction (Scheme 2.52).[69]

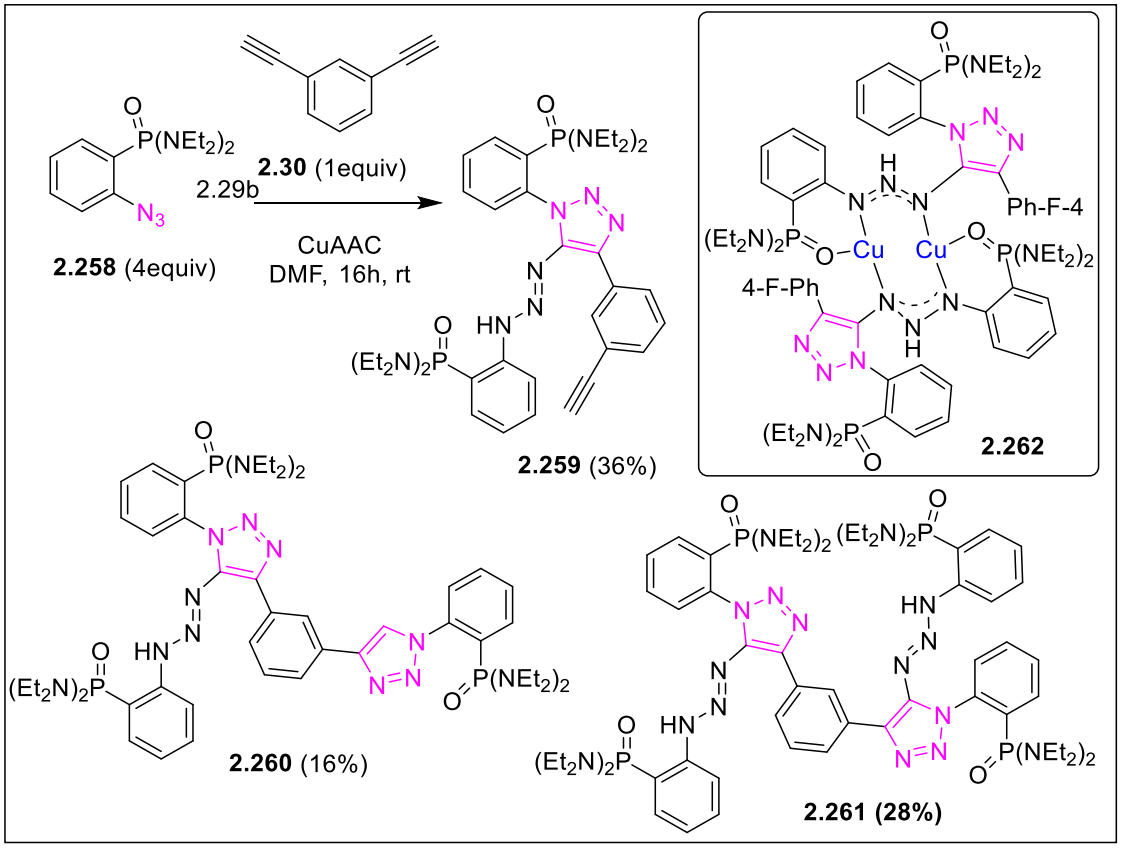

Scheme 2.52

Fluorinated boron-dipyrromethene (BODIPY) linked 1,2,3-bis triazole based on catechol was designed as chemosensor and synthesized by using conventional CuAAC strategy. Thus, two equivalents of azido-BODIPY **2.263** was reacted with one equivalent of 1,2-bis(prop-2-ynyloxy)benzene **2.264** to generate a new bifunctional fluorescent sensor **2.265**. Spectroscopic studies revealed that the sensor acted as a "turn-on" fluorescent probe for dual recognition of Hg(II) and Ag(I) ions. The sensor **2.265** clearly distinguished between Hg(II) and Ag(I) by the use of EDTA. ^{1}H NMR experiments suggested that the triazole moieties were involved in the recognition process (Scheme 2.53).[70]

The synthesis of a new tritriazolic compound namely, 1,10 -(2-[{4,5-bis(methoxycarbonyl)-1H-1,2,3-triazol-1-yl}methyl]-2-[(4-methylphenyl)sulfonamido]propane-1,3-diyl)bis(1H-1,2,3- triazole-4,5-dicarboxylate) **2.268**

was reported by using 1,3-dipolar cycloaddition reaction. The corresponding triazide **2.266** derived from the fully tosylated derivative **2.266** was reacted with excess of alkyne resulting in the formation of the desired cycloadduct **2.268**. The structure of the tristriazole **2.268** was elucidated by various spectroscopic and elemental analysis (Scheme 2.54).[71]

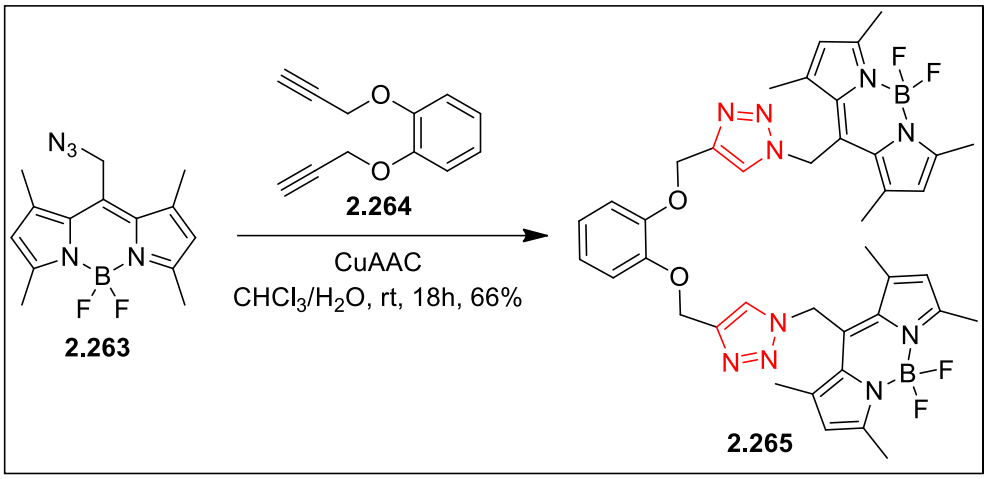

Scheme 2.53

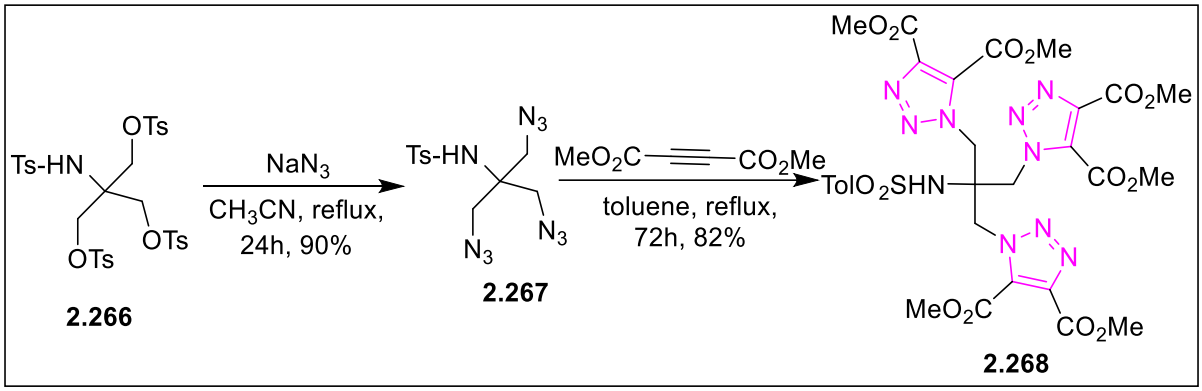

Scheme 2.54

A series of aryloxy-tethered and amide-linked symmetrical 1,2,3-triazole hybrids were synthesized by CuAAC approach. Thus, bisalkynes **2.269** or **2.264** (Scheme 2.55) were coupled with amidoazides **2.270/2.271** or **2.274** respectively. Twenty six such compounds were evaluated for their *in vitro* antifungal activity against different fungal strains as well as the enzymatic study for the inhibition of lanosterol 14 α-demethylase enzyme. Compound **2.272** was found to be most potent against all the tested fungal strains. Furthermore, the enzymatic study revealed that compounds **2.273** and **2.275** were the most promising inhibitors of the enzyme. The molecular docking study showed the highest binding affinity of **2.275** with the active site of the enzyme (Scheme 2.55).[72] Related symmetrical bis(urea-1,2,3triazole) hybrids were synthesized via click chemistry and tested against three bacterial strains (*Staphylococcus epidermidis*, *Escherichia coli* and *Bacillus subtilis*) and two fungal strains (*Aspergillus niger* and *Candida albicans*).[73]

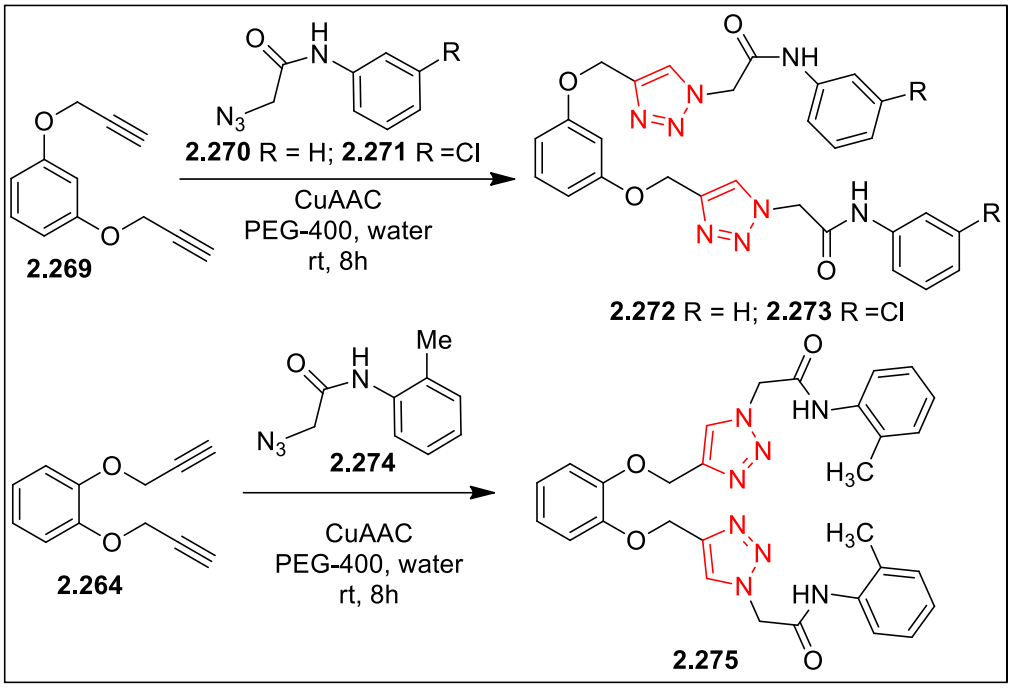

Scheme 2.55

An efficient method was developed to assemble modules onto diazide, triazide, and tetrazide platforms by consecutive azido-type selective triazole formations. Reaction sequences were selected based on the functional group tolerance. The strategy led to the preparation of tri- and di-triazolylated molecules **2.276-2.278** (Scheme 2.56). For the synthesis of the tetrafunctionalized probe **2.281**, the tetraazide **2.279** was reacted first with 1,3-diketone under basic conditions; triazolylation proceeded selectively at the unhindered aromatic azido group due to the stabilization of the anionic intermediate by the aryl group. The RuAAC reaction selectively triazolylated the unhindered benzyl azide group. Thirdly, the strain promoted reactions of cyclooctyne **2.280** at the 2,6-diisopropylphenyl azido group took place efficiently; the reaction was facilitated by the steric inhibition of resonance. The residual 1-adamantyl azido group was coupled with the terminal alkyne using $(MeCN)_4CuBF_4$ as the catalyst to afford the tetratriazole derivative **2.281** (Scheme 2.56).[74]

The bisalkyne **2.282** derived from the known *O*-cresolphthalein, a phthalein dye was coupled with benzylazide using $[Cu(PPh_3)_3Br]$ technique to afford a fiuorescent probe **2.283**, which was studied for its sensing abaility with a series of metal ions. The UV-visible study established the sensitivity exclusively towards Pb(II) ions with a measured detection limit of 13 µM at 2:1 stoichiometry of **2.283:Pb(II)** complex. (Scheme 2.57).[75]

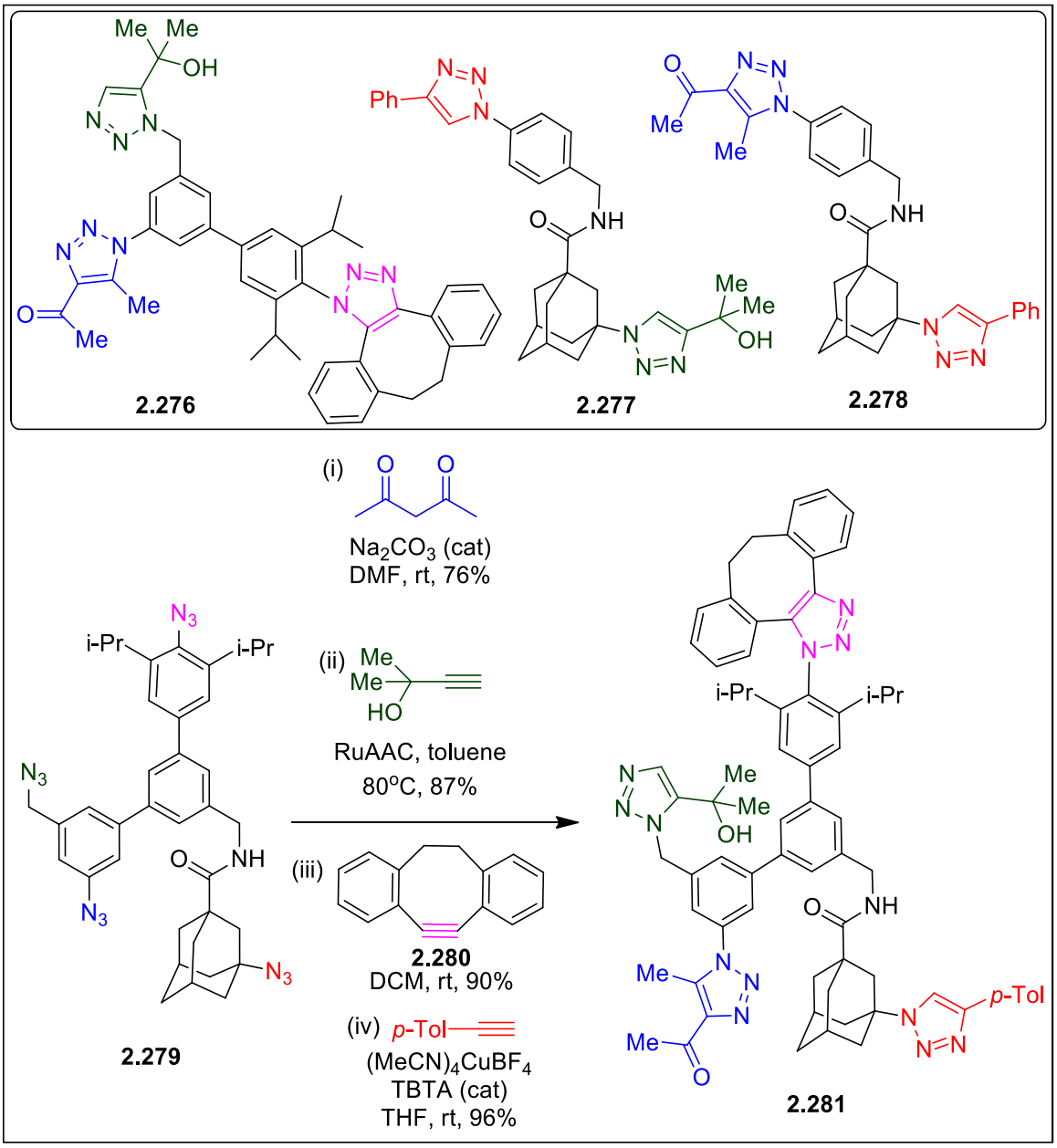

Scheme 2.56

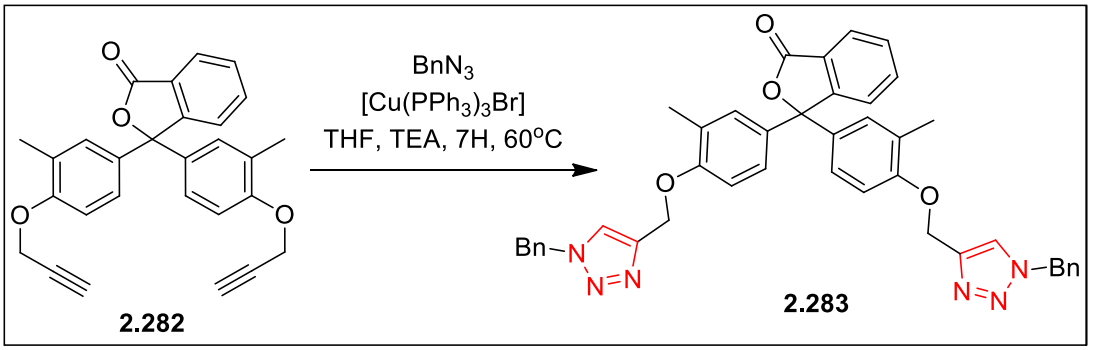

Scheme 2.57

1,4-Dihydroxyanthraquinone based 1,2,3-triazole linkers were used for their sensing behaviour for the selective detection of Fe(II) ions by UV–Visible spectroscopy. Thus, the bisalkyne **2.284** was reacted with the azide **2.285** to afford 1,4-DT based sensor **2.286**. UV–Visible absorption studies were performed with a set of metal ions such as Mn (II), Cd (II) Hg (II), Ni (II), Pb (II), Zn (II), Fe (II), Fe (III), Ce (III), Cr (III), Co (II), Ba (II), K (I) and Na (I). The significant change in absorption spectrum was observed for the probes with the addition of Fe (II) ions (Scheme 2.58).[76]

Benzene-based triazolylated semicircular hybrid molecules carrying different polar functionalities were synthesized and screened for their RNase A inhibitory potencies. The synthesis was started with the click coupling of the diazido benzoic acid derivative **2.287** with propargyl alcohol; the product **2.288** was mesylated to **2.289** and the latter was converted to the desired 3,5- bis[4-(sulfomethyl)-1H-1,2,3-triazol-1-yl]benzoic acid **2.290** using strategies for the synthesis of **2.179** and **2.180** reported above. In a series of ten such new compounds, the presence of the carboxylic acid group at the C1-position of the 1,3,5- trisubstituted benzene ring enhanced the inhibitory properties significantly. Furthermore, the studies revealed that the reduced arm lengths of 3,5-substituents resulted in a better geometric complementarity that made the molecules fit favorably in the semicircular cavity of the active site of RNase A as visualized by docking studies. Compound **2.290** exhibited the highest inhibition efficiency with a Ki value of 12 ± 0.9 µM (Scheme 2.59).[77]

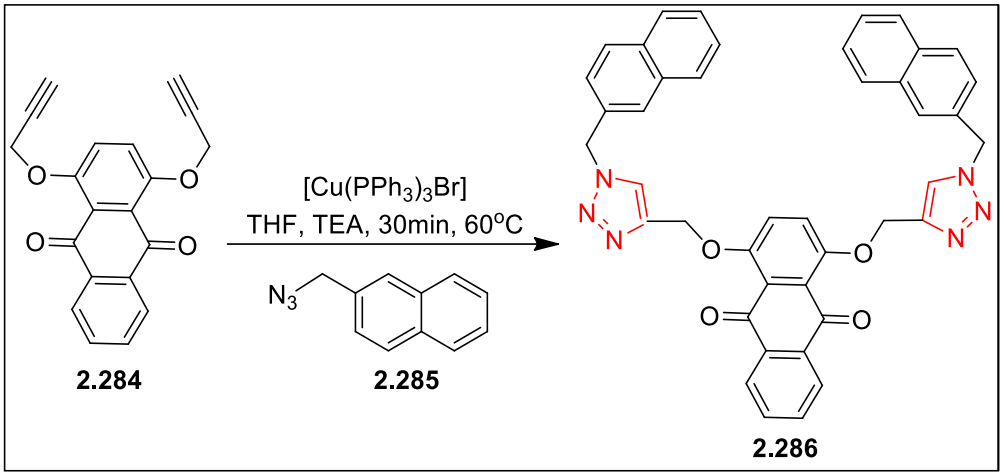

Scheme 2.58

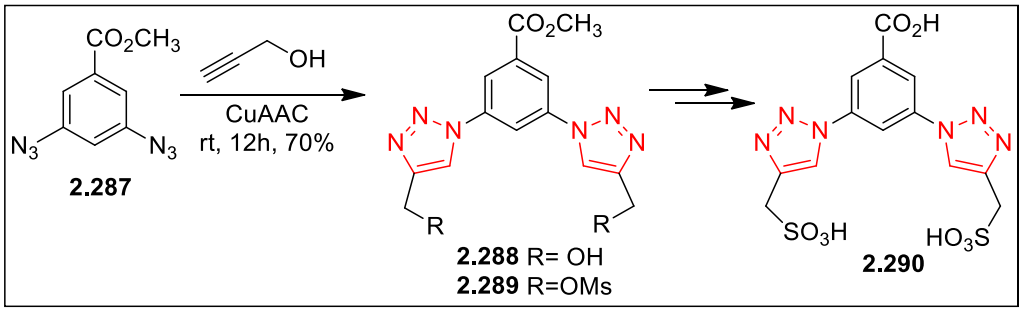

Scheme 2.59

3. N-(CH)n-C linked triazolamers

Triazolamers are triazole-based oligomers where monomeric triazole units are connected by "*N-(CH)$_n$-C*" linkage forming mostly a linear chain consisting of several triazole rings. From the structural elucidation, it was confirmed that oligomers adopt zigzag conformations, with an adjacent triazole unit turned in opposite directions.[78] The non-peptidic triazolmer was introduced in 2005 and was synthesized by iterative sequential growth cycle in a one pot manner. Oligomers composed of 1,4-DTs were reported as being reminiscent of a peptide β-strand conformation (see figure 1.1). The bioactivity evaluations of these nonpeptidic β-strand mimetics showed their potential as protease inhibitors.[9] On the other hand, the construction of peptido triazolamers were reported by incorporationg triazole rings in peptide backbone as alternating triazole and amide connectors.[9] Recently, the synthesis of homochiral and heterochiral 1,5-DT linked peptidotriazolamer was also reported. Synthetic strategy involved either solid phase or solution phase iterative protocols. Structural analysis revealed the self-dimerization property of these class of oligomers through hydrogen bonds. Those oligomers also acted as organogelators.[79] Structural analysis revealed that these oligomers adopted anti conformations, with an adjacent triazole unit turned in opposite directions (Figure 3.1).[80]

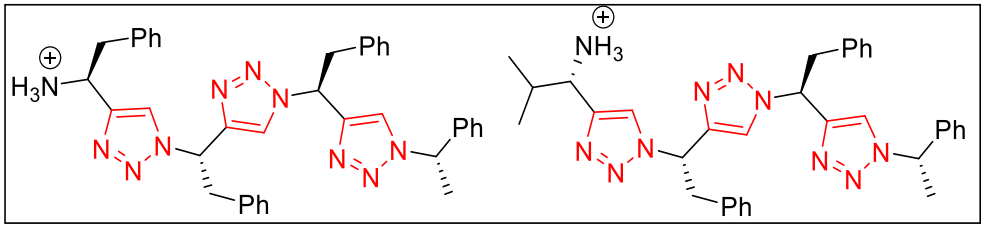

Figure 3.1

3.1. Non-peptido triazolamers

The 1,4-DTs were prepared by generating the azido derivative in situ from the amino acid methyl ester **3.1** and the former was coupled with the aminoalkyne **3.2** using CuAAC strategy. The monotriazole **3.3** was deprotected and the free amine was again azidolyzed and coupled with the same alkyne **3.2** to afford the dimer **3.4**. Repetition of the same sequence of reactions afforded the 1,3-substituted oligomers starting with the trimer **3.5**. The trimer represented a nonpeptidic scaffold capable of displaying protein-like side chains by replacing amide bonds with 1,2,3-triazole rings. Several such oligomers were synthesized and the overall conformation of these triazole oligomers was most likely dictated by dipole-dipole interactions between adjacent rings. 2D NMR study revealed that the backbones of selected triazolamers predominantly adopted zigzag structures arising from the anti- conformation, which was reminiscent of peptide β-strand conformation (Scheme 3.1).[80] Continuing with the same approach, the same group developed further an efficient one-pot, two-step sequence for the preparation of triazoles from the corresponding amino acid-derived amines and alkynes in solution. The one-pot sequence afforded the desired products in significantly higher yields than the previous method. A solid phase method was also developed in parallel.[81]

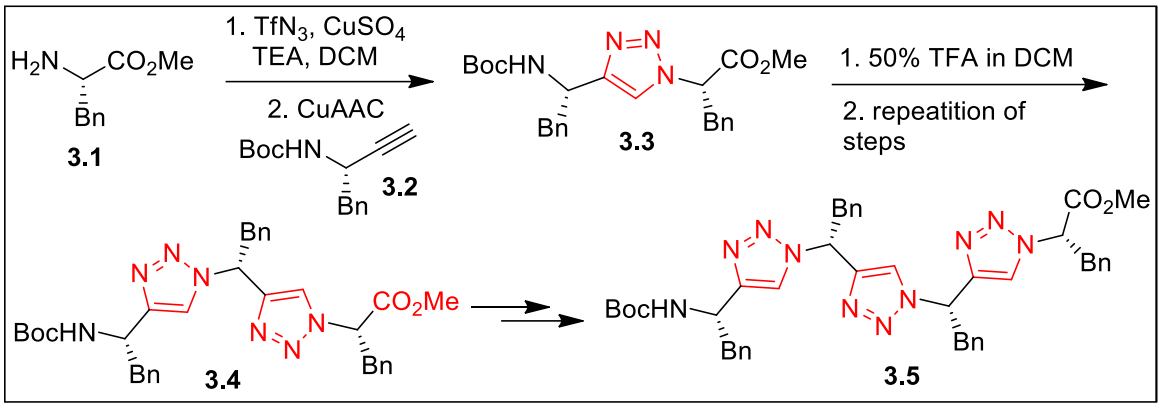

Scheme 3.1

A series of orthogonally protected 1,4-DT (e.g. **3.8a**) were prepared from the corresponding alkynols **3.6** and trialkylsilyl-propargyl azides **3.7** via 1,3-dipolar cycloaddition. The cycloadduct **3.8a** was deprotected to **3.8b** and the latter was coupled with **3.7** to get a dimer **3.9**. Repetition of the same strategy afforded the trimer **3.10**. By synthesizing the dimer **3.11** with a protected amino group, it was possible to extend the chain in a sequential and controlled fashion in either direction (azide or alkyne terminus); in this case, the alcohol and TMS moieties act as precursors/protecting groups for the azide and alkyne reactive groups, respectively. This methodology gave an easy access to triazole-based peptidomimetics in a controlled fashion (Scheme 3.2).[82] The same group used this strategy to increase the diversify of trazolamers by employing 1-phenyl-pent-4-yn-2-(*R*)-ol **3.6a** and trimethylsilyl-homopropargyl azides **3.7a** to afford chirally pure 1,4-DT heterotetramer **3.12,** which was shown to exist in a linear conformation in solution (Scheme 3.2).[83]

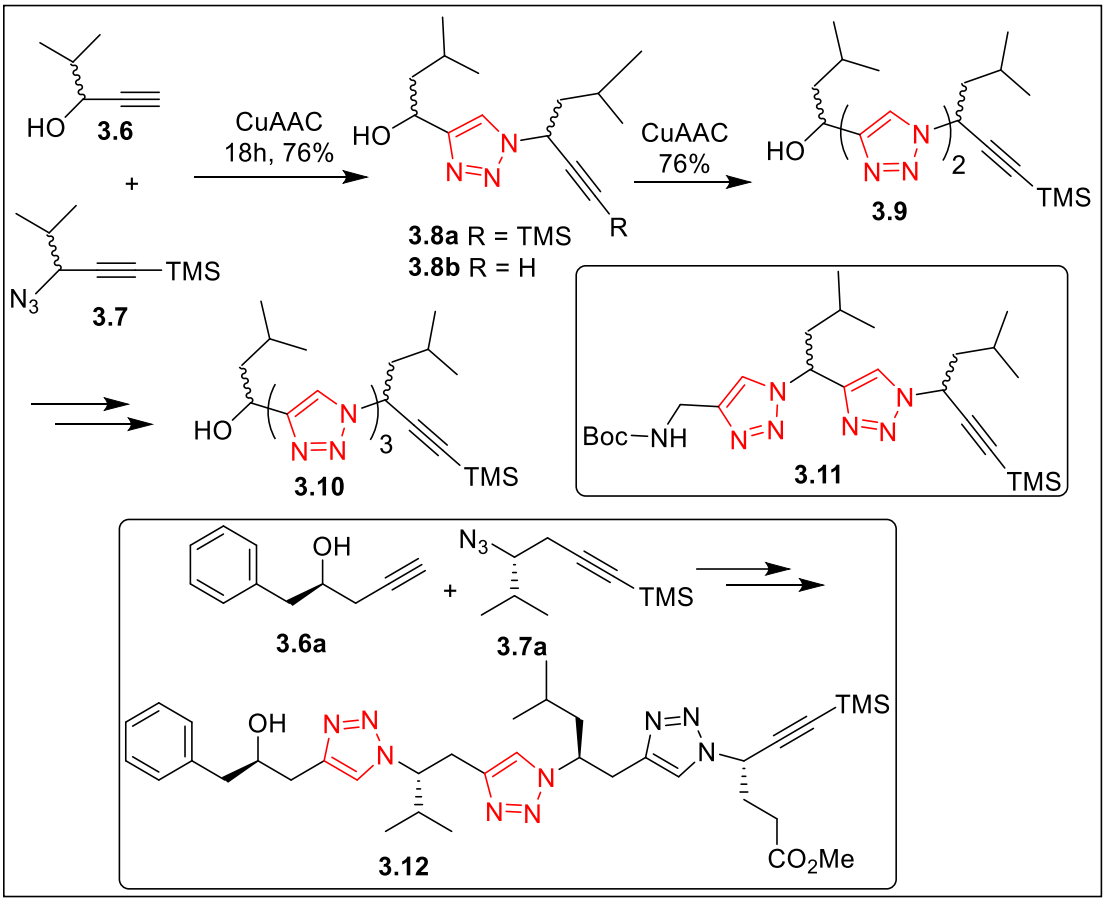

Scheme 3.2

In order to circumvent the conformational and chemical instabilities as well as poor pharmacological properties of peptides a new family of twenty nonpeptidic triazolamers were synthesized and tested for their activities against HIV-1 protease. A triazolamer **3.13** (Scheme 3.3), synthesized following strategies reported above, showed significant activity. However, a solid phase synthesis was utilized for the synthesis of triazolamer **3.18**. Thus, the pre-loaded amino acid **3.14** was deprotected and subjected to diazotransfer reaction using TfN_3. The azido compound **3.15**, thus generated was reacted with the Boc protected amino alkyne **3.2** under CuAAC conditions to afford the monotriazole **3.16**. The steps, deprotection, diazotransfer and click reaction using **3.2** to afford the traizolamer **3.17**. The resin was suspended in ethylenediamine:methanol to remove the resin and deprotected to finally afford triazolamer **3.18** after HPLC purification. Compounds **3.13** and **3.18** inhibited the enzyme activity with K_i values of roughly 25 µM. Oligomers like **3.13** and **3.18** composed of four triazole linkages (and five side chain groups) are the best leads in this group of compounds. Isopropyl groups in place of benzyl groups had detrimental effect. Docking study also justified the best activities of **3.13** and **3.18** (Scheme 3.3).[84]

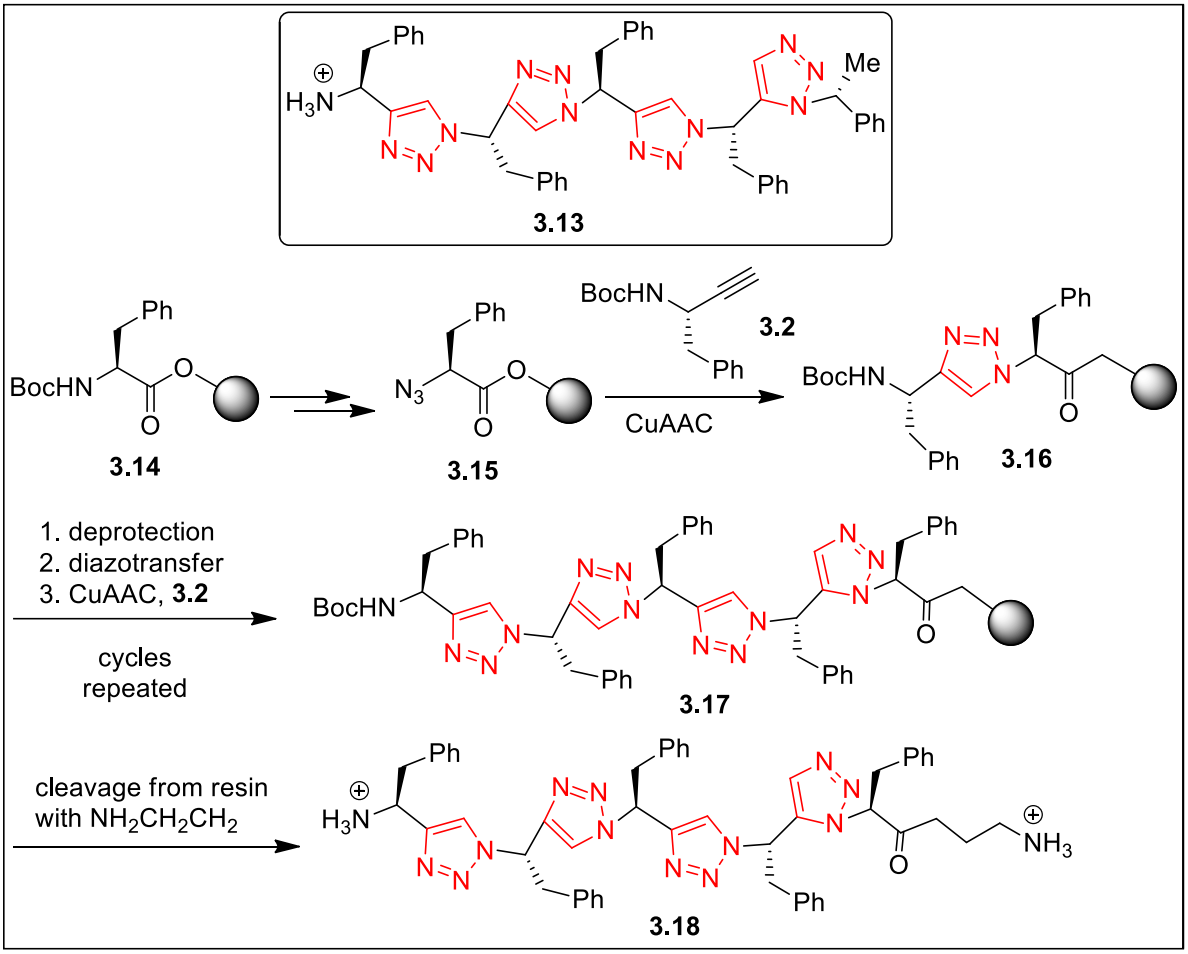

Scheme 3.3

Alkynes are known to form complexes with dicobalt octacarbonyl which can undergo oxidative degradation to liberate the alkyne. This strategy was used for the synthesis of orthogonally functionalized azido-alkynes as the building blocks of triazolamer. Thus, functionalized propargyl alcohols **3.19** were converted to cobalt hexacarbonyl azido alkynes **3.20** and the azido group of one of these building blocks **3.20** (R =H) was reacted with an external alkyne **3.21** avoiding any selfcoupling. Oxidative removal of cobalt with ceric ammonium nitrate (CAN) afforded the monotriazole **3.22**. The free akyne of **3.22** was reacted with the whole series of cobalt hexacarbonyl azido alkynes **3.20 (a-g)** to afford the dimers **3.23.** Reactions of the dimer **3.23** with methyl azidoacetate afforded a triazolamer **3.24** (Scheme 3.4).[85]

4-Bromo-1-butyne was used as the starting material for the synthesis of "-CH_2-CH_2-" linked triazolamers. Thus, CuAAC coupling of 4-Bromo-1-butyne with benzyl or n-octyl azide afforded the monomeric bromotriazoles **3.24a** in excellent yields. Conversion of the bromo derivative to the corresponding azido compounds **3.24b** followed by the CuAAC coupling of the latter with 4-Bromo-1-butyne generated a bromobistriazole **3.25** ready to undergo further azidolysis followed by triazolylation. The strategy led to the synthesis of several triazolamers such as **3.26** and **3.27** (Scheme 3.5).[86]

A series of short triazolamers were derived from quaternary amino acids. Thus, the monotriazole **3.30** (Scheme 3.6) was obtained from the CuAAC coupling of N-Boc protected 2-methyl-3-butyn-2-amine **3.29** with benzylic azides **3.28** functionalized at the *ortho*-position. The triazolamer chain was ready to be extended from

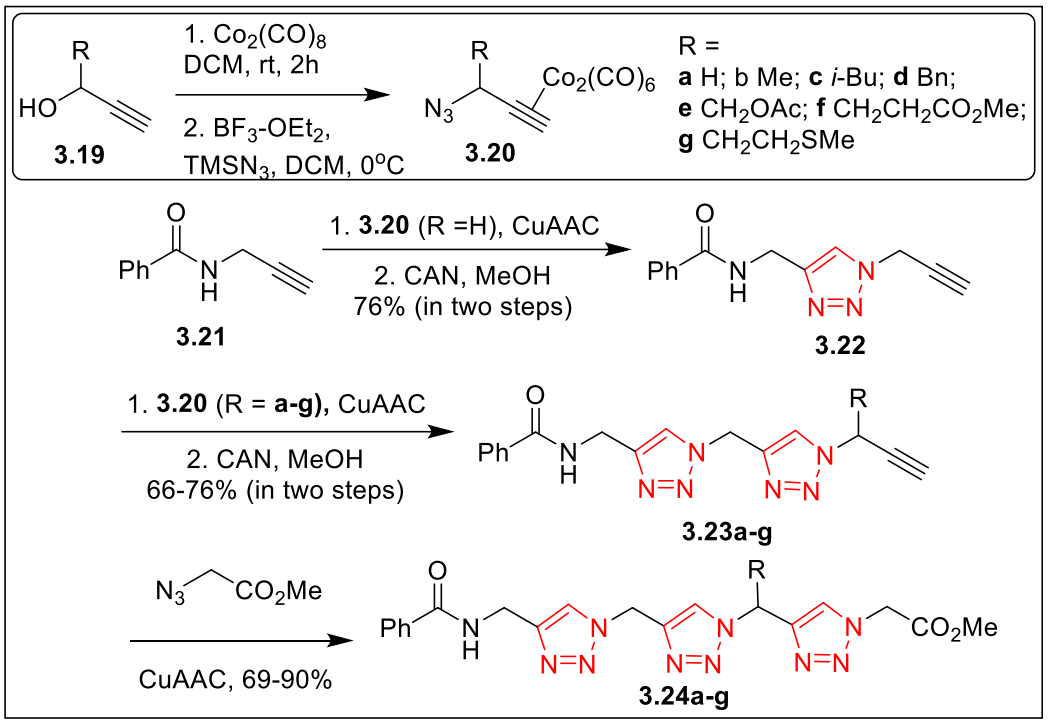

Scheme 3.4

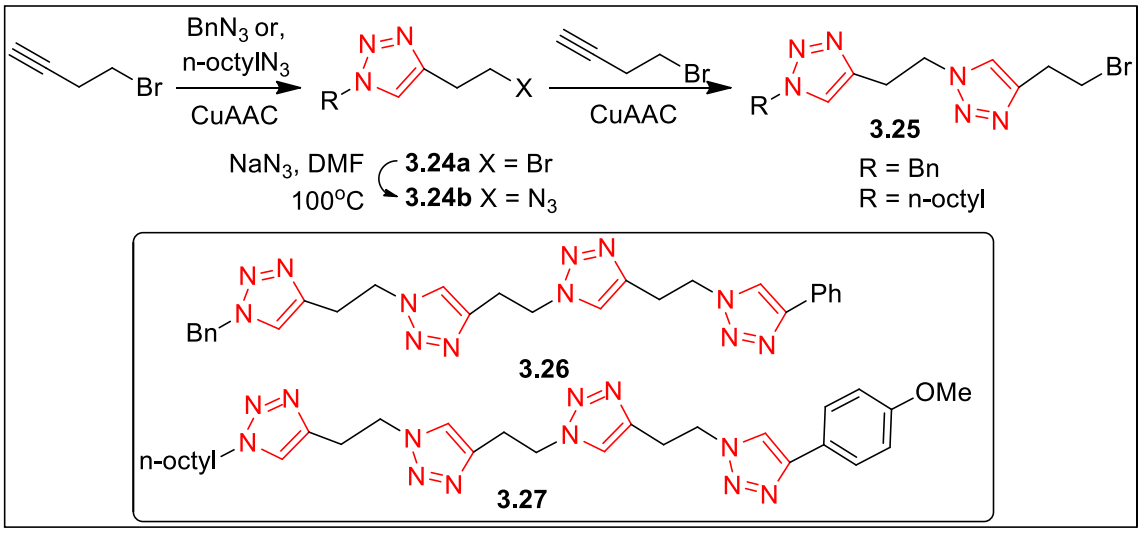

Scheme 3.5

the 'C-terminus' to the 'N-terminus' as in peptide synthesis. After amine deprotection of **3.30** and azide transfer reaction, the product was coupled with **3.29** to obtain the dimer **3.31**. The strategy was repeated one more time and at the end coupling of the second quaternary amino acid **3.32** afforded tetramers **3.33**. The ortho-substituted benzyl azides were used to induce a certain rotational constriction. NMR studies indicated that several conformations probably existed in solution together with aggregation. NMR and X-ray diffraction studies provided evidence that the oligomers existed as twisted strands or zig-zag structures, depending on the compound substituents. The presence of folded structures was observed for residues with bulky *N*-groups and rotationally restricted benzylic protons in solvents like chloroform and acetonitrile. The conformational

behaviour was shown to have similarities to that of natural peptides. The overall study identified the "conformational promiscuity" in this class of triazolamers mimicking peptide behaviour (Scheme 3.6).[87]

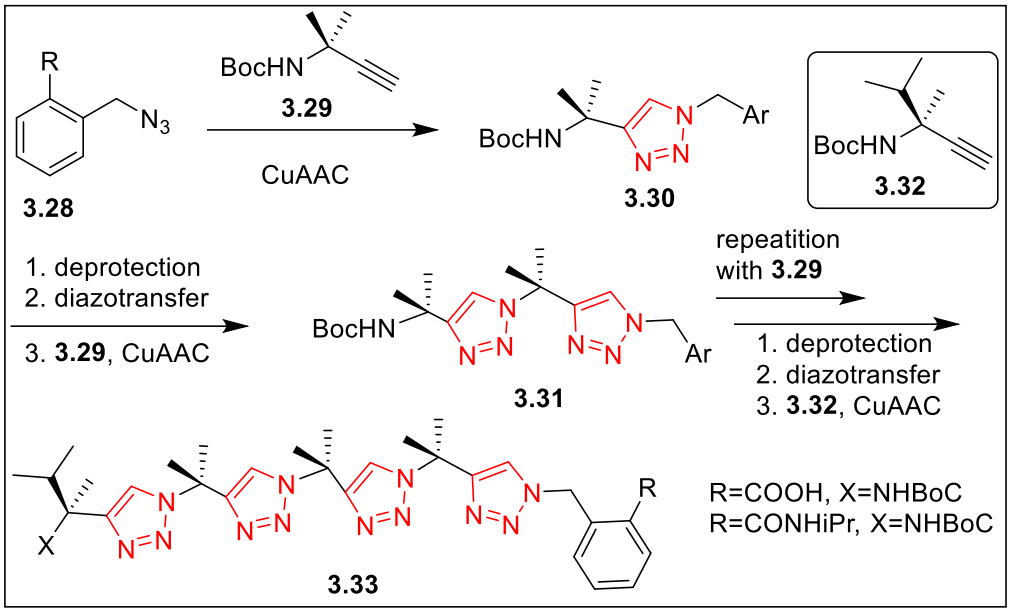

Scheme 3.6

α-Hydroxy-β-azidotetrazoles **3.35** (Scheme 3.7), easily prepared in one step from α,β-epoxynitriles **3.34**, was introduced as latent alkyne scaffolds for orthogonal CuAAC reactions performed on the same carbon atom. The tetrazole **3.35** was converted to a 1,4-DT tetrazole hybrid **3.36** using CuAAC reaction conditions. On treatment with N-(3-dimethylaminopropyl)-N'-ethylcarbodiimide (EDC) or diisopropylcarbodiimide (DIC), the tetrazole moiety was known to generate the alkyne residue. The intermediate was a tetraazaflvene **3.37**, which decomposed to vinylidene carbene **3.37a** and the carbene afforded the alkyne **3.38** via a Fritsch–Buttenberg–Wiechell rearrangement. A wide range of 1,4-DT tetrazole hybrids (as in **3.36**) were prepared and converted to the corresponding alkynes (as in **3.38**). Several bistriazoles were synthesized using this strategy. A tetrazole containing triazolamer **3.42** was prepared in steps by coupling **3.35** (X = Y =Et) with 1,4-DT containing alkyne **3.39** to afford a bistriazolamer (Scheme 3.7).[88]

In an attempt to design a crescent shaped structure as the potential inhibitor of RNase A, a 1,4-DT-1,4,5-TT-ribose hybrid molecule was introduced. Synthetic strategy involved azidation of ribosfuranosyl derivative **3.44** to **3.45**, followed by cycloaddition with dimethyl acetylenedicarboxylate (DMAD) to afford compound **3.46**. Compound **3.46** was subjected to deisopropylidenation followed by hydrolysis to generate the final product **3.47.** This final product was shown to be a moderate inhibitor of RNase A (Scheme 3.8).[51]

Minigastrin (H-Leu-Glu-Glu-Glu-Glu-Glu-Ala11-Tyr12-Gly13-Trp14-Met15-Asp16-Phe17-NH_2) is a potential drug for thyroid carcinoma. The radiolabeled shorter version of minigastrin, for example, leutetium (^{177}Lu) labeled tumor-targeting analog (DOTA-DGlu^{10}-Ala^{11}-Tyr^{12}-Gly^{13}-Trp^{14}-Nle^{15}-Asp^{16}-Phe^{17}-NH_2,) is a useful therapeutic agent for targeting such tumors. A truncated analog of minigastrin having a mono-1,4-DT instead of a single amide bond resulted in the stabilization and significant enhancement in the affinity of a peptidic ligand for the cholecystokinin-2 receptor (CCK2R). Therefore three 1,4-DT units were incorporated replacing appropriate amide positions for substitutions which contributed to enhanced stability or affinity in order to

probe for synergistic or additive effects. The synthesis of **3.56** was initiated with the preparation of α-amino alkynes **3.51**

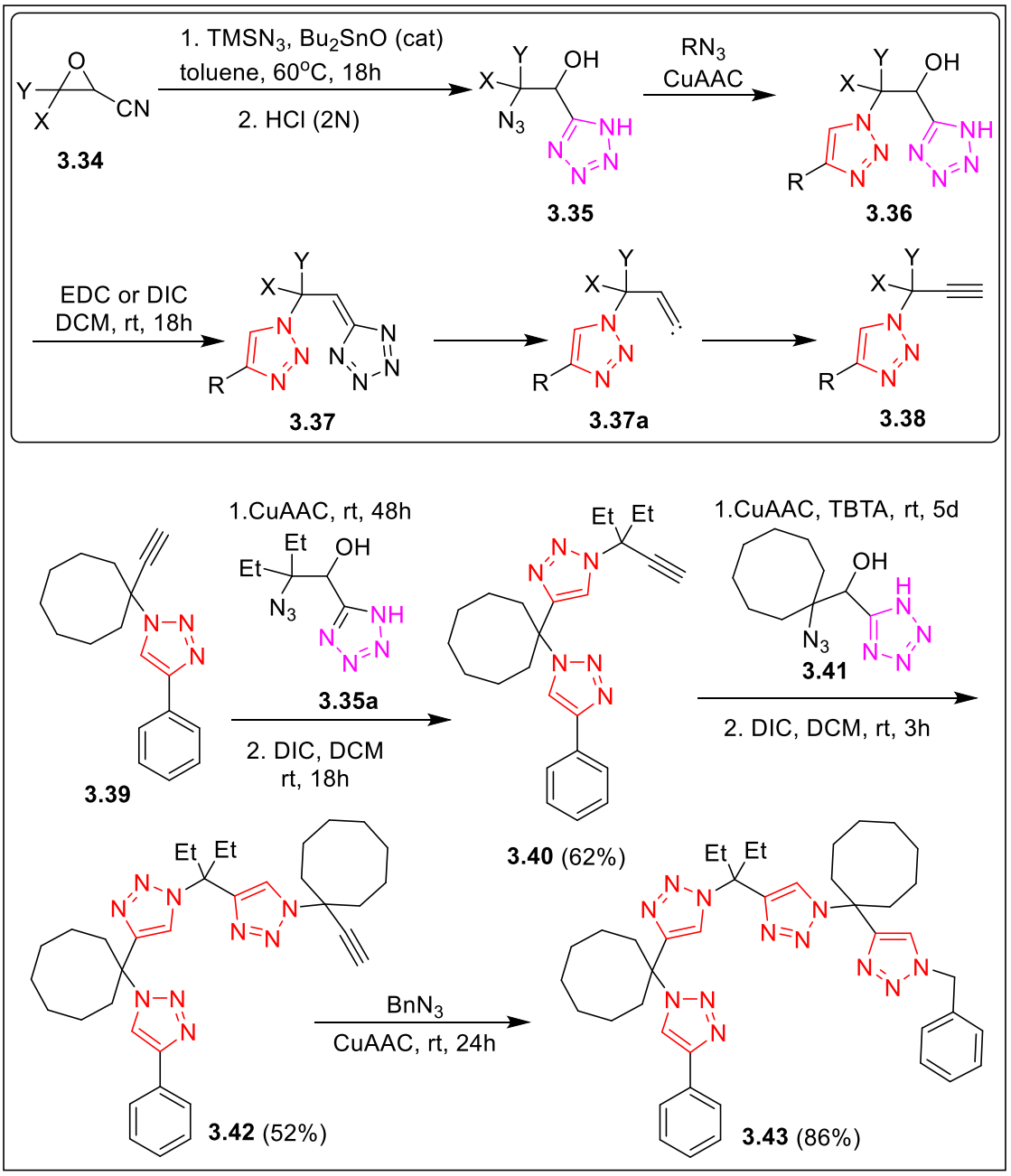

Scheme 3.7

(Scheme 3.9) from protected amino acids **3.48** which were convereted to the corresponding aldehydes **3.49**. These aldehydes **3.49** were converted to the alkynes using the Bestmann–Ohira reagent dimethyl (1-diazo-2-oxopropyl)phosphonate **3.50**. The α-amino alkynes **3.51** were analyzed for racemization by formation of a diastereomer which was characterized. If necessary, enantiomers of α-amino alkynes **3.51** were separated by semipreparative chiral HPLC. Azide precursors **3.55** were prepared on solid phase by standard solid-phase peptide synthesis (**3.52** → **3.53**) followed by a diazotransfer reaction of the deprotected *N*-terminal amine group **3.53** at the desired position using imidazole-1-sulfonyl azide·HCl **3.54**. The reaction of azide-

functionalized peptides with α-amino alkynes and tetrakis(acetonitrile)copper(I)·PF6 as catalyst yielded the 1,4-DTs also on the solid support. Completion of the peptide sequences including the final coupling of DOTA to the N-terminus of the peptidomimetics was accomplished by standard solid-phase peptide synthesis or repetition of the diazotransfer/Cu(I) coupling reaction sequence, respectively. The precursors for radio metal

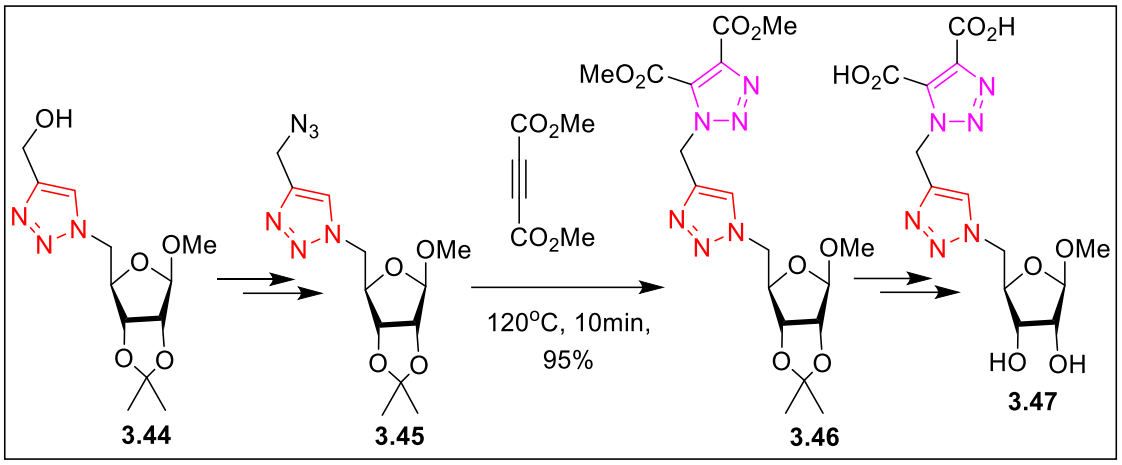

Scheme 3.8

labeling were obtained, after purification by semipreparative HPLC, in satisfying yields of 6–25% and high purities >95%. This study confirmed that the systematic replacement of single or multiple amide bonds in peptides with metabolically stable 1,4-DTs is a promising strategy for the designing of peptidomimetics with improved tumor-targeting properties (Scheme 3.9).[89,90]

3.2. Peptidotriazolamers

An alternative combination of amide and triazole linkage using solid phase synthesis generated unnatural peptidotriazoles (such as **3.66**). The butyne carboxylic acid **3.62** (Scheme 3.10) was attached to the solid support **3.61** using usual peptide coupling reagents. The best condition identified for Cu(I) based coupling was to use excess of CuI and ascorbic acid in presence of 20% piperidine in DMF. This reaction condition coupled azide **3.57** and also deprotected the amino group to afford free amino 1,4-DT **3.64**. A series of enantiomerically pure azido-amines **3.57**-**3.60** were synthesized for this study. Another peptide coupling of **3.64** with **3.62** afforded **3.65** ready for the next click reaction with **3.58**. Henceforth, the same reaction cycles were repeated until **3.58** was attached to generate peptidotriazolamer **3.66** obtained after cleavage, deprotection purification. This approach provided a strategy for the synthesis of peptidomimetics with triazole-mixed backbones (Scheme 3.10).[91]

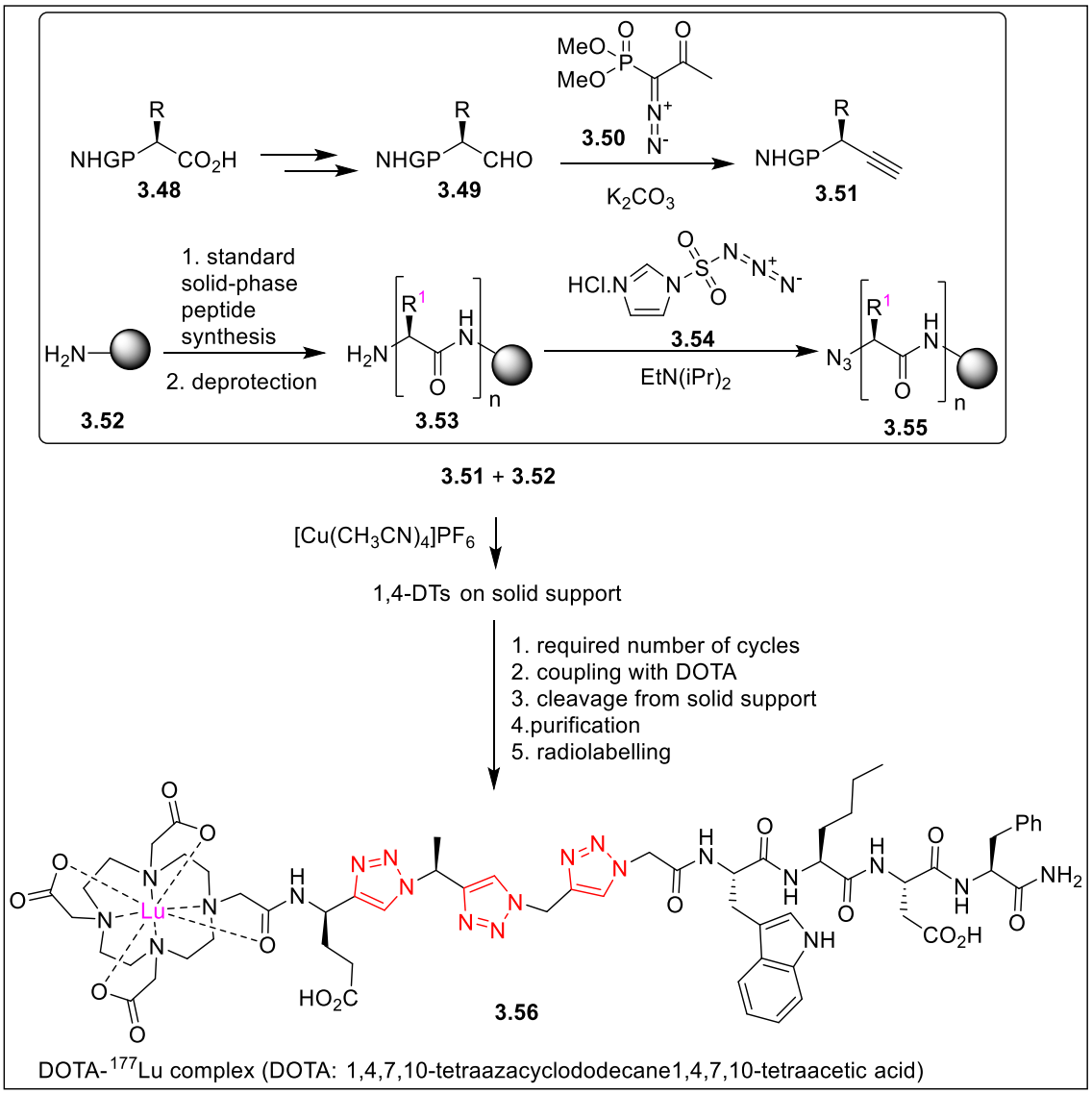

Scheme 3.9

Efforts are currently underway to synthesize cyclic peptides and peptidomimetics. However, cyclization of tetra-, penta-, and hexapeptides made of L-amino acids is known to be problematic, particularly in the absence of glycine, proline, or a D-amino acid. 1,4-DTs are known for inducing □-turn in cyclic peptides. The efficiency of click reaction was examined in the macrocyclization of resin-bound tri-, tetra-, penta-, hexa-, and heptapeptides in the absence of turn-promoting amino acids. Thus, the amino acids were incorporated on the resin carrying the monomeric alkyne **3.67** via usual peptide synthesis. Usual peptide synthesis afforded the linear oligomers **3.68** (n = 1-5). The azido-alkyne oligomers were allowed to undergo cyclization using non-catalytic Cu(I) assisted reactions. Although the crude yields of these reactions were >95%, the yields of the monomeric 1,4-DT fused triazoles **3.69** ranged between 0-27% because the majority of the products were lost on HPLC purification. For n=1 only dimeric cyclic product **3.70** was formed. This study demonstrated that the efficiency of cyclization was dependent on the length, sequence etc of the linear peptide but indicated the potential of resin-based strategy for peptidomimetic synthesis (Scheme 3.11).[92]

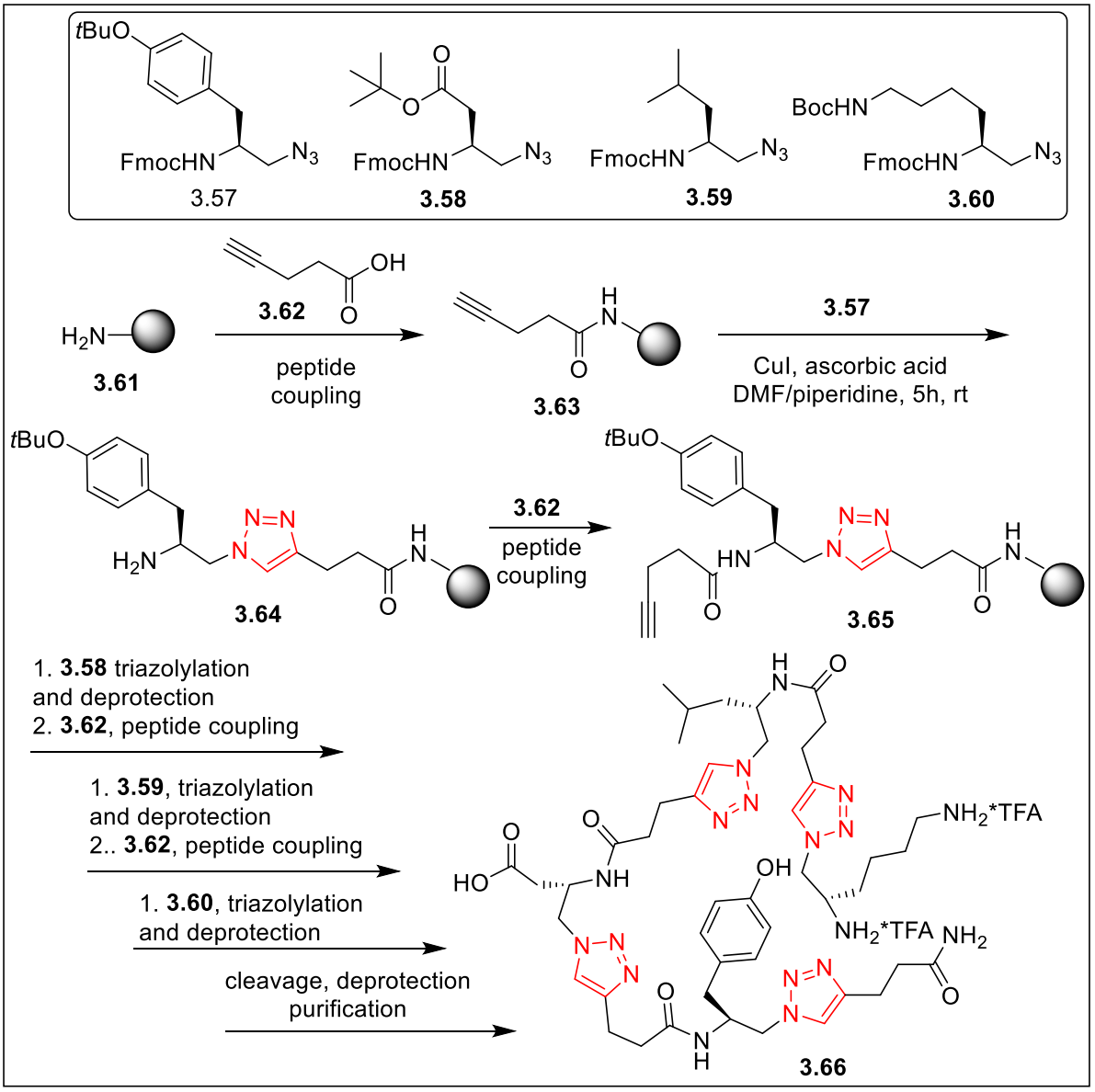

Scheme 3.10

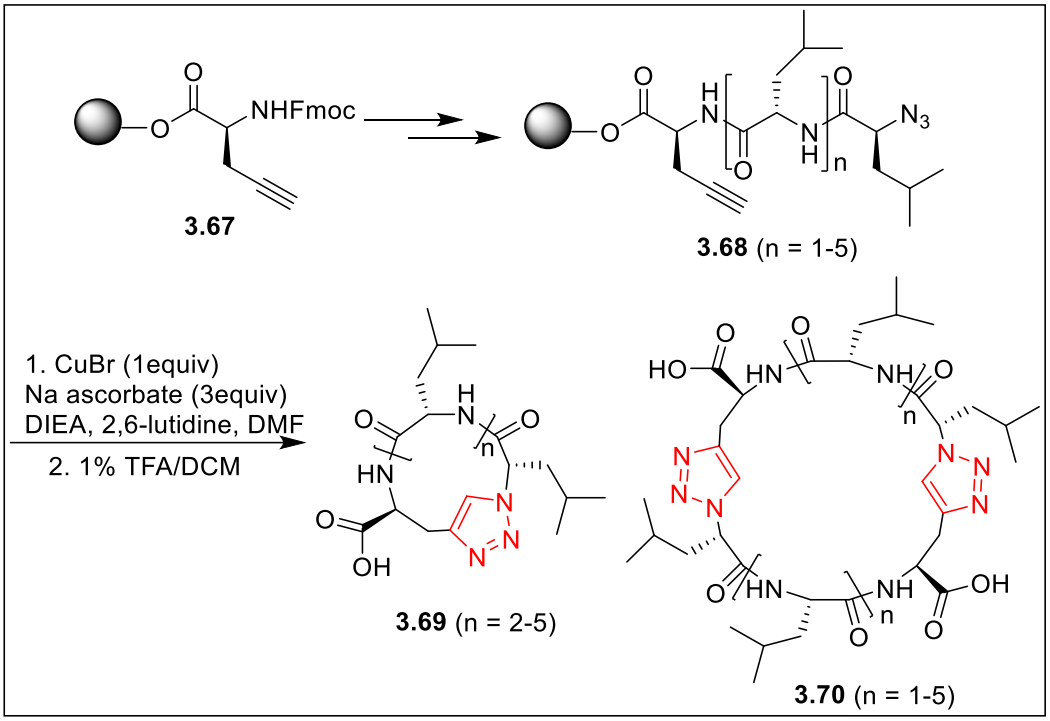

Scheme 3.11

Two epimeric series of foldamers characterized by the presence of a repeating α,ε-dipeptide units were constructed where the ε-unit contained two heterocycles: a 1,4-DT unit and a 4-carboxy-5-methyloxazolidin-2-one, while the α-unit was an alanine moiety. Thus, D-Thr-OMe **3.71** (Scheme 3.12) was cyclized with triphosgene at room temperature to give (4R,5S)-4-methylcarboxylate-5-methyloxazolidin-2-one which was finally converted to the azido derivative **3.72** in several steps in 79% overall yield. The azide **3.72** on reaction with benzyl propiolate afforded the 1,4-DT residue and the product was subjected to peptide coupling to afford L-Ala-D-oxd-1,4-DTCO$_2$Bn monomeric unit **3.73**. Using this approach several oligomers, such as **3.74** having L,D configuration were prepared. For comparison of conformational preferences with L, L oligomers, the monomeric building block L-Ala-L-oxd-1,4-DTCO$_2$Bn **3.77** was prepared from the free amino compound **3.76** obtained from L-Thr-OMe **3.75**. Oligomers such as **3.78** were prepared from the monomeric unit **3.77**. The L ,D series of oligomers formed ordered β-turn foldamers but the L, L series was not ordered. Simulations showed that an ordered L, L trimer was energetically (2 kcal/mol) higher than the more stable nonfolded extended conformations. Both series were titrated with Cu(II), which formed complexes with both the series, but the complexation could not impose order to the L, L series. Therefore, a small modification of the skeleton contributed dramatically to the conformational aspects of oligomer. Moreover, the foldamers made of L,D unit may be introduced in a peptidomimetic for a stable β-turn (Scheme 3.12).[93]

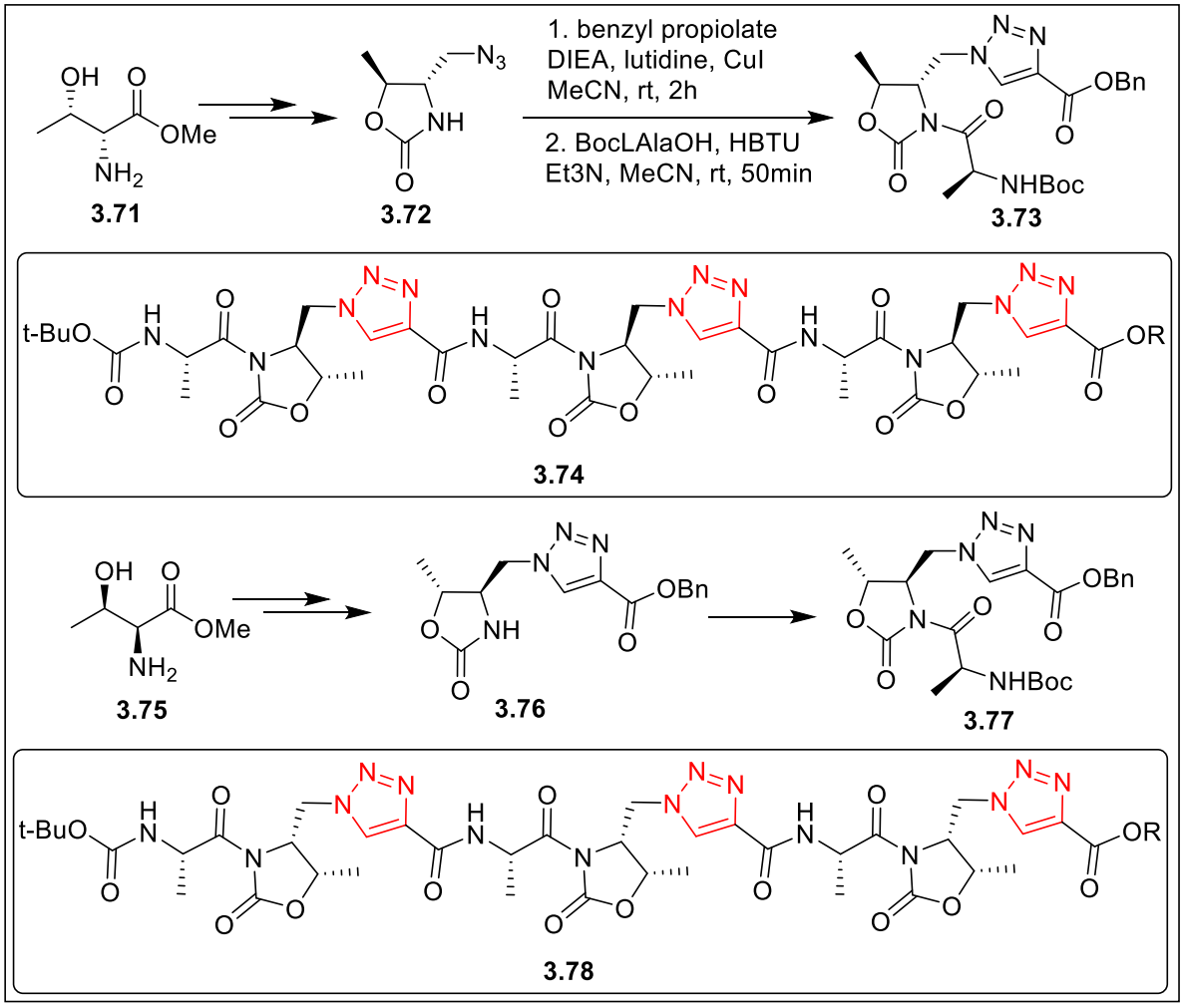

Scheme 3.12

In an attempt to explore whether tris(triazole) peptides could self-assemble into spherical nanoarchitectures as suggested in scheme 3.13 (inset box), a series of oligotriazole peptides **3.81** were synthesized by coupling a tripropargylamine scaffold **3.80** with azidopeptide units **3.79** under Cu(I) catalytic conditions. Since oligotriazole Cu(I) complexes (e.g. from TBTA, scheme 2.3) can catalyze triazole formation, the autocatalytic reproduction of tris(triazole) peptides was possible. In this case the tripodal tris(triazole) ligands were decorated with three peptide arms (as in **3.81**). Transmission electron microscopy (TEM) revealed the presence of several populations of spherical compartments (150, 600 and 900 nm average diameter for **3.81a, c, d**, respectively), consistent with nanosphere architectures. Nanospherical architectures of the azido-modified peptide precursors **3.79a, c, d** were not observed in TEM under the same hydration conditions, demonstrating that peptide tris(triazole) formation was necessary to trigger sphere assembly. These results provided strong evidence that the oligotriazole peptides, functioned as Cu(I) ligand and autocatalyze the formation of additional oligotriazoles in the presence of Cu(I) and appropriate azide and alkyne precursors. These oligotriazoles self-assembled spontaneously into peptide-based nanospheres. Aromatic π-stacking effectscould be the probable driving force for nanosphere formation (Scheme 3.13).[94]

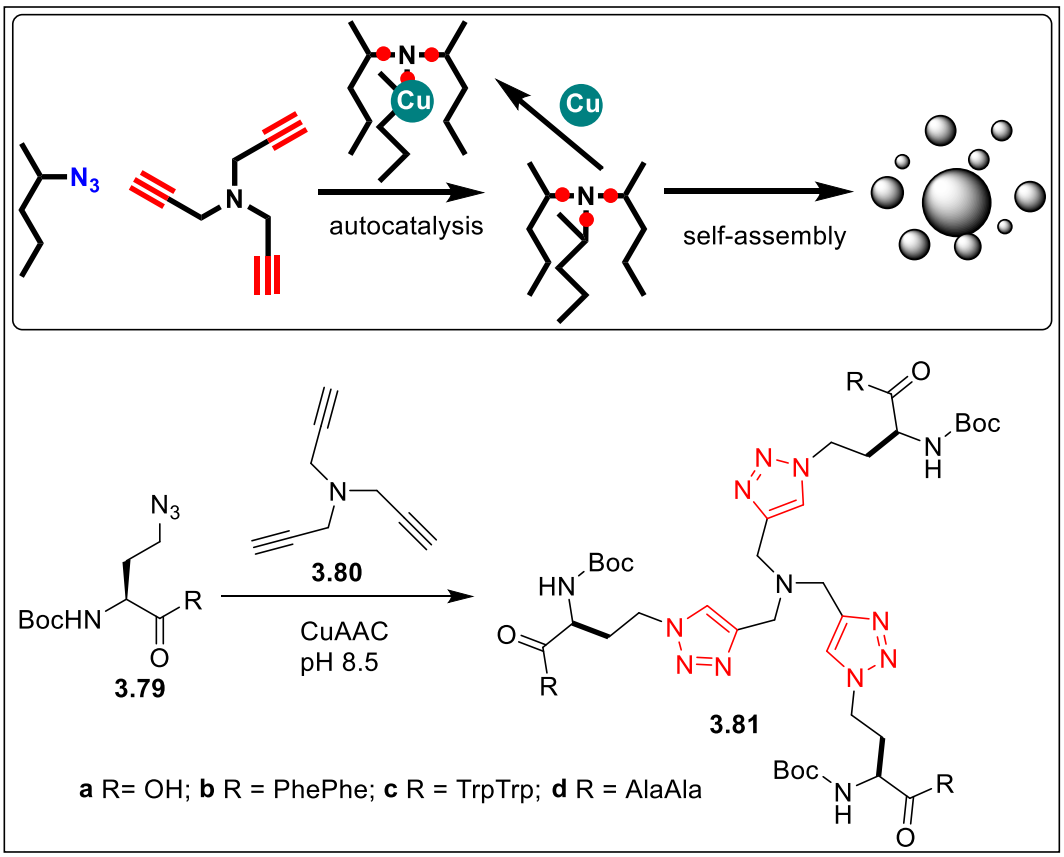

Scheme 3.13

A route has been designed to synthesize conformationally versatile peptidomimetic foldamers, such as **3.82** and **3.83** (Scheme 3.14) containing chiral 1,5-disubstituted triazoles in an alternating fashion with amide bonds. Six different homo- and heterochiral building blocks Boc-Xaa[5Tz]Yaa-OBzl such as **3.86** and **3.89** were synthesized in high yields. Thus, ruthenium-catalyzed azide–alkyne cycloaddition (RuAAC) combined chiral propargylamines **3.84** and and α-azido acids **3.85** under under microwave conditions to afford 3.86. Similarly, **3.87** and **3.88** afforded **3.89**. Epimerization during the formation of the peptide bonds was prevented by a base-free carbodiimide-mediated preactivation and the application of sym-collidine, as a mild base, for the successive coupling steps. Using the combination of triazolylation and peptide chemistry cycles, 1,5-DT derivatives **3.86** and **3.89** were eventually converted to peptidotriazolamer **3.32** and **3.83**. While the homochiral peptidotriazolamer **3.82** formed a compact β-turn-like structure, the heterochiral peptidotriazolamer 37 with alternating chirality adopts a polyproline I-like conformation [95] Same research group synthesized an alternative class of peptidomimetics containing 1,4-DTs and amide bonds in an alternating fashion. The synthesis was also based on chiral propargylamines and chiral α-azido acids as mentioned in scheme 3.14. Homo- and heterochiral tetra-, hexa-, and heptamers based on two different sequences as well as a homochiral oligomer, in which every second sidechain was replaced by a proton, were synthesized. Thus, for example, the homochiral oligomer **3.90a** (Scheme 3.15) and the heterochiral oligomer **3.91a** were prepared in a stepwise fashion using repeat cycles of reaction sequences from **3.90** and **3.91** respectively. Molecular modeling of the Boc-Ala-ValΨ[4Tz]Phe-LeuΨ[4Tz]Phe-LeuΨ[4Tz]Val-OAll sequence (homo- and heterochiral) as well as a Gly-substituted derivative revealed a compact folded conformation in DMSO. The conformation of these molecules remains compactly folded in water as well, due to the

hydrophobic character of the non-polar side chains. The homochiral compound folded into a regular helical structure and the heterochiral one showed a twisted "S"-shape (Scheme 3.15).[79]

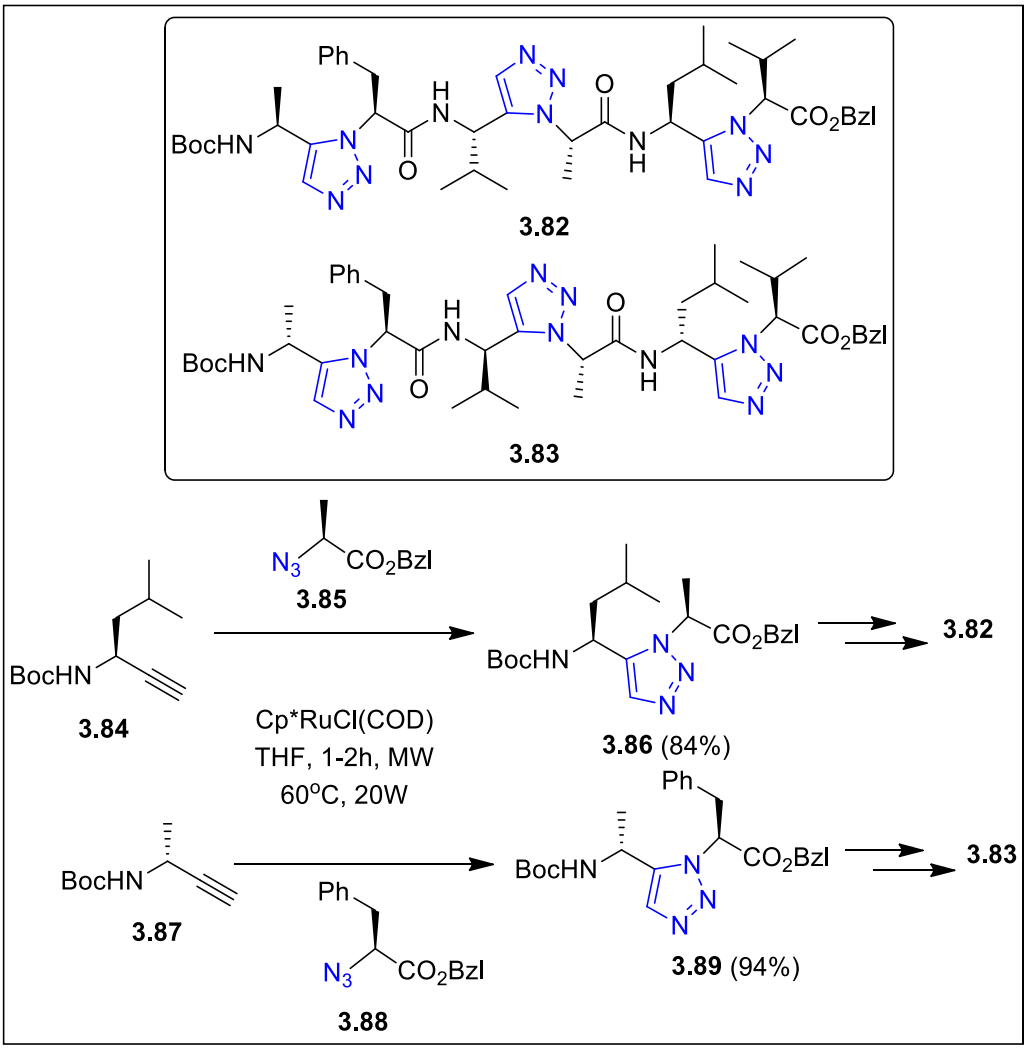

Scheme 3.14

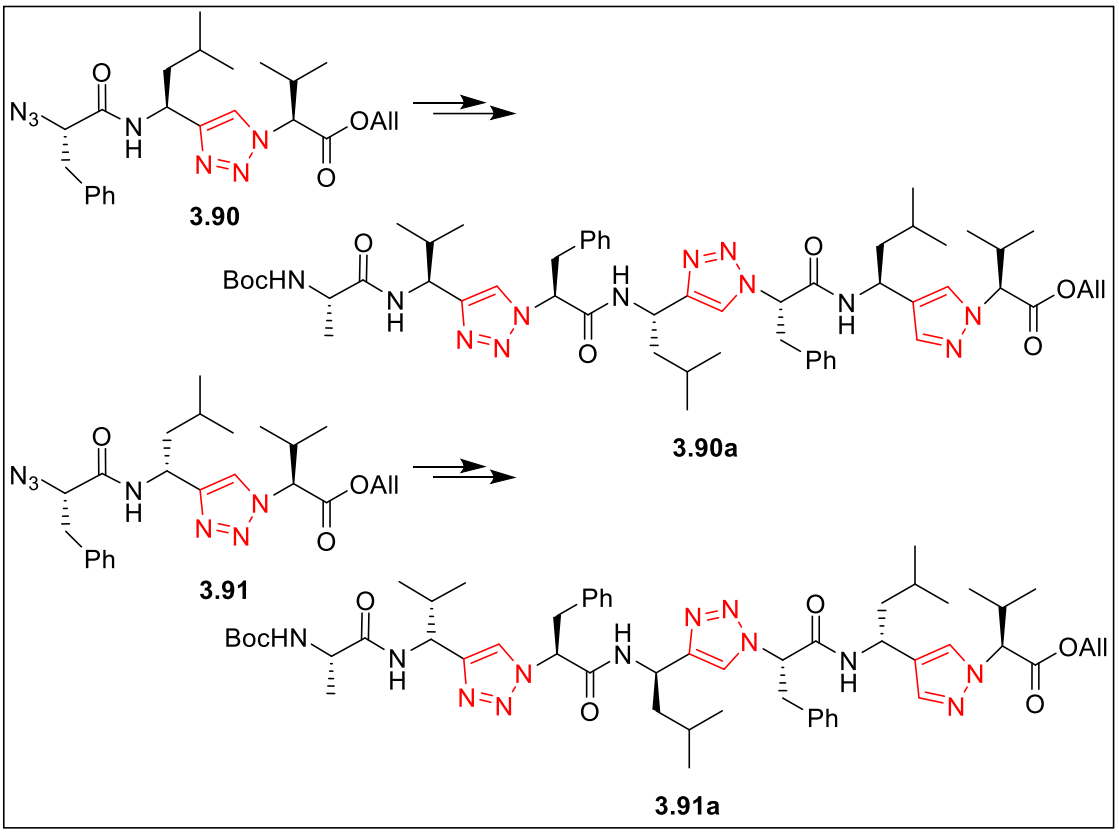

Scheme 3.15

To study the utility of chiral triazoles in the synthesis of foldamer, enantiomerically pure 1,5-DT (*S*)-**3.93** was synthesized by coupling chiral alkyne **3.92** with 2-azidoacetate under RuAAC conditions. LiOH mediated hydrolysis of one part of **3.93** led to the corresponding carboxylic acid, and TFA treatment of another portion of **3.93** generated **3.93B** with the free N-terminal. Amide coupling of **3.93A** and **3.93B** afforded the bistriazolyl (*S,S*)-**3.94**. Repetition of amide synthesis generated 1,5-DT based trimer (S,S,S)-**3.94a**. 2D NOESY NMR experiments revealed that the corresponding non-chiral trimer existed in a turn-like conformer but no such correlation was observed for (S,S,S)-**3.94a**. Further analysis of the spectra of (*S,S,S*)-**3.94a** indicating a twisted conformer. A systematic quantum chemical study was performed on all monomers (**3.93a**-**d**), indicating their capacity to form several low energy conformers. These studies would be useful in the design and synthesis of new classes of foldamers from 1,5-DT based scaffolds (Scheme 3.16).[96]

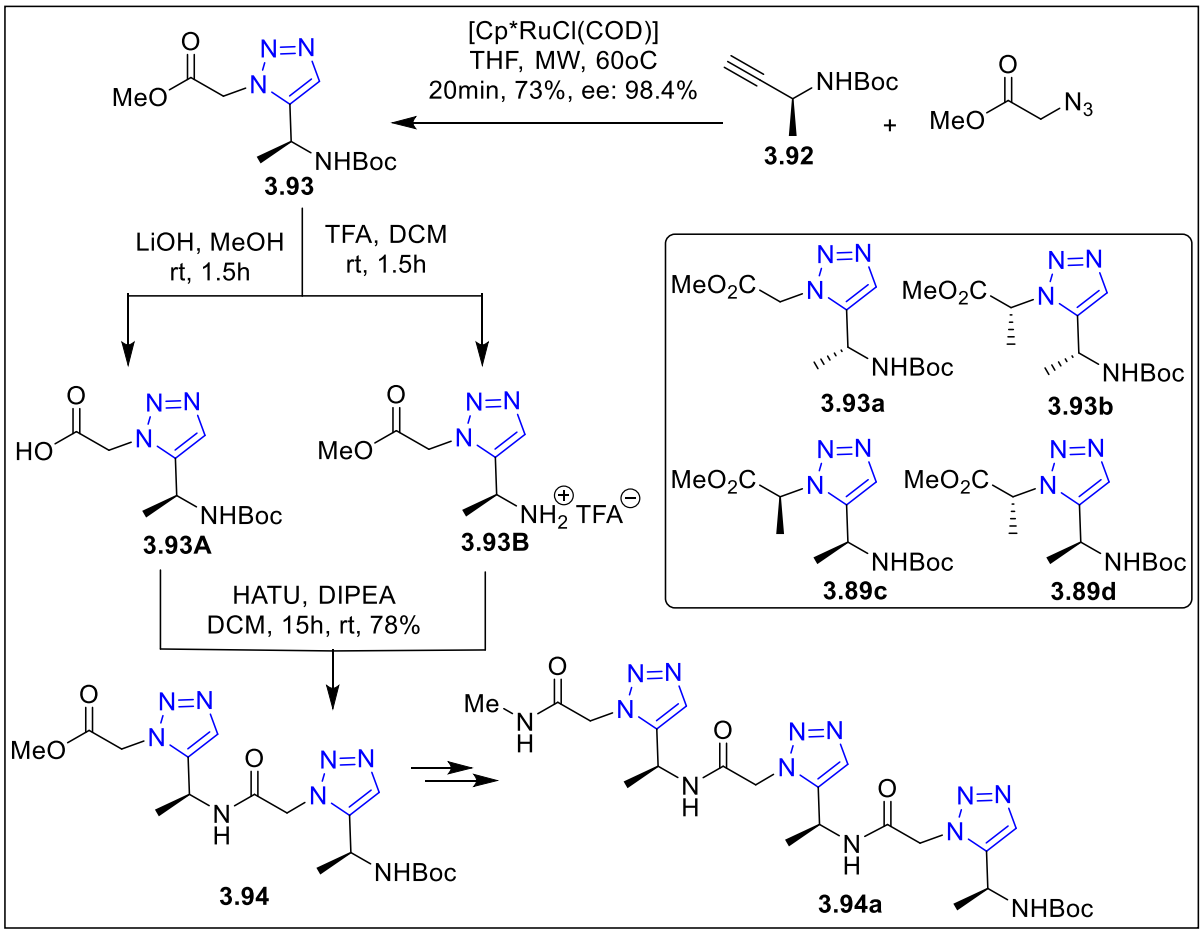

Scheme 3.16

From the few reports on fluorinated foldamers, it was known that the fluorinated peptoids and CF_3-β-peptides adopted an helical conformation while oligomers of cis-2-amino-1-fluorocyclobutane-1-carboxylic acid and of 2-fluoro-aryl substituted α,β-amino acid adopted strand-like secondary structure. Therefore, for the synthesis of a new family of fluorinated foldamers, the asymmetric Zinc-mediated Barbier type propargylation of the (*R*) isomer of trifluoromethyl (*R*)-*tert*-butanesulfinyl aldimine **3.95** (Scheme 3.17) afforded the corresponding (*R,RS*) CF_3-homopropargylic amine **3.96**. The CuAAC reaction between **3.96** and ethyl 2-azidoacetate, afforded the trifluoromethyl 1,4-DT monomer **3.97**. ^{19}F NMR confirmed that there was no epimerization. The 1,4-DT monomer **3.97** was saponified to **3.98** using LiOH to avoid epimerization; another part of **3.97** was subjected to an acidic cleavage of its N-protection to give **3.99**. Amide coupling reaction of **3.98** and **3.99** afforded the bistriazolide **3.100**. Repetition of deprotection and amide coupling reactions and final purification generated the desired tetramer **3.101**. The combination of similar cycloaddition and amidation strategy using the 1,4-DT monomer **3.102** afforded the backbone fluorinated tetramer **3.103**. Foldamers based on CF_3-1,4-DT amino acids were capable of adopting short multi-stranded β-sheet-like structures. The driving forces in these structures were consisted of electrostatic, π-stacking and dipole-dipole interactions of triazole units. On the other hand, foldamers based on 1,4-DT-CF_2 units adopted elongated β-strand like structures, stabilized by electrostatic interaction between fluorine atoms and their neighboring protons (Scheme 3.17).[97]

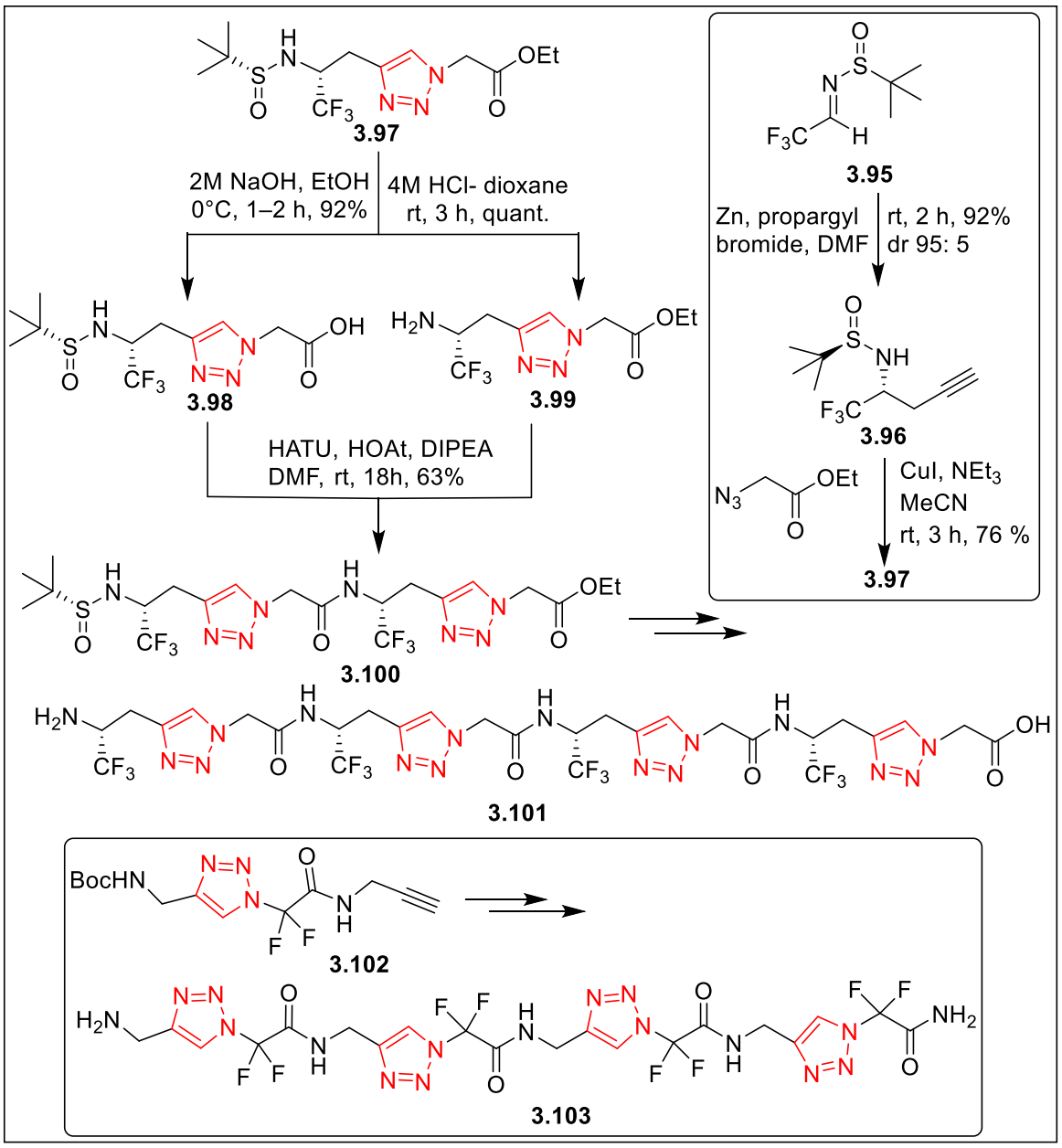

Scheme 3.17

Conclusions

This review summarized recently reported synthetic approaches and versatile applications of oligo-1,2,3-triazolylated molecules. An attempt was made to highlight two different structural motifs of oligotriazoles. In one hand, a series of multiple trazolyl units were connected by versatile organic building blocks and on the other hand, one triazole unit was connected with another by "*N*-(CH)n-*C*" linkage to generate triazolamers.

The triazolamers were categorized in two subsections i.e. non-peptido and peptido triazolamers. Synthetic strategy of most of these oligo-1,2,3-triazoles is based on click chemistry and biased towards CuAAC reactions to construct 1,4-DT units. There are limited number of reports on the use of RuAAC strategy for the synthesis of 1,5-DT units. However, the metal free vinyl sulfone route, developed by the authors' group was also used to

obtain 1,5-DTs. There were several examples of aromatic/heteroaromatic building blocks-triazole hybrid oligomers which lead to the formation of anion templated foldamers; these oligomers were used as recognition motif.[12] In limited number of reports, 1,4,5-trisubstituted 1,2,3-triazoles (1,4,5-TT) were also used in combination with 1,4- and 1,5-DTs.

Although, in general the oligotriazole synthesis and their applications in material science and biology (Section 2) remain a thriving area of research, the field of triazolamers (Section 3) remained underexplored. It was obvious that the fewer examples of triazolamers cited in this review, indicated the potential of this class of molecules to emerge as a promising family of chemical entities with completely unknown properties for applications in biological and material science. The ease of synthesis of 1,4-DT units also enabled researchers to work with mostly 1,4-DT-based oligo-1,2,3-triazoles and triazolamer. Undoubtedly, all these molecules had shown broad spectrum of applications. It should be noted, however that the applications of 1,5-DT based oligotriazoles[47] and triazolamers[79,96] were heavily under-explored. Probably due to synthetic complexity, oligotriazoles and triazolamers constructed using differently substituted triazoles, such as, 1,4-DT/1,5-DT,[45] 1,4-DT/1,4,5-TT; 1,5-DT/1,4,5-TT[74] etc remained unexplored. Availability of these classes of compounds would certainly provide new chemical entities with new properties. Hopefully, this minireview would help researchers from various areas of chemistry, biology and material science to explore the unchartered areas of oligotriazoles and triazolamers.

Acknowledgements

T.P. thanks all the past and present MSc project students, research scholars, and postdoctoral fellows for their contributions toward the development of research on 1,2,3-triazole linked hybrid molecules, especially oligotriazole based molecules and vinyl sulfone chemistry for the synthesis as well as relaed studies of 1,5-DTs in his laboratory. Financial support from Science and Engineering Research Board (SERB), Department of Science and Technology, Government of India (project no. CRG/2019/000375), Department of Science and Technology, India (project no. SB/S1/OC-30/2014), Department of Biotechnology, Ministry of Science and Technology, New Delhi (project no. BT/PR6189/BRB/10/1150/2012), the Council of Scientific and Industrial Research, India, and the Indo-French Centre for the Promotion of Advanced Research is gratefully acknowledged. T. P. also thanks the thanks the Indian Institute of Technology Kharagpur for internal supports. R.P. thanks the Indian Institute of Technology Kharagpur for a research fellowship.

References

1. Singh, H.; Sindhu, J.; Khurana, J.M. *RSC Adv.* **2013**, *3*, 22360.
https://doi.org/10.1039/C3RA44440F
2. Michael, A. *J. Prakt. Chem.* **1893**, *48*, 94.
https://doi.org/10.1002/prac.18930480114
3. Huisgen, R.; Szeimies, G.; Mobius, L. *Chem. Ber.* **1967**, *100*, 2494.
https://doi.org/10.1002/cber.19671000806
4. Tornøe, C. W.; Christensen, C.; Meldal, M. *J. Org. Chem.* **2002**, *67*, 3057.
https://doi.org/10.1021/jo011148j
5. Rostovtsev, V. V.; Green, L. G.; Fokin, V. V.; Sharpless, K. B. *Angew. Chem. Int. Ed.* **2002**, *41*, 2596.

https://doi.org/10.1002/1521-3773(20020715)41:14<2596::AID-ANIE2596>3.0.CO;2-4
6. Zhang, L.; Chen, X.; Sharpless, K. B.; Fokin, V. V. *J. Am. Chem. Soc.* **2005**, *46*, 15998.
https://doi.org/10.1021/ja054114s
7. Pedersen, D. S.; Abell, A. *Eur.J.Org.Chem.* **2011**, 2399.
https://doi.org/10.1002/ejoc.201100157
8. Rani, A.; Singh, G.; Singh, A.; Maqbool, U.; Kaur, G.; Singh, J. *RSC Adv*. **2020**, *10*, 5610.
https://doi.org/10.1039/C9RA09510A
9. Wang, X.; Zhang, X.; Ding, S. *Polym. Chem.* **2021**, *12*, 2668.
https://doi.org/10.1039/D1PY00123J
10. Yoshida, S. *Org. Biomol. Chem.* **2020**, *18*, 1550.
https://doi.org/10.1039/C9OB02698C
11. Zheng, Z.-J.; Ding, W.; Xu, Z.; Xu, L.-W. *Beilstein J. Org. Chem.* **2015**, *11*, 2557.
https://doi.org/10.3762/bjoc.11.276
12. Foyle, E. M.; White, N. G. *Chem Asian J.* **2021**, *16*, 575.
https://doi.org/10.1002/asia.202100040
13. Huo, J.; Hu, H.; Zhang, M.; Hu, X.; Chen, M.; Chen, D.; Liu, J.; Xiao, G.; Wang, Y.; Wen, Z. *RSC Adv.* **2017**, *7*, 2281.
https://doi.org/10.1039/C6RA27012C
14. Katrizky, A. R.; Singh, S. K.; Meher, N. K.; Doskocz, J.; Suzuki, K.; Jiang, R.; Geoffroy L. Sommen, G. L.; David A. Ciaramitaro, D. A.; Steeld, P. J. *Arkivoc* **2006**, *(v)*, 43.
https://doi.org/10.3998/ark.5550190.0007.505
15. Cheshev, P.; Marra, A.; Dondoni, A. *Org. Biomol. Chem.* **2006**, *4*, 3225.
https://doi.org/10.1039/B609734K
16. Conte, M. L.; Chambery, A.; Marra, A.; Dondoni, A. *SYNLETT* **2009**, *16*, 2679.
https://doi.org/10.1055/s-0029-1217751
17. Conte, M. L.; Marra, A.; Chambery, A.; Gurcha, S. S.; Besra, G. S.; Dondoni, A. *J. Org. Chem.* **2010**, *75*, 6326.
https://doi.org/10.1021/jo100928g
18. Juwarker, H.; Lenhardt, J. M.; Pham, D. M.; Craig, S. L. *Angew. Chem. Int. Ed.* **2008**, *47*, 3740.
https://doi.org/10.1002/anie.200800548
19. Juwarker, H.; Lenhardt, J. M.; Castillo, J. C.; Zhao, E.; Krishnamurthy, S.; Jamiolkowski, R. M.; Kim, K.; Craig, S. L. *J. Org. Chem.* **2009**, *74*, 8924.
https://doi.org/10.1021/jo901966f
20. Qin, A.; Lam, J. W. Y.; Jim, C. K. W.; Zhang, L.; Yan, J.; Haussler, M.; Liu, J.; Dong, Y.; Liang, D.; Chen, E.; Jia, G.; Tang, B. Z. *Macromolecules* **2008**, *41*, 3808.
https://doi.org/10.1021/ma800538m
21. Wang, Y.; Li, F.; Han, Y.; Wang, F.; Jiang, H. *Chem. Eur. J.* **2009**, *15*, 9424.
https://doi.org/10.1002/chem.200900546
22. Nuzzi, A.; Massi, A.; Dondoni, A. *QSAR Comb. Sci.* **2007**, *26*, 1191.
https://doi.org/10.1002/qsar.200740079
23. Dondoni, A. *Org. Biomol. Chem.* **2010**, *8*, 3366.
https://doi.org/10.1039/c002586k
24. Türka, M.; Cos¸gun, S.; C¸elika, S. U.; Erdemi, H.; Gérardin-Charbonnier, C.; Bozkurt, A. *Synth. Met.* **2011**, *161*, 665.
https://doi.org/10.1016/j.synthmet.2011.01.010

25. Ghorai, A.; Gayen, A.; Kulsi, G.; Padmanaban, E.; Laskar, A.; Achari, B.; Mukhopadhyay, C.; Chattopadhyay, P. *Org. Lett.* **2011**, *13*, 5512.
https://doi.org/10.1021/ol2022356
26. Rolfe, A.; Painter, T. O.; Asad, N.; Hur, M. Y.; Jeon, K. O.; Brzozowski, M.; Klimberg, S. V.; Porubsky, P.; Neuenswander, B.; Lushington, G. H.; Santini, C.; Hanson, P. R. *ACS Comb. Sci.* **2011**, *13*, 511.
https://doi.org/ 10.1021/co200093c
27. Corrales, R. C. N. R.; Souza, N. B.; Pinheiro, L. S.; Abramo, C.; Coimbra, E. S.; Silva, A. D. D. *Biomed. Pharmacother* **2011**, *65*, 198.
https://doi.org/10.1016/j.biopha.2010.10.013
28. Zornik, D.; Meudtner, R. M.; Malah, T. E.; Thiele, C. M.; Hecht, S. *Chem. Eur. J.* **2011**, *17*, 1473.
https://doi.org/10.1002/chem201002491
29. Cendret, V.; Francois-Heude, M.; Me´ndez-Ardoy, A.; Moreau, V.; Ferna´ndez, J. M. G.; Djedaı¨ni-Pilard, F. *Chem. Commun.* **2012**, *48*, 3733.
https://doi.org/10.1039/c2cc30773a
30. Singh, P.; Parvesh Singh, P.; Kumar, M.; Gut, J.; Philip J. Rosenthal, P. J.; Kewal Kumar, K.; Kumar, V.; Mahajan, M. P.; Bisetty, K. *Bioorg. Med. Chem. Lett.* **2012**, *22*, 57.
https://doi.org/10.1016/j.bmcl.2011.11.082
31. Potratz, S.; Mishra, A.; Bäuerle, P. *Beilstein J. Org. Chem.* **2012**, *8*, 683.
https://doi.org/10.3762/bjoc.8.76
32. You, L.-Y.; Chen, S.-G.; Zhao, X.; Liu, Y.; Lan, W.-X., Zhang, Y., Lu, H.-J., Cao, C.-Y.; Li, Z.-T. *Angew. Chem. Int. Ed.* **2012**, *51*, 1657.
https://doi.org/10.1002/anie.201106996
33. Liu, Y.-H.; Zhang, L.; Xu, X.-N.; Li, Z.-M.; Zhang, D.-W.; Zhao, X.; Li, Z.-T. *Org. Chem. Front.* **2014**, *1*, 494.
https://doi.org/10.1039/c4qo00047a
34. Zhang, J.; Chow, H.-F.; Chan, M.-C.; Chow, G. K.-W.; Kuck, D. *Chem. Eur. J.* **2013**, *19*, 15019.
https://doi.org/10.1002/chem.201300682
35. Roberts, D. A.; Schmidt, T. W.; Crossley, M. J.; Sebastien, P. *Chem. Eur. J.* **2013**, *19*, 12759.
https://doi.org/10.1002/chem.201301133
36. Shang, J.; Gallagher, N. M.; Bie, F.; Li, Q.; Che, Y.; Wang, Y.; Jiang, H. *J. Org. Chem.* **2014**, *79*, 5134.
https://doi.org/10.1021/jo500582c
37. Hirsch, B. E.; McDonald, K. P.; Flood, A. H.; Tait, S. L. *J. Chem. Phys.* **2015**, *142*, 101914.
https://doi.org/10.1063/1.4906895
38. Mudraboyina, B. P.; Obadia, M. M.; Abdelhedi-Miladi, I.; Allaoua, I.; Drockenmuller, E. *Eur. Polym. J.* **2015**, *62*, 331.
https://doi.org/10.1016/j.eurpolymj.2014.08.025
39. Campo, V. L.; Ivanova, I. M.; Carvalho, I.; Lopes, C. D.; Carneiro, Z. A.; Saalbach, G.; Schenkman, S.; Silva, J. S.; Nepogodiev, S. A.; Field, R. A. *Tetrahedron* **2015**, *71*, 7344.
https://doi.org/10.1016/j.tet.2015.04.085
40. Shang, J.; Wei Zhao, W.; Li, X.; Wang, Y.; Jiang, H. *Chem. Commun.* **2016**, *52*, 4505.
https://doi.org/10.1039/c5cc10422j
41. Zhao, W.; Huang, F.; Wang, Y.; Li, Q.; Shang, J.; Che, Y.; Jiang, H. *Tetrahedron Lett.* **2016**, *57*, 1691.
https://doi.org/10.1016/j.tetlet.2016.03.008
42. Wang, Y.; Zhao, W.; Bie, F.; Wu, L.; Li, X.; Jiang, H. *Chem. Eur. J.* **2016**, *22*, 5233.
https://doi.org/10.1002/chem.201504910

43. Fujino, T.; Suzuki, T.; Okada, K.; Kogashi, K.; Yasumoto, K.-i.; Sogawa, K.; Isobe, H. *J. Org. Chem.* **2016**, *81*, 8967.
https://doi.org/10.1021/acs.joc.6b01618
44. Ishmetova, R. I.; Yachevskii, D. S.; Ignatenko, N. K.; Slepukhin, P. A.; Efimov, I. V.; Bakulev, V. A.; Rusinov, G. L.; Filyakova, V. I.; Charushin, V. N. *Russ.Chem.Bull.* **2016**, *65*, 1268.
https://doi.org/10.1007/s11172-016-1446-4
45. Bose, A.; Pathak, T. *Adv Carbohydr Chem Biochem* **2020**, *78*, 1 and references cited therein.
https://doi.org/10.1016/bs.accb.2020.10.001
46. Erhardt, H.; Mohr, F.; Kirsch, S. F. *Chem. Commun.* **2016**, *52*, 545.
https://doi.org/10.1039/c5cc08163g
47. Dey, S.; Sarkar, T.; Majumdar, A.; Tanmaya Pathak, T.; Ghosh, K. *ChemistrySelect* **2017**, *2*, 2034.
https://doi.org/10.1002/slct.201601933
48. Khanapurmatha, N.; Kulkarnia, M. V.; Joshib, S. D.; Kumar, G. N. A. *Bioorg. Med. Chem.* **2019**, *27*, 115054.
https://doi.org/10.1016/j.bmc.2019.115054
49. Salta, J.; Reissig, H.-U. *Eur. J. Org. Chem.* **2020**, 4361.
https://doi.org/10.1002/ejoc.202000618
50. Salta, J.; Arp, F. F.; Kühne, C.; Reissig, H.-U. *Eur. J. Org. Chem.* **2020**, 7333.
https://doi.org/10.1002/ejoc.202001389
51. Das, A.; Dasgupta, S.; Pathak, T. *Org. Biomol. Chem.* **2020**, *18*, 6340.
https://doi.org/10.1039/d0ob01286f
52. Arévalo-Ruiza, M.; Samir Amrane, S.; Rosuc, F.; Belmonte-Reche, E.; Peñalver, P.; Mergny, J.-L.; Morales, J. C. *Bioorganic Chemistry* **2020**, *99*, 103786.
https://doi.org/10.1016/j.bioorg.2020.103786
53. Carreiro, E. P.; Sena, A. M.; Puerta, A.; Padrón, J. M.; Burke, A. J. *Synlett* **2020**, *31*, 615.
https://doi.org/10.1055/s-0039-1690781
54. Yerrabellya, J. R.; Gogulaa, T.; Erukalaa, Y. G.; Yerrabelly, H.; Gabriella, S. *Chem. Data Collect* **2020**, *29*, 100523.
https://doi.org/10.1016/j.cdc.2020.100523
55. Bunchuay, T.; Docker, A.; Eiamprasert, U.; Surawatanawong, P.; Brown, A.; Beer, P. D. *Angew. Chem. Int. Ed.* **2020**, **59**, 12007.
https://doi.org/10.1002/anie.202001125
56. Deshmukh, T. R.; Khare, S. P.; Krishna, V. S.; Sriram, D.; Sangshetti, J. N.; Khedkar, V. M.; Shingate, B. B. *Synth. Commun.* **2020**, *50*, 271.
https://doi.org/10.1080/00397911.2019.1695275
57. Lawal, N. S.; Bala, M. D. *J. Mol. Struct.* **2020**, *1200*, 127124.
https://doi.org/10.1016/j.molstruc.2019.127124
58. Stalina, A.; Kandhasamyd, S.; Kannane, B. S.; Verma, R. S.; Ignacimuthu, S.; Kima, Y.; Qingsonga, S.; Chena, Y.; Palani, P. *Bioorg. Chem.* **2020**, *96*, 103579.
https://doi.org/10.1016/j.bioorg.2020.103579
59. Sunitha, V.; Kumar, K.; Jalapathi, P.; Lincoln, C. A. *Russ. J. of Gen. Chem.* **2020**, *90*, 154.
https://doi.org/10.1134/S1070363220010247
60. Joseph, R. *ACS Omega* **2020**, *5*, 6215.
https://doi.org/10.1021/acsomega.0c00595

61. Georghiou, P. E.; Rahman, S.; Alrawashdeh, A.; Alodhayb, A.; Vallurua, G.; Unikela, K. S.; Bodwell, G. J. *Supramol Chem* **2020**, *32*, 325.
https://doi.org/10.1080/10610278.2020.1739686
62. Juraj, N. P.; Krklec, M.; Novosel, T.; Perić, B.; Vianello, R.; Raić-Malić, S.; Kirin, S. I. *Dalton Trans.* **2020**, *49*, 9002.
https://doi.org/10.1039/d0dt01244k
63. Bayrak, F.; Oral, A.; Ay, K. *Maced. J. Chem. Chem. Eng.* **2021**, *40*, 75.
https://doi.org/10.20450/mjcce.2021.2220
64. Hazarika, S. I.; Mahata, G.; Pahari, P.; Pramanik, N.; Atta, A. K. *Inorganica Chim. Acta* **2020**, *507*, 119582.
https://doi.org/10.1016/j.ica.2020.119582
65. Wang, X.; Zhang, X.; Sun, Y.; Ding, S. *Macromolecules* **2021**, *54*, 9437.
https://doi.org/10.1021/acs.macromol.1c01371
66. Çelik, F.; Türkan, F.; Aras, A.; Atalar, M. N.; Karaman, H. S.; Ünver, Y.; Kahriman, N. *Bioorg. Chem.* **2021**, *107*, 104606.
https://doi.org/10.1016/j.bioorg.2020.104606
67. Rathinam, S.; Hjalmarsdottir, M. A.; Thygesen, M. B.; Masson, M. *Carbohydr. Polym.* **2021**, *267*, 118162.
https://doi.org/10.1016/j.carbpol.2021.118162
68. Nu´nez-Villanueva, D.; Hunter, C. A. *Chem. Sci.* **2021**, *12*, 4063.
https://doi.org/10.1039/d0sc06770a
69. Navarro, Y.; Lopez, J. G.; Iglesias, M. J.; Ortiz, F. L. *Org. Lett.* **2021**, 23, 334.
https://doi.org/10.1021/acs.orglett.0c03838
70. Saiyasombata, W.; Kiatisevi, S. *RSC Adv.* **2021**, *11*, 3703.
https://doi.org/10.1039/d0ra09686e
71. Fall, S.A.K.; Hajib, S.; Karai, O.; Aouine, Y.; Boukhssas, S.; Faraj, H.; Alami, A. *Molbank* **2021**, *2021*, M1186.
https://doi.org/10.3390/M1186
72. Deshmukh, T. R.; Khedkar, V. M.; Jadhav, R. G.; Sarkate, A. P.; Sangshetti, J. N.; Tiwarif, S. V.; Shingate, B. B. *New J. Chem.* **2021**, *45*, 13104
https://doi.org/10.1039/d1nj01759d
73. Poonia, N.; Lal, K.; Kumar, A. *Res. Chem. Intermed.* **2021**, *47*, 1087.
https://doi.org/10.1007/s11164-020-04318-1
74. Yoshida, S.; Sakata, Y.; Misawa, Y.; Morita, T.; Kuribara, T.; Ito, H; Koike, Y.; Isao Kii, I.; Hosoya, T. *Chem. Commun.* **2021**, *57*, 899.
https://doi.org/10.1039/d0cc07789e
75. Saini, P.; Singh, G.; Kaur, G.; Singh, J.; Singh, H. *J. Mol. Struct.* **2022**, *1251*, 131985.
https://doi.org/10.1016/j.molstruc.2021.131985
76. Saini, P.; Sushma; Singh, G.; Kaur, G.; Singh, J.; Singh, H. *Inorg. Chem. Commun.* **2022**, *141*, 109524.
https://doi.org/10.1016/j.inoche.2022.109524
77. Das, A.; Dasgupta, S.; Pathak, T. *Bioorg. Med. Chem.* **2022**, *71*, 116888.
https://doi.org/10.1016/j.bmc.2022.116888
78. Agouram, N.; El Hadrami, E.M.; Bentama, A. *Molecules* **2021**, *26*, 2937.
https://doi.org/10.3390/molecules26102937
79. Schröder, D. C.; Kracker, O.; Fröhr, T.; Góra, J.; Jewginski, M.; Nieß, A.; Antes, I.; Latajka, R.; Marion, A.; Sewald, N. *Front. Chem.* **2019**, *7*:155.
https://doi.org/10.3389/fchem.2019.00155

80. Angelo, N. G.; Arora, P. S. *J. Am. Chem. Soc.* **2005**, *127*, 17134.
https://doi.org/10.1021/ja056406z
81. Angelo, N. G.; Arora, P. S. *J. Org. Chem.* **2007**, *72*, 7963.
https://doi.org/10.1021/jo701292h
82. Montagnat, O. D.; Lessene, G.; Hughes, A. B. *Tetrahedron Lett.* **2006**, *47*, 6971.
https://doi.org/10.1016/j.tetlet.2006.07.131
83. Montagnat, O. D.; Lessene, G.; Hughes, A. B. *J. Org. Chem.* **2010**, *75*, 390.
https://doi.org/10.1021/jo9021887
84. Jochim, A. L.; Miller, S. E.; Angelo, N. G.; Arora, P. S. *Bioorg. Med. Chem. Lett.* **2009**, *19*, 6023.
https://doi.org/10.1016/j.bmcl.2009.09.049
85. Tsukada, Y.; Yamada, K.; Kunishima, M. *Tetrahedron Lett.* **2011**, *52*, 3358.
https://doi.org/10.1016/j.tetlet.2011.04.082
86. Fiandanese, V.; Iannone, F.; Marchese, G.; Punzi, A. *Tetrahedron* **2011**, *67*, 5254.
https://doi.org/10.1016/j.tet.2011.05.040
87. Solà, J.; Bolte, M.; Alfonso, I. *Org. Biomol. Chem.* **2015**, *13*, 10797.
https://doi.org/10.1039/c5ob01461a
88. Wright, K.; Quinodoz, P.; Drouillat, B.; Couty, F. *Chem. Commun.* **2017**, *53*, 321.
https://doi.org/10.1039/c6cc08294g
89. Grob, N. M.; Häussinger, D.; Deupi, X.; Schibli, R.; Behe, M.; Mindt, T. L. *J. Med. Chem.* 2020, 63, 9, 4484.
https://doi.org/10.1021/acs.jmedchem.9b01936
90. Grob, N. M.; Schmid, S.; Schibli, R.; Behe, M.; Mindt, T. L. *J. Med. Chem.* **2020**, *63*, 4496.
https:// doi.org/10.1021/acs.jmedchem.9b01937
91. Zhang, Z.; Fan, E. *Tetrahedron Lett.* **2006**, *47*, 665.
https://doi.org/10.1016/j.tetlet.2005.11.111
92. Turner, R. A.; Oliver, A. G.; Lokey, R. S. *Org. Lett.* **2007**, *9*, 5011.
https://doi.org/10.1021/ol702228u
93. Milli, L.; Larocca, M.; Tedesco, M.; Castellucci, N.; Ghibaudi, E.; Cornia, A.; Calvaresi, M.; Zerbetto, F.; Tomasini, C. *J. Org. Chem.* **2014**, *79*, 5958.
https://doi.org/10.1021/jo500963n
94. Brea, R. J.; Devaraj, N. K. *Nat. Commun.* **2017**, 8: 730, 1.
https://doi.org/10.1038/s41467-017-00849-1
95. Oliver Kracker, O.; Góra, J.; Krzciuk-Gula, J.; Marion, A.; Neumann, B.; Stammler, H.-G.; Nieß, A.; Antes, I.; Latajka, R.; Sewald, N. *Chem. Eur. J.* **2018**, *24*, 953.
https://doi.org/10.1002/chem.201704583
96. Stålsmeden, A. S.; Paterson, A. J.; Szigyártó, I. C.; Thunberg, L.; Johansson, J. R.; Beke-Somfai, T.; Kann, N. Org. Biomol. Chem., 2020, 18, 1957.
https://doi.org/10.1039/d0ob00168f
97. Arenas, J. L.; Xu, Y.; Milcent, T.; Heijenoort, C. V.; Giraud, F.; Ha-Duong, T.; Crousse, B.; Ongeri, S. *ChemPlusChem* **2021**, *86*, 241.
https://doi.org/10.1002/cplu.202000791

Authors' Biographies

Rashmita Pan obtained her B. Sc. and M. Sc. degrees in Chemistry in 2016 and 2018 respectively from Presidency University, Kolkata. She started her Ph.D. program at Indian Institute of Technology Kharagpur under the supervision of Professor Tanmaya Pathak from 2018. Her current research focuses on the synthesis and applications of various biologically relevant poly-1,2,3-triazoles.

Tanmaya Pathak was born in Kolkata and obtained his Master of Science degree from Jadavpur University, Kolkata, India. After a brief stay at the research centre of Organon (India) Ltd, he carried out his doctoral research with Professor Jyoti Chattopadhyaya, Uppsala University (1988). He joined the National Chemical Laboratory, Pune, India as a scientist in 1991 after two years of postdoctoral research with Professor David Gani, Southampton University (and later St. Andrews University). He spent the year 1997 in the University of Karlsruhe, Germany at the laboratory of Professor Herbert Waldmann as an Alexander von Humboldt Fellow. In 2001 he moved to the Department of Chemistry of the Indian Institute of Technology, Kharagpur, India as an Associate Professor and became a Professor in 2004. He was the head of the department during 2014-2017 and currently continuing in the same department as a Professor with Higher Administrative Grade. He, in collaboration with a French colleague secured a research grant from "Indo–French Centre for the Promotion of Advanced Research" during 2006-2009. He teaches organic chemistry at all levels of bachelor and master degrees with a special interest in Biomolecules and Medicinal Chemistry. His research is focused on carbohydrate modifications and the synthesis of modified nucleosides. His group has extensively worked on the applications of vinyl sulfone modified carbohydrates as Michael acceptors leading to the synthesis of modified carbohydrates, carbocycles and heterocycles. More recently, his group showed the applications of vinyl sulfone as 2π partners in the metal free synthesis of 1,5-disubstituted 1,2,3-tiazoles and oligotriazoles. He has also worked on the design of carbohydrate or nucleoside based inhibitors of ribonuclease A. His free time is spent by reading Bengali novels, watching movies and listening to music.

